u^b

Lake-based paleoseismology in central Sulawesi, Indonesia

Inaugural dissertation
of the Faculty of Science,
University of Bern

presented by

Nicolas, Tournier

from France

Supervisor of the doctoral thesis:
Prof. Dr. Hendrik Vogel
Prof. Dr. Flavio S. Anselmetti

Institute of Geological Sciences
University of Bern

WISSEN
SCHAFFT
WERT.

u^b

Lake-based paleoseismology in central Sulawesi, Indonesia

Inaugural dissertation
of the Faculty of Science,
University of Bern

presented by

Nicolas, Tournier

from France

Supervisor of the doctoral thesis :
Prof. Dr. Hendrik Vogel
Prof. Dr. Flavio S. Anselmetti
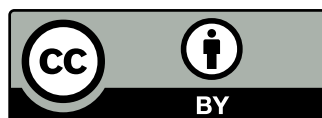Institute of Geological Sciences
University of Bern

Accepted by the Faculty of Science.

Bern, **19.09.2024**

The Dean
Prof. Dr. Marco Herwegh

WISSEN
SCHAFFT
WERT.

Note to myself: don't forget to paste a quote to look clever.

Nicolas Tournier

II

Abstract

Earthquakes are the main cause of considerable human losses and damage on Earth. The most active seismic areas are now widely studied. However, the hazard potential and recurrence rate of major earthquake events remains poorly understood for some seismic faults. This is the case of the island of Sulawesi, in eastern Indonesia. Although the magnitude 7.5 Palu earthquake in 2018 focused seismological research on the section that ruptured, the Palu-Koro fault runs for hundreds of kilometers across the island of Sulawesi. The entire fault is considered to be a potential source of earthquakes, yet it is understudied.

Seismic risk evaluation is crucial to prepare populations for major earthquakes, and thus limit fatalities and damage. Analysing the seismic hazard is an essential part of this evaluation. It consists of identifying past earthquakes and their recurrences and then estimating the probability of return of these types of events, based on the principle that if an earthquake of a given magnitude has occurred in a region in the past, a similar event could occur in the same region in the future.

Instrumental and historical records of earthquakes on the island of Sulawesi only cover the last 100 years. This time range prevents the identification of major earthquakes with magnitudes greater than 6, as their return periods exceed the seismological records. While it is difficult to study seismic evidence in a tropical setting, due to the enhanced erosion and the dense vegetation, paleoseismology is here essential in evaluating the island's seismic hazard. Lake Towuti and Lake Poso are two ancient tectonic lakes located in central Sulawesi. The sediments act as natural seismographs and cover several hundreds thousands years. Core samples

and sediment boreholes taken at Lake Towuti, in complement of seismic reflection data, have enabled to understand how the lake reacted to climatic and tectonic fluctuations. On the other hand, bathymetric and seismic data from Lake Poso have made it possible to identify and correlate slope collapse deposits triggered by seismic events, and also to observe fault structures directly beneath the sediment surface, revealing tectonic activity.

Acknowledgment

My first thanks naturally go to Hendrik and Yuda, without whom this project would never have started. I would also like to thank Hendrik for his confidence from the start of this long adventure.

Then, I would like to express my gratitude to all those who have contributed scientifically, directly or indirectly, to this project. Many thanks to Flavio and Stefano for your experience with bathymetric and seismic data, Mudrik and Danny for their knowledge of the island of Sulawesi, and Renaldo for your advice on carrying out a successful thesis.

Our fieldwork at Lake Poso would not have been so easy without the precious help of the locals. I would like to express my warmest thanks to Herson and his family, whose hospitality is the best in this world. Thanks also to Marthen, who had the patience to share his boat with us for 17 days to carry out the bathymetric survey. Aside from the scientific aspect, I would like to extend my deepest thanks to the Indonesian community that I had the chance to meet during the 4 years of my thesis. Whether in Indonesia, Switzerland, Italy or US, my encounters with Indonesians have always been very easy and pleasant. So Terima kasih Ahmad, Zahrah, Arga, Taufan, Abang, Yola and the Unta Air of Jakarta.

Starting a PhD thesis during Covid-19 is not the best idea if you want to enjoy student life. However, my life here in Switzerland would have been rather complicated without the friends I have made. First, a big thanks to Adri, who endured me during these four years in Bern and on the field. You're the only one who fits into the category of friend, colleague, office mate and roommate on excursions or seminars. Secondly, I'd like to thank Quan Quan, Giulia, Renaldo,

Aliisaa, and Laura for all the good times I had in Bern and elsewhere.

Thanks go to those who have been by my side and helped me get through. Thank you to Nicolas and Enguerrand who made it possible for me not to think for a single second about my work for entire days. Merci également à ma famille et surtout à mes parents pour m'avoir laissé la liberté dans mes choix de parcours et pour m'avoir soutenu dans mes décisions. Finally, my wholehearted thanks to Alexandra. The first months were difficult, but your patience was my fuel. You are probably the only person who has kept me on track to get to the end of this work. A chapter is ending for me, but a new book is beginning for us.

Contents

4 The large-magnitude earthquake potential of an active strike-slip fault system in Lake Poso, Central Sulawesi, Indonesia   101

5 Conclusion and outlook   133

List of abreviations

BP   before present

kyr   thousand years

LF   Lawanopo Fault

LGM   Last Glacial Maximum

Ma   million years

masl   metre above sea level

mblf   metre below lake floor

MCE   maximum credible earthquake

MF   Matano Fault

MTD   mass transport deposit

Mw   moment magnitude

PGA   peak ground acceleration

PKF   Palu-Koro Fault

TDP   Towuti Drilling Project

TWT   two-way travel time

List of Figures

XIII

XV

List of Tables

Chapter 1

Introduction

Picture of an onshore tectonic feature from a boat on Lake Poso (personal collection).

1 Background and motivation

1.1 Global tectonic and seismology

Global tectonics describes the deformation of the Earth, including seismicity and volcanism (Kearey et al., 2009). Deformation is mostly located at the boundaries of the major tectonic plates (Figure 1.1). These plates comprise the surface layers of the Earth, along with the oceanic crust and the terrestrial crust. Consequently, the tectonic plates generate multidirectional pressure between themselves, accumulating stress (Crétaux et al., 1998). When the stress becomes too strong, the rupture point is reached, and all the accumulated energy is suddenly released in the form of earthquakes. Therefore, most earthquakes recorded on the earth are located along the tectonic plate boundaries.
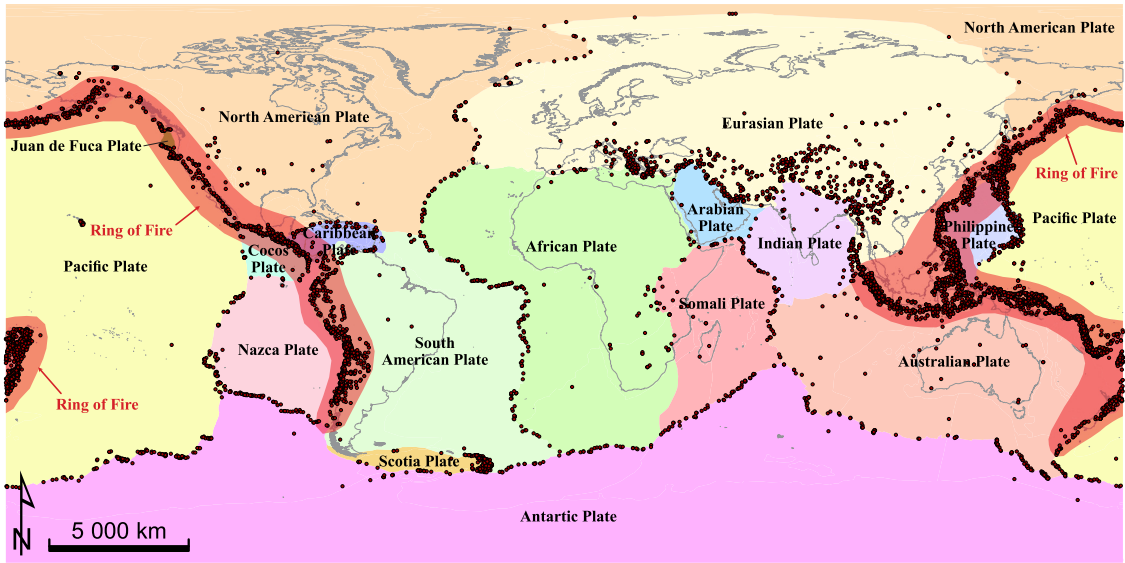
Figure 1.1: Map of the world's tectonic Great Plates. The red dots are earthquakes of magnitude ≥ 5 recorded over the last 20 years (USGS catalogue: https://earthquake.usgs.gov/earthquakes/search/).

The seismic risk combines hazard and vulnerability (Silva et al., 2020). The seismic hazard is the probability of triggering an earthquake in a defined area at

a specified time. It can be quantified with the Peak Ground Acceleration (PGA), which determines the maximal amplitude in speed that an earthquake can generate to the ground (Midorikawa, 1993; Figure 1.2). The vulnerability is the exposure of populations and infrastructures to natural events. It can be evaluated with the capacity of communities to resist and react to these disasters. Therefore, a seismic risk can be insignificant if low-magnitude earthquakes occur in a dense population area with shake-proof buildings. In contrast, it is possible to record very high magnitude earthquakes in the middle of oceans, with no danger to the human population (without considering tsunami hazard).
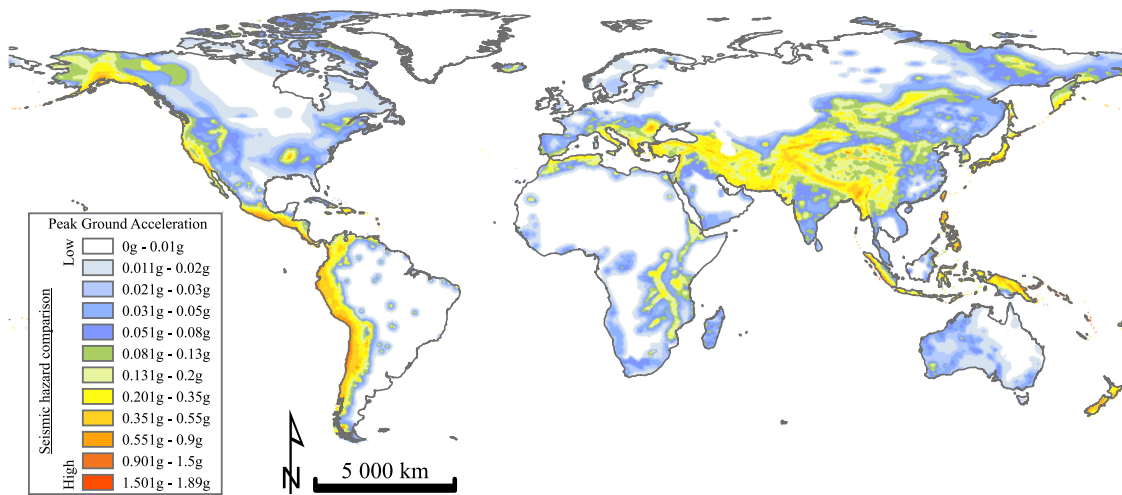
Figure 1.2: Global seismic hazard map showing the distribution of the Peak Ground Acceleration (PGA) with a 10% probability of being exceeded in 50 years (data: Johnson et al. (2023)).

Nevertheless, the world's population has increased exponentially since the beginning of the 19th century, extending high vulnerability regions over areas with high seismic hazard (Freire and Aubrecht, 2012). South-East Asia and Japan are likely the most relevant examples of the increase in seismic risk. The seismic hazard is the third most recurrent natural disaster on Earth (8% of all the natural hazards), after floods (43%) and Storms (28%). But if we look at the number of casualties, it emerges as the main cause of fatality, responsible for 56% of all casualties linked to

natural disasters (Wallemacq et al., 2018). Compared with weather forecasts, which are available for a few days in advance, the seismic hazard is almost considered unpredictable. Therefore, improving our knowledge of these natural disasters is essential to improve population awareness and preparation.

The intensity scale is used to estimate the strength of an earthquake spatially and assess the impact on human perception and material damage (Gutenberg and Richter, 1942). The intensity of an earthquake is a subjective parameter estimated with the feeling effects. The intensity evaluation is processed *a posteriori* by surveying the local population and estimating the damage and ground deformation. This method is essential for the estimation of the seismic risk. It appears that the composition of the substratum is decisive on the effect of shaking (Trifunac and Brady, 1975). Soft sediments amplify the ground movement and can be accentuated by the water content in the sediment, triggering a liquefaction effect (Jalil et al., 2021). At the same distance from the epicentre, the damage to buildings installed on alluvial sediments is typically more severe than infrastructures settled on hard rock, in the mountains, for example.

1.2 Seismic cycles

The seismic hazard is integrated into earthquake forecasting. It is founded on two principles: Where and when will the next earthquake occur? Plate tectonics already indicate the probably location of most earthquakes: along active faults and plate boundaries (Figure 1.1). To assess the timing, it is important to study the evolution of fault dynamics. The frequency, intensity and probability of triggering a major earthquake are the essential parameters for modelling earthquake projections.

Short-term prediction (days to weeks) would likely be the most useful way to alert and protect populations. It consists of analysing the early warning signals, composed of foreshocks or earthquake swarms (Kagan and Knopoff, 1987), and can also be indicated by spontaneous groundwater level changes (Koizumi, 2013), and occasionally abnormal release of radon from the crust (Ghosh et al., 2009). However, these analysis methods are at best indicators for an upcoming event but

still too unreliable to predict the exact timing of the next event. It is, therefore, fundamental to enhance earthquake forecasting using long-term predictions to better predict future events and improve seismic risk preparedeness.

The long-term prediction is based on a certainty that when an earthquake occurs in an area, another one will occur in the future. The tectonic stress of faults follows a cycle of energy accumulation and release (Robert and Bousquet, 2013). The recurrence time is fundamental to determining the long-term prediction. It is estimated by calculating the time average between several historical earthquakes, depending on the magnitude. The Gutenberg - Richter law (Gutenberg and Richter, 1949) states the relation between the magnitude and the total number of earthquakes in a specific region and a period of time for a minimum magnitude (Figure 1.3). Therefore, a significant threat concerns high-magnitude earthquakes (M $\geq$ 7) because the recurrence interval may exceed the instrumental and historical record of past earthquakes.
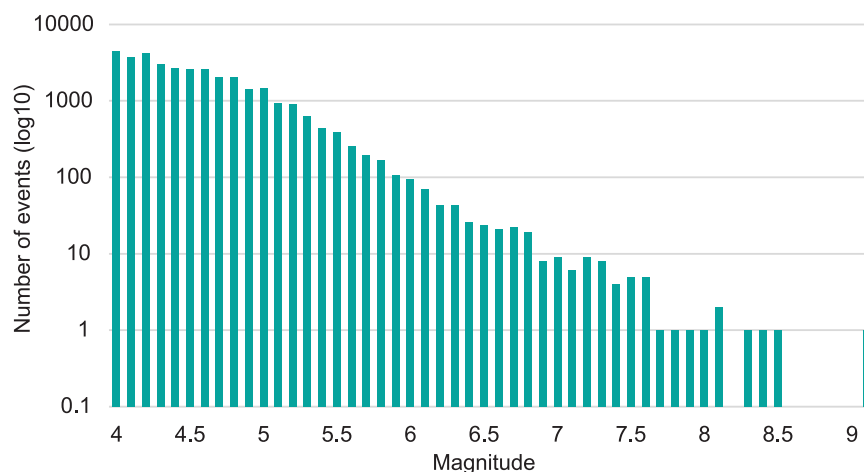
Figure 1.3: Number of earthquakes by the magnitude, recorded in Indonesia from 1970 to 2022 with a depth $\leq$ 40 km. Source: ISC - https://doi.org/10.31905/D808B830

The principle of seismic cycles was introduced for the first time at the beginning of the 20th century, after the San-Frnacisco Mw 7.9 earthquake in 1906 (Reid, 1910). The theory divides seismic deformation into two phases (Figure 1.4): a phase of slow elastic deformation, accumulating stress energy (interseismic), followed

by a phase of spontaneous rupture (coseismic). With that theory, it would be relatively easy to model the earthquake recurrence, especially in the case of a regular seismic cycle, assuming that earthquakes are triggered with the same time interval and at a constant released stress (Shimazaki and Nakata, 1980). Nevertheless, long-term paleoseismologic studies show more complex patterns, with periods of activity, including several earthquakes, followed by periods of quiescence Wallace (1987). During the long interseismic phase, faults continue to accumulate stress. The gap between two coseismic phases also depends on the region and the motion rate between the plates. A supercycle can last from several hundreds of years to millions of years (Salditch et al., 2020).

2 Paleoseismology

2.1 Earthquake recording methods

Various disciplines are applied to identify past earthquakes on different time scales (Figure 1.5). Analytical instruments and the modern seismographic network are highly effective for detecting tremors, even of low magnitudes, and provide precise locations of the epicentres (McCalpin, 2009). Nevertheless, they cannot be used for events triggered before their inventions. Historical documents and archeoseismology are similar because they are related to the populations. Historical documents can be precise in time, but their magnitude can only be estimated based on the descriptions. Archeoseismology, on the contrary, is less precise on the timimg of the earthquakes, but the magnitudes are estimated with physical parameters measured in the field. Both disciplines are also heterogeneous in spatial and temporal distribution over the world. Neotectonics studies the structural deformation of the Earth's crust since the Miocene. This discipline focuses on the geomorphology of landscapes and the topography to identify areas and periods of tectonic activity. Therefore, only high-magnitude events can leave evidence of their effects.
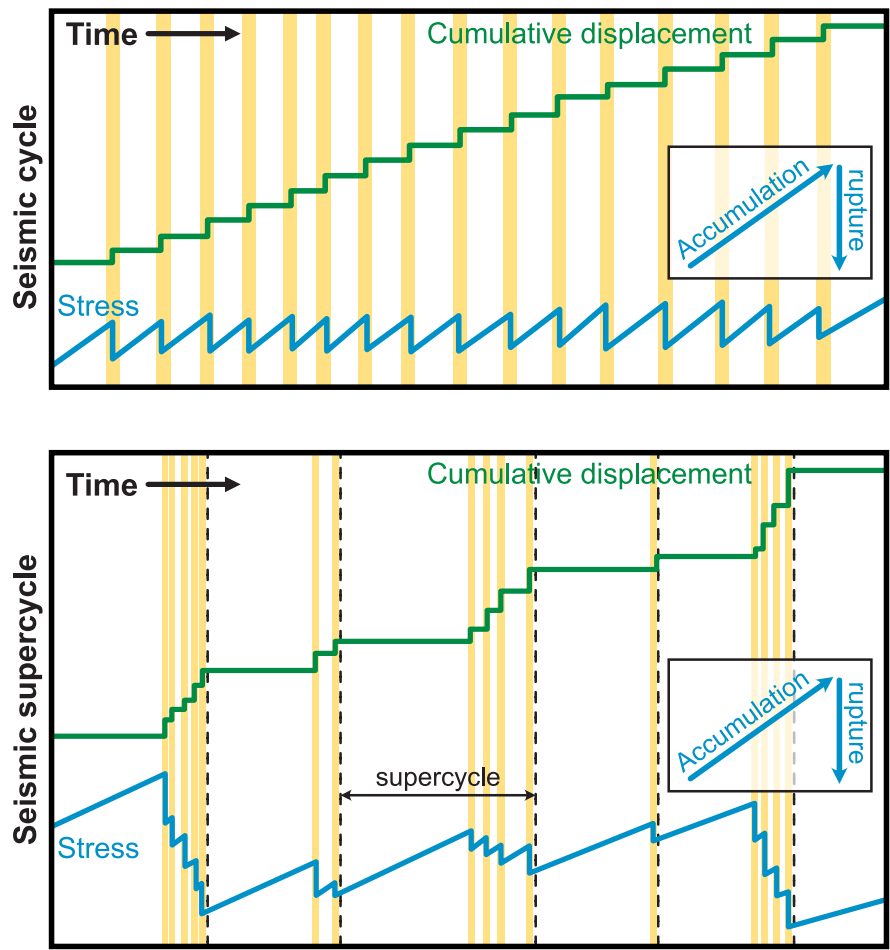
Figure 1.4: Conceptual periodic seismic cycle (top) and clustered supercycle (bottom). Earthquakes are represented by the yellow lines (modified from Salditch et al. (2020)).
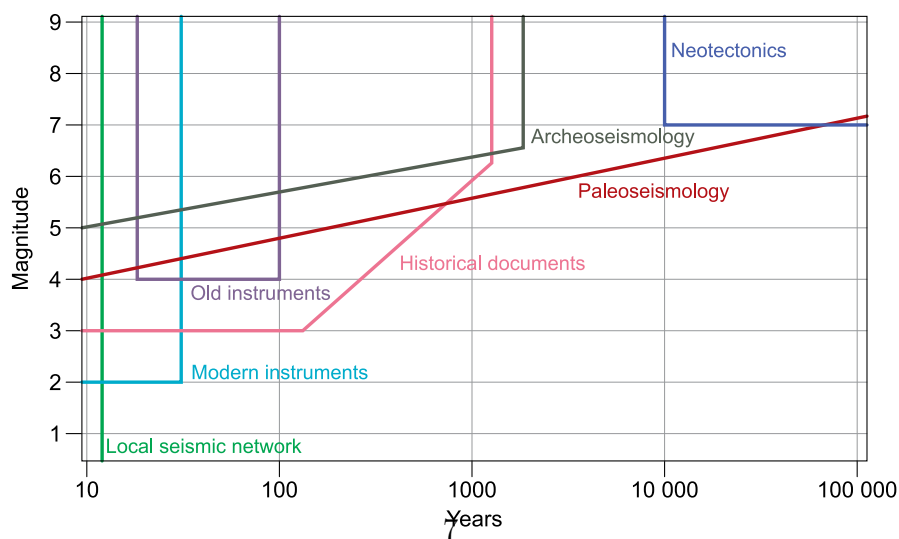
Figure 1.5: Conceptual range of magnitudes and timescales covered by the different disciplines involved in the earthquake studies. (modified from McCalpin (2009)).

Earthquake databases rarely span several centuries, such as in the USA (Stover and Coffman, 1993) or Europe (Grünthal and Wahlström, 2012). Major earthquakes generally have recurrence periods exceeding these catalogues, and coseismic and interseismic phases can compromise interpretations over short periods of time. Offshore paleoseismology can fill these geographical and spatial blanks. This discipline can be applied to almost all the world's oceans, seas, and lakes, providing continuous global coverage for up to several million years (Colman et al., 2003; Kutterolf et al., 2018).

2.2   Principle of the lacustrine records

On-shore investigations can indicate fault movements precisely, but the surveys must be located exactly on the fault lineament (Gastineau, 2022). Additionally, lakes record the climate and natural events (earthquakes, floods, storms, tsunamis, volcanic eruptions) in all the catchment areas. They are, therefore, essential for identifying off-fault seismic events. However, it is important to first differentiate between earthquake-related deposits and those triggered by other natural hazards. All these event deposits are associated with gravity-driven flows, identified by upward-grading (normal grading) beds (Goldfinger, 2011). It is, therefore, essential to characterised event deposits, such as slumps, mass transport deposits (MTD), and turbidites, and identify their source to establish the stratigraphy of the lake (Figure 1.6), which is generally representative of the catchment area (Sabatier et al., 2022).

Event-deposit identification has been used for decades worldwide, as examples in Chile (Wils et al., 2020), in Alaska (Praet et al., 2017), in the Alps (Wilhelm et al., 2017), in East-Africa (Maitituerdi et al., 2022), in Japan (Shiki et al., 2000), in Middle East (Lu et al., 2017), in Cascadia (Morey Ross, 2020). The magnitude, distance of the epicenter to the lake, and bedrock/subtrate type are the control parameters that trigger lake floor destabilisation. In general, a minimum intensity of VI is necessary to trigger turbidites and MTDs (Van Daele et al., 2015). However, lakes act differently, depending on the region, the compaction (Alsop et al., 2016), the sedimentation rate (McHugh et al., 2002), or the pore-water pressure (Blumberg et al., 2008). These parameters can be used to qualitatively assess the sensitivity of lakes to record earthquakes in their sediments.
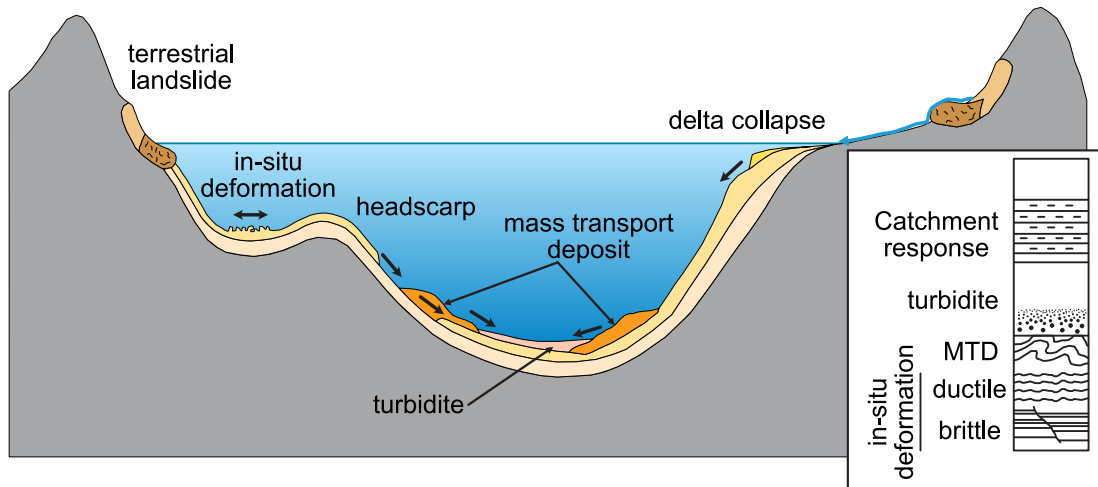
Figure 1.6: Earthquake-related depositional processes and sediment sections associated with the different types of earthquake-related deposits (modified from Sabatier et al. (2022)).

The identification of earthquake-related deposits is based on their spatial and temporal extent. Geophysical mapping of MTDs and turbidites using high-resolution multibeam bathymetric and seismic reflection data is crucial for charactirising the depositional processes on a basin scale. In addition, analysis of seismo-turbidites from multiple sediment cores can help to identify their sedimentary sources and to date individual events. Petrophysical and geochemical analysis allow the understanding of sediment composition and depositional processes.

2.3 Classification of Paleoseismic evidence

Palaeoseismological studies use geological features to determine the intensity or the magnitude of prehistoric earthquakes and their spatio-temporal characteristics. They focus on geomorphic expressions contrasting with the nonseismic deposition and erosion processes (background or climate-control). The classification of paleoseismic evidence is based on location and time (McCalpin, 2009). Evidence of past earthquakes distinguishes all features directly related to certain fault sections (on-fault) from the physical responses of the deformation or the shaking (off-fault).

On-fault evidence encompasses instantaneous (coseismic) geomorphic and stratigraphic expressions like fault scarps, fissures, folds, pressure ridges, and unconformities. It induces delayed responses (postseismic) with, for example, fissure fills and slope instabilities along the fault segments. Off-fault evidence is essentially related to sediment deposition processes and is mostly induced by the shaking rather than by the movement of the fault itself They occur in an extended area surrounding the rupture zone, up to several hundred kilometres, depending on the intensity of the earthquake (even several thousand in the case of tsunamis). Tilted surfaces, uplifted or subsided shorelines, fluid escapes, Mass Transport Deposits (MTD) and turbidites are considered coseismic expressions. Delayed responses include sediment unconformities because of the subsurface deformation, erosion, and change in sedimentation rates.

3 Study sites

Indonesia (Southeast Asia) is located along the active Ring of Fire. The vulnerability of the large and unprepared population inside a high seismic hazard area makes this archipelago one of the highest seismic risk places in the world (Figure 1.2). In 2004, an earthquake with a magnitude of 9.1 occurred in Sumatra, triggering a large tsunami that caused more than 227,000 fatalities.

Indonesia is currently the fourth most populated country. Since the beginning of the 20th century, it has grown from 70 million inhabitants in 1950 to more than 280 million today. However, earthquake research is lacking in this area. The pre-industrial major events are poorly documented. Therefore, the only knowledge of past earthquakes is probably the memories of people. Yet the return periods of major earthquakes can exceed generations, which means that the population is unaware of the seismic risk in regions that have not experienced major earthquakes in the recent past. Indeed, the most destructive earthquakes generally have return periods of hundreds or thousands of years. For example, since the Mw 9.1 Sumatra earthquake, several studies have highlighted the temporality of major seismic events in this area, with a return period of about 200 years (Philibosian

and Meltzner, 2020; Salditch et al., 2020; Sieh et al., 2008). The PGA map of Indonesia (Figure 1.7) highlights the Sunda subduction zone along the Sumatra western shoreline. Nevertheless, a high seismic hazard is also estimated with the PGA on the Island of Sulawesi.
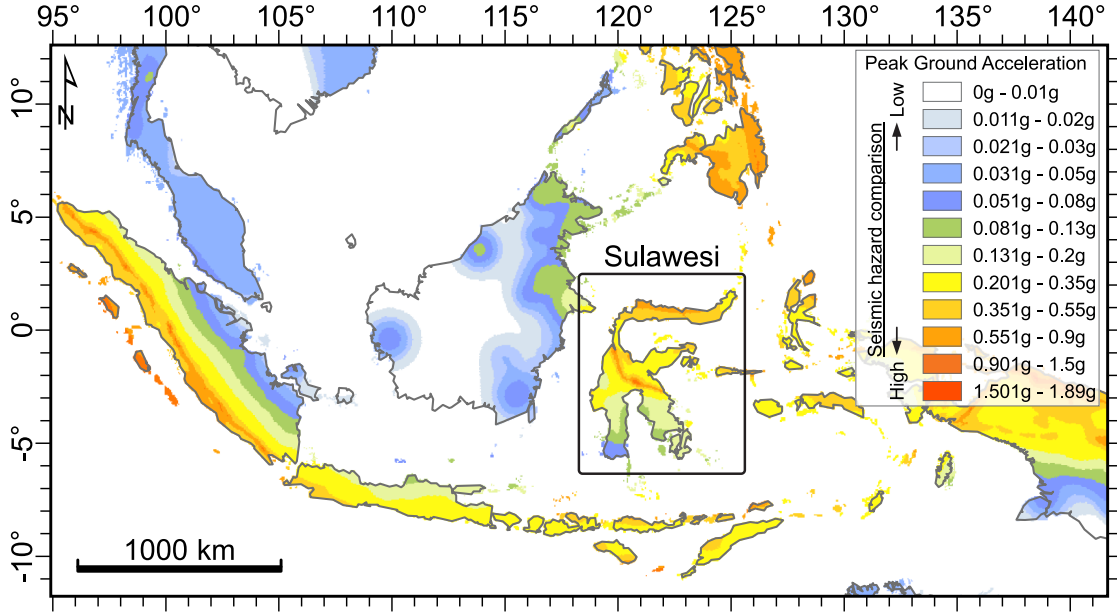
Figure 1.7: Indonesian map showing the distribution of the Peak Ground Acceleration (PGA) with a 10% probability of being exceeded in 50 years (data: Johnson et al. (2023)).

3.1   Sulawesi

The Island of Sulawesi is located at the junction of the Eurasian, Philippine, Pacific and Australian plates (Figure 1.8). Delineated to the north by the North Sulawesi Trench, to the East by the Tolo Thrust and to the west by the Makassar Strait. The particular shape of the island is due to a complex geodynamic history of collisions and rotations of continental blocks and oceanic crust (Hamilton, 1972). The island can be divided into two geological zones. The western arc is composed of a Middle Cretaceous metamorphic basement, overlayed by Tertiary and Quaternary volcanic formations (Katili, 1978). The eastern arc, formed by a Cretaceous subduction complex, is composed of the East Sulawesi Ophiolite formation (Silver et al., 1983b). The stress induced by the North Sulawesi Trench and the Tolo Thrust

is accommodated by the Sulawesi strike-slip fault system, including the Palu-Koro Fault (PKF), the Matano Fault (MF) and the Lawanopo Fault (LF) (Silver et al., 1983a). A west-dipping slab subduction of the eastern Sulawesi block created the western volcanic arc since the early Oligocene and obducted the ophiolite nappe to the east. At the end of the collision, the slab is detached and exhumed by collapse (Villeneuve et al., 2002).

For the Mw 7.5 Palu earthquake in 2018, scientists were able to measure directly on land the rupture (Bao et al., 2019). However, in this tropical setting, a high erosion rate and a dense vegetation cover hamper the study of earthquakes triggered more than a few decades ago. There is also a paucity of historic documentation or archeological evidence of past events. Therefore, lacustrine paleoseismology is a promising approach likely the last discipline to provide more comprehensive insight into the seismic evolution of Sulawesi and recurrence of strong earthquake in the past. Two ancient lakes are located along the Sulawesi fault system: Lake Towuti (southeast of Central Sulawesi) and Lake Poso (Central Sulawesi). These two lakes are promising sites for recording the spatial extent and timing of past earthquakes a spatial and temporal study of the earthquakes recorded in the sediments.

3.2 Lake Towuti

Lake Towuti (2.75° S, 121.5° E) is the largest tectonic lake in Indonesia (Russell and Bijaksana, 2012). With a surface of 552 km^2 and a maximum depth of 203 m water depth, the lake is one of the three interconnected ancient (1 to 4 Ma ago) lakes of the Malili Lake system, with upstream Lake Matano and Lake Mahalona, associated with two satellite lakes, Lontoa and Masapi (Figure 1.9). The location provides a unique site for paleoclimate studies and understanding the Indo-Pacific Warm Pool (IPWP). The geology around Lake Towuti is composed of ultrabasic (ophiolitic) rocks releasing high concentrations of iron, nickel and chromium into the lake (Morlock, 2018). The Malili Lake system is delineated by strike-slip faults to the north by the Matano Fault and to the south by the Lawanopo Fault (Watkinson and Hall, 2017).
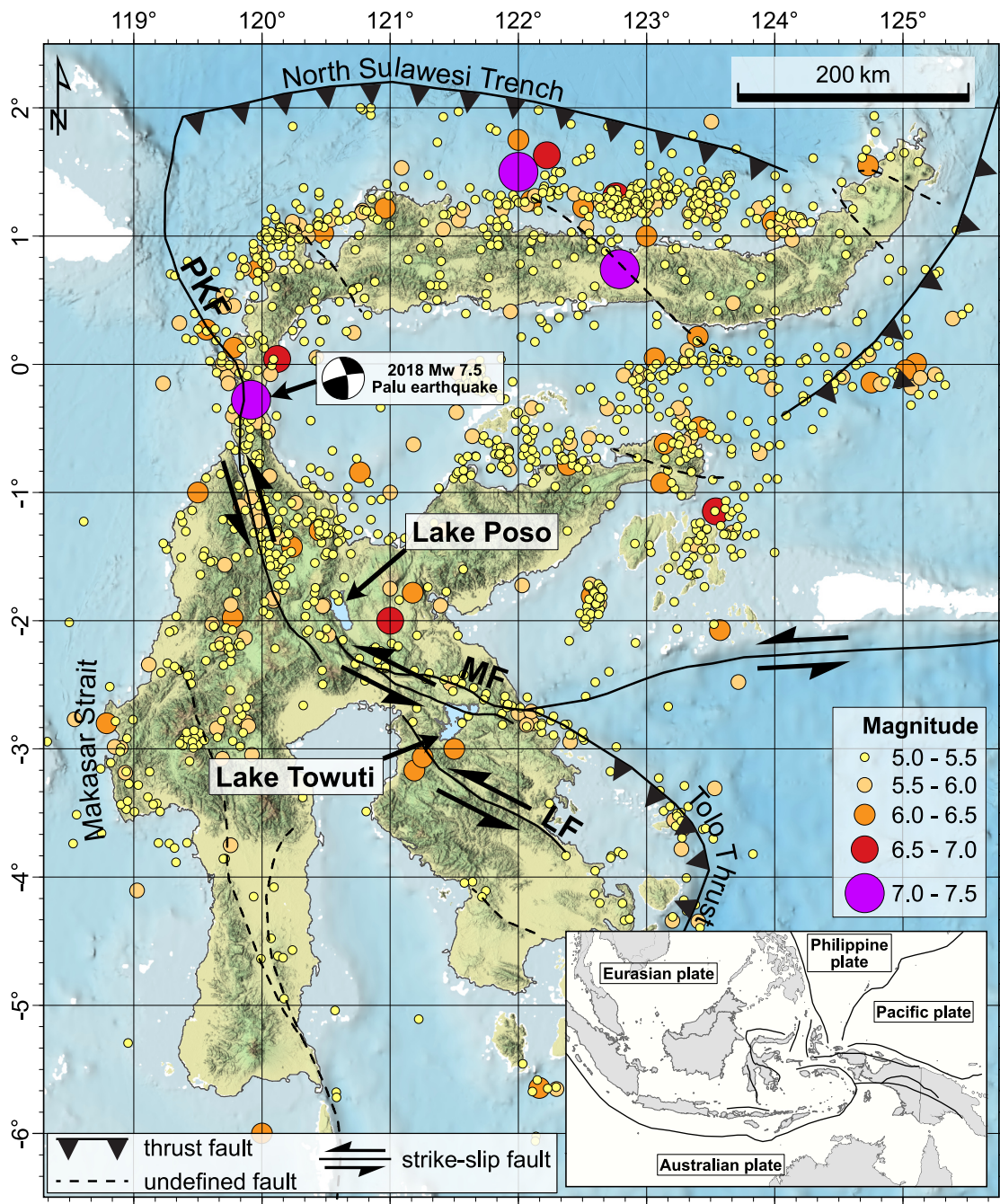
Figure 1.8: Tectonic map of the Island of Sulawesi, representing the earthquakes recorded from 1960 to 2024, with a magnitude ≥ 5 and depth ≤ 40 km (source: ISC bulletin catalogue: http://www.isc.ac.uk/iscbulletin/search/catalogue/. PKF: Palu-Koro Fault, MF: Matano Fault, LF: Lawanopo Fault)

Between 2007 and 2013, three surveys of seismic reflection data (CHIRP, airgun multi-channel and airgun single-channel), totalling more than 1000 km of lines, were collected at Lake Towuti. In addition, 12 sediment piston cores have been sampled, covering the upper 10 - 20 m of sediment in various parts of the lake (Russell and Bijaksana, 2012). This preliminary phase of the Towuti Drilling Project (TDP) illustrated the potential for paleoclimate records of the lake. In 2015, the TDP recovered 1000 m of sediment cores from three sites and reached bedrock at more than 160 metres below the lake floor (mblf). The ages calculated on these boreholes estimate the formation of the permanent Lake Towuti to be $\sim$ 1 Ma old (Russell et al., 2020).
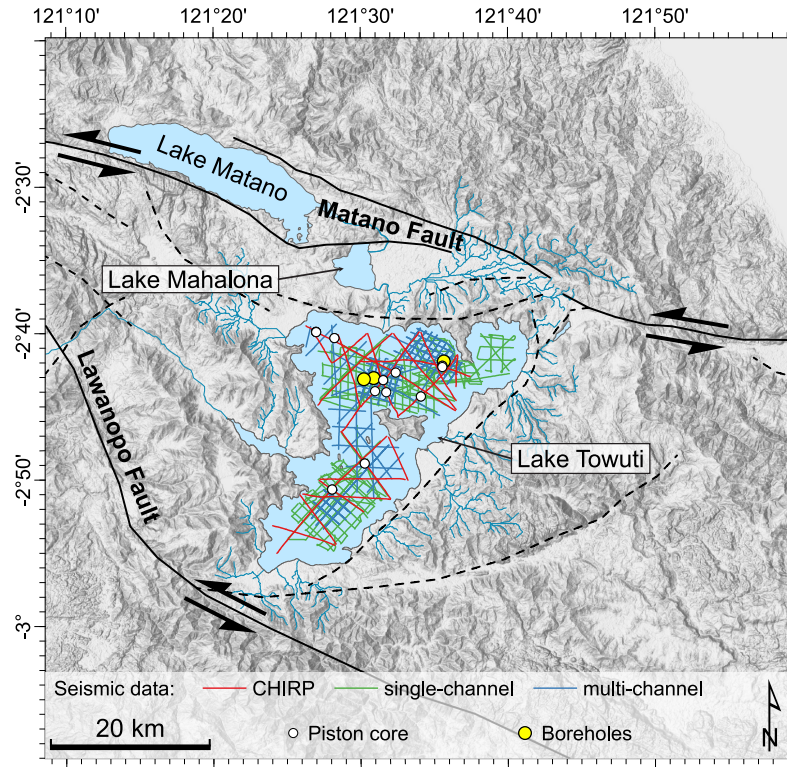
Figure 1.9: Morphological map of the Malili Lake system and the data collected on Lake Towuti for the Towuti Drilling Project. The plain lines are faults included in the Sulawesi strike-slip fault system, and the dashed lines represent the undefined secondary faults.

14

3.3 Lake Poso

Lake Poso (1°54'49.0" S, 120°36'40.5" E) is located in central Sulawesi at 485 meters above sea level (masl), 30 km to the north of the PKF. Its formation initiated ∼ 2 Myr ago (Monnier et al., 1995) and resulted in a succession of extensions and retrogressions of a half-graben, open to the sea and the Gulf of Tomini until the Pleistocene (Hamilton, 1972).
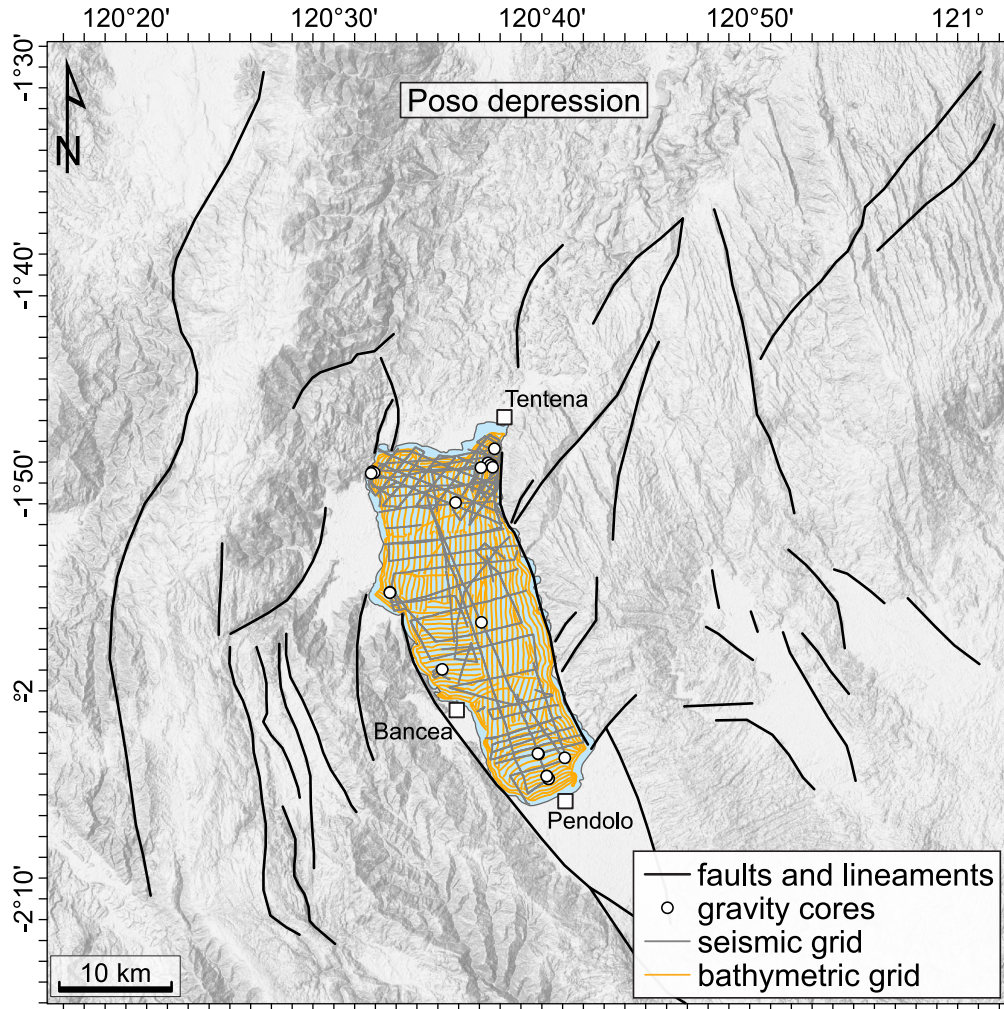
Figure 1.10: Morphological map of the surroundings of Lake Poso with the gravity core locations, the seismic and the bathymetric grids. The faults and other lineaments are reported from Watkinson and Hall (2017).

15

Field work of the Poso Project started in November 2022. After complex logistics for sending the material to Indonesia and to Lake Poso, a bathymetric survey was conducted for the first time on the island of Sulawesi. In total, ~ 950 km of track lines were surveyed in 17 days. The preliminary results were used to plan the seismic survey. About 576 km of seismic reflection profiles were recorded to image ~ 40 m subsurface sediment of the lake. In addition, 23 short cores were sampled with an ETH-style gravity corer. The locations were selected based on the bathymetry and the seismic profiles.
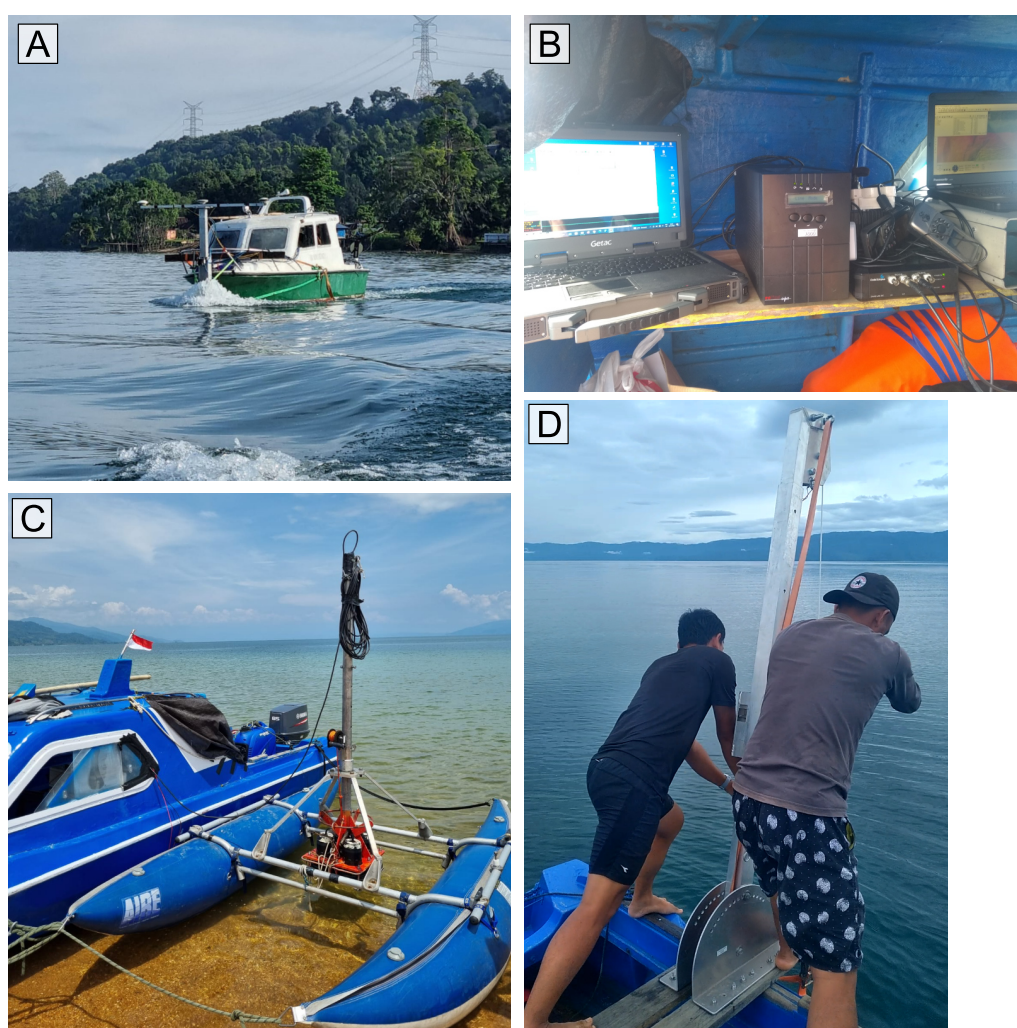
Figure 1.11: Images of the (A) bathymetric acquisition, (B and C) seismic acquisition, and (D) coring during the field mission on Lake Poso in 2022.

4 Outline of this thesis

There is a significant disparity in the study sites, with much more research conducted in the northern hemisphere than in the southern hemisphere. On the island of Sulawesi, the earthquakes recorded by instrumental instruments are located mainly along the northern section of the PKF. High-magnitude earthquakes can likely occur in central Sulawesi and along the Matano Fault, for example, with the 2011 Mw 6.1 earthquake to the north of Lake Matano (Watkinson and Hall, 2017). The distribution of the PGA in Indonesia also indicates a high seismic hazard in this area (Figure 1.7. Without historical documents on past earthquakes, paleoseismology is the best discipline to improve earthquake records and estimate the return periods of devastating earthquakes.

The initial phase of this study was to analyse how tropical lakes react to earthquakes and climate change. It is important to differentiate between various processes and the response of the lake environment in terms of sedimentation or water level. All these parameters determine the sensitivity of a lake to record natural hazards.

- Chapter 2 of this thesis identifies the evolution of the sensitivity of Lake Towuti by comparing climatic fluctuation with the record of event deposits. This study site was ideal for this initial phase because a large amount of data is already available from the Towuti Drilling Project, which focused on the palaeo-environmental and palaeo-climatic studies of the lake. This chapter uses seismic reflection correlated with piston cores to conduct a high-resolution study of the past 40 kyr.

- Chapter 3 is a preliminary stage in the continuity of Chapter 2. After identifying the sensitivity of Lake Towuti over the last 40 kyr, a correlation between borehole data and single-channel seismic reflection is carried out to estimate the return period of turbidites over 1 Ma. In addition, a detailed seismic stratigraphy between the different basins of the lake will highlight the geomorphological evolution of Lake Towuti.

- Chapter 4 is the first paleoseismological study on Lake Poso. The data

collected at the lake in 2022 show the considerable potential of this site for paleoseismological studies. This pioneering project in Sulawesi will provide an overview of past seismological evidence using bathymetric and seismic acquisition data.

5 References

Alsop, G., Marco, S., Weinberger, R., and Levi, T. (2016). Sedimentary and structural controls on seismogenic slumping within mass transport deposits from the Dead Sea Basin. *Sedimentary Geology*, 344:71–90.

Bao, H., Ampuero, J.-P., Meng, L., Fielding, E. J., Liang, C., Milliner, C. W. D., Feng, T., and Huang, H. (2019). Early and persistent supershear rupture of the 2018 magnitude 7.5 Palu earthquake. *Nature Geoscience*, 12(3):200–205.

Blumberg, S., Lamy, F., Arz, H., Echtler, H., Wiedicke, M., Haug, G., and Oncken, O. (2008). Turbiditic trench deposits at the South-Chilean active margin: A Pleistocene–Holocene record of climate and tectonics. *Earth and Planetary Science Letters*, 268(3-4):526–539.

Colman, S., Karabanov, E., and Nelson, C. (2003). Quaternary Sedimentation and Subsidence History of Lake Baikal, Siberia, Based on Seismic Stratigraphy and Coring. *Journal of Sedimentary Research*, 73(6):941–956.

Crétaux, J.-F., Soudarin, L., Cazenave, A., and Bouillé, F. (1998). Present-day tectonic plate motions and crustal deformations from the DORIS space system. *Journal of Geophysical Research*, 103(B12):30167 – 30181.

Freire, S. and Aubrecht, C. (2012). Integrating population dynamics into mapping human exposure to seismic hazard. *Natural Hazards and Earth System Sciences*, 12(11):3533–3543.

Gastineau, R. (2022). *Paléosismologie lacustre et géophysique appliquées au lac d'Iznik (Turquie): contribution à l'étude de la branche médiane de la Faille Nord-Anatolienne.* PhD Thesis, Université Grenoble Alpes, Grenoble.

Ghosh, D., Deb, A., and Sengupta, R. (2009). Anomalous radon emission as precursor of earthquake. *Journal of Applied Geophysics*, 69(2):67–81.

Goldfinger, C. (2011). Submarine Paleoseismology Based on Turbidite Records. *Annual Review of Marine Science*, 3(1):35–66.

Grünthal, G. and Wahlström, R. (2012). The European-Mediterranean Earthquake Catalogue (EMEC) for the last millennium. *Journal of Seismology*, 16(3):535–570.

Gutenberg, B. and Richter, C. F. (1942). Earthquake magnitude, intensity, energy, and acceleration. *Bulletin of the Seismological Society of America*, 32(3):163–191.

Gutenberg, B. and Richter, C. F. (1949). *Seismicity of the Earth and associated phenomena*. Princeton University Press, Princeton, New Jersey.

Hamilton, W. B. (1972). Tectonics of the Indonesian Region. Report 72-1978. Edition: -.

Jalil, A., Fathani, T. F., Satyarno, I., and Wilopo, W. (2021). Liquefaction in Palu: the cause of massive mudflows. *Geoenvironmental Disasters*, 8(1):21.

Johnson, K., Villani, M., Bayliss, K., Brooks, C., Chandrasekhar, S., Chartier, T., Chen, Y.-S., Garcia-Pelaez, J., Gee, R., Styron, R., Rood, A., Simionato, M., and Pagani, M. (2023). Global Seismic Hazard Map.

Kagan, Y. Y. and Knopoff, L. (1987). Statistical Short-Term Earthquake Prediction. *Science*, 236(4808):1563–1567. Publisher: American Association for the Advancement of Science.

Katili, J. A. (1978). Past and present geotectonic position of Sulawesi, Indonesia. *Tectonophysics*, 45(4):289–322.

Kearey, P., Vine, F., and Klepeis, K. (2009). *Global tectonics*. Wiley-Blackwell, Oxford, 3rd edition.

Koizumi, N. (2013). Earthquake prediction research based on observation of groundwater. *Synthesiology*, 6(1):24–33.

Kutterolf, S., Schindlbeck, J. C., Robertson, A. H. F., Avery, A., Baxter, A. T., Petronotis, K., and Wang, K.-L. (2018). Tephrostratigraphy and Provenance From IODP Expedition 352, Izu-Bonin Arc: Tracing Tephra Sources and Volumes From the Oligocene to Recent. *Geochemistry, Geophysics, Geosystems*, 19(1):150–174. Publisher: John Wiley & Sons, Ltd.

Lu, Y., Waldmann, N., Ian Alsop, G., and Marco, S. (2017). Interpreting Soft Sediment Deformation and Mass Transport Deposits as Seismites in the Dead Sea Depocenter: Disturbances in the Dead Sea depocenter. *Journal of Geophysical Research: Solid Earth*, 122(10):8305–8325.

Maitituerdi, A., Van Daele, M., Verschuren, D., De Batist, M., and Waldmann, N. (2022). Depositional history of Lake Chala (Mt. Kilimanjaro, equatorial East Africa) from high-resolution seismic stratigraphy. *Journal of African Earth Sciences*, page 104499.

McCalpin, J., editor (2009). *Paleoseismology*. Number v. 95 in International geophysics series. Academic Press, Burlington, MA, 2nd ed edition. OCLC: ocn318100432.

McHugh, C. M., Damuth, J. E., and Mountain, G. S. (2002). Cenozoic mass-transport facies and their correlation with relative sea-level change, New Jersey continental margin. *Marine Geology*, 184(3-4):295–334.

Midorikawa, S. (1993). Semi-empirical estimation of peak ground acceleration from large earthquakes. *New horizons in strong motion: Seismic studies and engineering practice*, 218(1):287–295.

Monnier, C., Girardeau, J., Maury, R. C., and Cotten, J. (1995). Back-arc basin origin for the East Sulawesi ophiolite (eastern Indonesia). *Geology*, 23(9):851.

Morey Ross, A. E. (2020). *Investigations into the Paleoseismic Potential of Small, Shouthern Cascadia Lakes.* PhD Thesis, Oregon State University, US.

Morlock, M. (2018). *Depositional modes and post-depositional mineral formation in a Pleistocene sediment record from Lake Towuti, Indonesia.* PhD Thesis, Universität Bern, Bern.

Philibosian, B. and Meltzner, A. J. (2020). Segmentation and supercycles: A catalog of earthquake rupture patterns from the Sumatran Sunda Megathrust and other well-studied faults worldwide. *Quaternary Science Reviews*, 241:106390.

Praet, N., Moernaut, J., Van Daele, M., Boes, E., Haeussler, P. J., Strupler, M., Schmidt, S., Loso, M. G., and De Batist, M. (2017). Paleoseismic potential of sublacustrine landslide records in a high-seismicity setting (south-central Alaska). *Marine Geology*, 384:103–119.

Reid, H. (1910). *The mechanics of the earthquake*, volume II of *The Cafifornia Earthquake of April 18, 1906, Report of the State Earthquake Investigation Commission.* Washington, D.C., carnegie institution of washington edition.

Robert, C. and Bousquet, R. (2013). *Géosciences - La dynamique du système Terre.* Belin edition.

Russell, J. M. and Bijaksana, S. (2012). The Towuti Drilling Project:

Paleoenvironments, Biological Evolution, and Geomicrobiology of a Tropical Pacific Lake. *Scientific Drilling*, 14:68–71.

Russell, J. M., Vogel, H., Bijaksana, S., Melles, M., Deino, A., Hafidz, A., Haffner, D., Hasberg, A. K., Morlock, M., von Rintelen, T., Sheppard, R., Stelbrink, B., and Stevenson, J. (2020). The late quaternary tectonic, biogeochemical, and environmental evolution of ferruginous Lake Towuti, Indonesia. *Palaeogeography, Palaeoclimatology, Palaeoecology*, page 109905.

Sabatier, P., Moernaut, J., Bertrand, S., Van Daele, M., Kremer, K., Chaumillon, E., and Arnaud, F. (2022). A Review of Event Deposits in Lake Sediments. *Quaternary*, 5(3):34.

Salditch, L., Stein, S., Neely, J., Spencer, B. D., Brooks, E. M., Agnon, A., and Liu, M. (2020). Earthquake supercycles and Long-Term Fault Memory. *Tectonophysics*, 774:228289.

Shiki, T., Kumon, F., Inouchi, Y., Kontani, Y., Sakamoto, T., Tateishi, M., Matsubara, H., and Fukuyama, K. (2000). Sedimentary features of the seismo-turbidites, Lake Biwa, Japan. *Sedimentary Geology*, 135(1-4):37–50.

Shimazaki, K. and Nakata, T. (1980). Time-predictable recurrence model for large earthquakes. *Geophysical Research Letters*, 7(4):279–282.

Sieh, K., Natawidjaja, D. H., Meltzner, A. J., Shen, C.-C., Cheng, H., Li, K.-S., Suwargadi, B. W., Galetzka, J., Philibosian, B., and Edwards, R. L. (2008). Earthquake Supercycles Inferred from Sea-Level Changes Recorded in the Corals of West Sumatra. *Science*, 322(5908):1674–1678.

Silva, V., Amo-Oduro, D., Calderon, A., Costa, C., Dabbeek, J., Despotaki, V., Martins, L., Pagani, M., Rao, A., Simionato, M., Viganò, D., Yepes-Estrada, C., Acevedo, A., Crowley, H., Horspool, N., Jaiswal, K., Journeay, M., and Pittore, M. (2020). Development of a global seismic risk model. *Earthquake Spectra*, 36(1_suppl):372–394. Publisher: SAGE Publications Ltd STM.

Silver, E. A., McCaffrey, R., Joyodiwiryo, Y., and Stevens, S. (1983a). Ophiolite emplacement by collision between the Sula Platform and the Sulawesi Island Arc, Indonesia. *Journal of Geophysical Research: Solid Earth*, 88(B11):9419–9435. Publisher: John Wiley & Sons, Ltd.

Silver, E. A., McCaffrey, R., and Smith, R. B. (1983b). Collision, rotation, and the initiation of subduction in the evolution of Sulawesi, Indonesia. *Journal of*

Geophysical Research: Solid Earth, 88(B11):9407–9418.

Stover, C. W. and Coffman, J. (1993). Seismicity of the United States, 1568-1989 (revised). Report 1527. Edition: -.

Trifunac, M. D. and Brady, A. G. (1975). On the correlation of seismic intensity scales with the peaks of recorded strong ground motion. *Bulletin of the Seismological Society of America*, 65(1):139–162.

Van Daele, M., Moernaut, J., Doom, L., Boes, E., Fontijn, K., Heirman, K., Vandoorne, W., Hebbeln, D., Pino, M., Urrutia, R., Brümmer, R., and De Batist, M. (2015). A comparison of the sedimentary records of the 1960 and 2010 great Chilean earthquakes in 17 lakes: Implications for quantitative lacustrine palaeoseismology. *Sedimentology*, 62(5):1466–1496.

Villeneuve, M., Gunawan, W., Cornee, J.-J., and Vidal, O. (2002). Geology of the central Sulawesi belt (eastern Indonesia): constraints for geodynamic models. *International Journal of Earth Sciences*, 91(3):524–537.

Wallace, R. E. (1987). Grouping and migration of surface faulting and variations in slip rates on faults in the Great Basin province. *Bulletin of the Seismological Society of America*, 77(3):868–876.

Wallemacq, P., Below, R., and McLean, D. (2018). UNISDR and CRED report: Economic Losses, Poverty & Disasters (1998 - 2017). Technical report, Centre for Research on the Epidemiology of Disasters.

Watkinson, I. M. and Hall, R. (2017). Fault systems of the eastern Indonesian triple junction: evaluation of Quaternary activity and implications for seismic hazards. *Geological Society, London, Special Publications*, 441(1):71–120.

Wilhelm, B., Vogel, H., and Anselmetti, F. S. (2017). A multi-centennial record of past floods and earthquakes in Valle d'Aosta, Mediterranean Italian Alps. *Natural Hazards and Earth System Sciences*, 17(5):613–625.

Wils, K., Van Daele, M., Kissel, C., Moernaut, J., Schmidt, S., Siani, G., and Lastras, G. (2020). Seismo-Turbidites in Aysén Fjord (Southern Chile) Reveal a Complex Pattern of Rupture Modes Along the 1960 Megathrust Earthquake Segment. *Journal of Geophysical Research: Solid Earth*, 125(9):e2020JB019405. Publisher: John Wiley & Sons, Ltd.

Chapter 2

Climate-controlled sensitivity of lake sediments to record earthquake-related mass wasting in tropical Lake Towuti during the past 40 kyr

Aerial picture of Lake Towuti (photo: indonesia-tourism).

Climate-controlled sensitivity of lake sediments to record earthquake-related mass wasting in tropical Lake Towuti during the past 40 kyr

Tournier, N.[1], Fabbri, S.C.[1,2], Anselmetti, F.S.[1], Cahyarini, S.Y.[3], Bijaksana, S.[4], Wattrus, N.[5], Russell, J.M.[6], Vogel, H.[1]

[1]Institute of Geological Sciences & Oeschger Centre of Climate Change Research, University of Bern, Baltzerstr. 1+3, 3012, Bern, Switzerland

[2]Edytem, Université Savoie Mont-Blanc, CNRS, 5, bd de la Mer Caspienne, Le Bourget-du-Lac, France

[3]Research Centre for Climate and Atmosphere, National Research and Innovation Agency (BRIN), Indonesia

[4]Faculty of Mining and Petroleum Engineering, Institut Teknologi Bandung, 15 Bandung, 40132, Indonesia

[5]Large Lakes Observatory & Dept. of Earth and Environmental Sciences, University of Minnesota Duluth, Duluth, MN, 55812, USA

[6]Department of Earth, Environmental, And Planetary Sciences, Brown University, Box 1846, Providence, RI, 02912, USA

Climate-controlled sensitivity of lake sediments to record earthquake-related mass wasting in tropical Lake Towuti during the past 40 kyr

Abstract

Located at the triple junction of the Pacific, Eurasian and Sunda plates, the Island of Sulawesi in Indonesia is one of the most tectonically active places on Earth. This is highlighted by the recurrence of devastating earthquakes such as the 2018 Mw 7.5 earthquake that damaged the city of Palu and caused several thousand fatalities in central Sulawesi. The majority of large-magnitude earthquakes on Sulawesi are related to stress release along major strike-slip faults such as the Palu-Koro Fault and its southern extensions, the Matano and Lawanopo Faults. To date, information on the frequency and magnitude of past major events on these faults is limited to instrumental records and historical sources restricted to the last century, whereas information from natural archives is completely lacking. Lake-sediment records can fill this gap, but a detailed assessment of the various factors that influence the sensitivity of sediment successions to past earthquakes is required to evaluate their suitability. Lake Towuti, situated in Eastern Sulawesi, is known for its paleoclimate record and also promises to be a key site to generate a paleoseismology record for Sulawesi. The lake lies close to the highly active Matano and Lawanopo strike-slip faults and thereby is an ideal archive for past earthquakes that have occurred in the surrounding area. Here we combine high-resolution chirp seismic data with lithostratigraphic and petrophysical data of sediment piston cores to assess the recurrence of seismically generated mass-transport and turbidite deposits. Three major seismic-stratigraphic units are distinguished in the upper ~10 m of the sediment succession and linked to differences in the frequency of mass-wasting during the past 60 kyrs. The evidence of a more turbidite-prone period between 12 and 40 ka is roughly coincident with a dry phase and associated lake-level lowstand during the last glacial period at Lake Towuti. Hence, we suggest that climate strongly influences the sensitivity of slopes to fail during seismic shaking in this tropical setting as a consequence of lowstand-forced sediment redeposition from the shelves onto the slopes and into the basins. As climate significantly impacts the sensitivity of the lacustrine sediments to record earthquake-related mass wasting deposits, we suggest that the frequency of mass-transport deposits can additionally be employed as a quantitative indicator for past changes in hydroclimate in these tropical settings.

1 Introduction

When the crustal deformation rate of a region is low, or when the release of fault energy through small earthquakes is frequent, there is a necessity to observe major seismic events over long time periods to successfully reveal their recurrence pattern (Lafuente et al., 2014; Moernaut et al., 2014). This relates to the extended recurrence period of strong earthquakes that is often longer than the time covered by both instrumental and historical records (Kremer et al., 2017). To identify periods and regions with moreactive seismic activity and to evaluate fault activity and evolution, it is therefore necessary to extend our knowledge of the temporal and spatial distribution of seismic events.

The Island of Sulawesi, in Eastern Indonesia, is located on the 'Ring of Fire' that encircles the entire Pacific Ocean. Consequently, it is subject to frequent and severe earthquakes (Bellier et al., 2001). In 2018, a magnitude 7.5 earthquake in Palu (Bao et al., 2019; Omira et al., 2019; Wu et al., 2021) caused several thousand fatalities and massive material damage. The earthquake-induced damage was further enhanced by an associated tsunami heavily affecting the shorelines along the Gulf of Palu. Seismic events of this magnitude are regarded as exceptional in the region, though, based on the documented and recorded 13 moment magnitude (Mw) 7+ earthquakes since 1924, they occur on average every decade on the Island of Sulawesi. Less powerful earthquakes strike more frequently. About one Mw 6.0 to 6.9 earthquake occurs every year and Mw 5.0 to 5.9 earthquakes occur nine times per year on average (depths <35 km), as documented in the Sulawesi earthquake catalogue (1924 – 2022) of the International Seismological Center (ISC) (Willemann and Storchak, 2001). The Island of Sulawesi is segmented by three major strike-slip faults (Fig. 2.1): the Palu-Koro (PKF), the Matano (MF) and the Lawanopo (LF) Faults. These faults cut across the island from NW to SE and define a major transform zone between the eastern and the western parts of the island (Fig. 2.1A), between the North Sulawesi Trench and the Tolo thrust (Silver et al., 1983). The entire Island of Sulawesi is split into multiple rotating tectonic microblocks, which accommodate the entire collision of the area by crustal rotation rather than by orogenesis. While the south-eastern part of Sulawesi rotates anticlockwise, the north-eastern part rotates clockwise (Socquet et al., 2006). Most of the earthquakes, and particularly the shallow large magnitude ones, typically have their epicenters along the three crustal faults PKF, MF and LF. Therefore, stress is generally transferred via left-lateral movement along those faults, accompanied by a rotation of various tectonic microblocks (Socquet et al., 2006; Villeneuve et al., 2002),

rather than by crustal shortening. Earthquakes are also concentrated along the North Sulawesi subduction zone (Fig. 2.1).
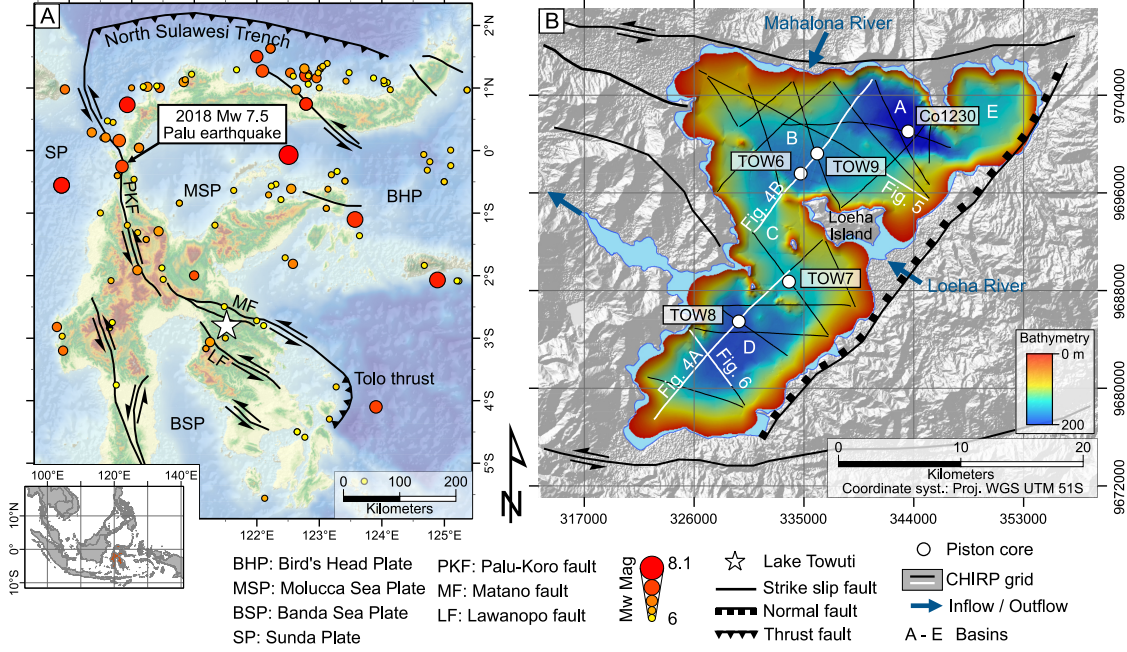
Figure 2.1: (A) Seismo-tectonic map of the Island of Sulawesi. Earthquakes from 1924 to 2022 are displayed, with a Mw magnitude ≥ 6 and a depth ≤ 35 km. (B) Bathymetric map of Lake Towuti with the high-resolution CHIRP seismic grid and the location of the piston cores.

The oldest earthquakes on Sulawesi recorded by the United States Geological Survey (USGS) and the ISC date back to the early 1900s. To date, only few paleoseismological studies are available to extend the earthquake catalogue beyond instrumental and historical records (Irsyam et al., 2020; Natawidjaja et al., 2020). However, the expansion of our knowledge of the region's seismic event history is vital to improve our understanding of the seismic and tsunamigenic hazard in the region (i.g. Daryono et al. (2021); Watkinson and Hall (2017); Wils et al. (2021b)). Given the severity of the few instrumentally recorded earthquakes and the population increase in city centres and agglomeration areas, better estimates on the earthquake cycle (e.g. recurrence period and pattern) are essential. The September 2018 Mw 7.5 earthquake in Palu has recently generated considerable attention to the hazard potential of the PKF while such awareness is currently absent for other areas of Sulawesi. For example, the south-eastern part of

Sulawesi remains poorly studied despite the presence of the similarly active MF and LF. Historical events call for the generation of a paleorecord of similar events, which will allow better estimates of recurrences and magnitudes and, consequently, better adaptation to these natural hazards through mitigation measures (building stability, education, etc.).

Lake Towuti represents the ideal site to generate a long regional paleoseismic record. It has a continuous >1 Myr sedimentary record (Russell et al., 2020b), large surface area-to-depth ratio with gently inclined slopes Morlock et al. (2019); Vogel et al. (2015) necessary for off-fault recording of seismic shaking (e.g. turbidites, mass movements), a large number of available drill and piston core records (Russell et al., 2020b,1; Vogel et al., 2015), and a dense grid of seismic reflection data (Russell et al., 2016). Tectonically, the Towuti basin formed by fault movement of the MF (an eastward extension of the PKF) and its conjugated fault structures, making it possible to directly analyse the creation of tectonically-controlled sediment accommodation space on local and regional scales. However, the lake and its catchment also experienced considerable changes in climate, lake level and land cover over its ~1 Myr history (Russell et al., 2020b), making it essential to understand how these environmental processes might interact with tectonic changes to influence the lake's paleoseismic record.

The sedimentary fill of lakes represents a continuous timeline over thousands of years, very sensitive to climatic (Ariztegui et al., 2001; Guyard et al., 2007), seismic (Avşar et al., 2015; Chapron, 1999; Howarth et al., 2014,2; Oswald et al., 2021; Schwestermann et al., 2020; Strasser et al., 2013; Talling, 2021) and volcanic (Chassiot et al., 2016; Shinohara et al., 2015) processes. Lakes constitute an essential archive for the study of geological events and processes and are among the very few continental depositional environments that continuously record changes over geological time-scales. Most long-lived lakes form in volcanic (Moernaut et al., 2010; Wils et al., 2021a), impact Melles et al. (2012); Shanahan et al. (2006) or tectonically active areas involving either extensional (e.g. East African, Russell et al. (2020a)), collisional (subduction zones in Chile, Alaska, Japan, Chapron et al. (2006); Inouchi et al. (1996); Kempf et al. (2020); Moernaut et al. (2014); Praet et al. (2017), transtensional regimes (Gastineau et al., 2021; Hage et al., 2017; Hubert-Ferrari et al., 2020) or a combination thereof (e.g. Japan and Indonesia, Shiki et al. (2000); Watkinson and Hall (2017)), creating and sustaining accommodation space over time, and hence making them invaluable paleoseismology archives. Therefore, lakes are ideal sites to provide a better understanding on earthquake recurrence patterns, fault behaviour and seismic hazard assessment.

Several criteria have to be met for a lacustrine setting to serve as an ideal archive of past earthquake events. Most importantly, factors such as sedimentation rate and earthquake intensity are critical (Wilhelm et al., 2016a). Generally, low sedimentation rates cause a slow charging of subaqueous slopes with fresh sediments, and therefore the probability to record earthquake-induced subaqueous mass movements may be low, leading to a less sensitive setting (Moernaut, 2020). On the other hand, sites characterized by lower sedimentation rate offer more easily accessible long-term records through sediment coring. Slope inclination is also a significant factor in the susceptibility of lakes to experience sediment failures (Pohl et al., 2020). A steeper slope increases the gravitational stress relative to the strength and stability of the sediments. However, a gentle inclined slope can also generate mass movements and soft sediment deformations (Avşar et al., 2016; Molenaar et al., 2021), especially following an earthquake (Field et al., 1982). During seismic shaking, liquefaction can destabilize the sediments either on land, as documented by the devastating landslide triggered by the 2018 Palu earthquake (Tohari et al., 2021; Watkinson and Hall, 2019), or within water filled basins (Boncio et al., 2020). Several studies indicate an intensity of $> VI$ is necessary to trigger mass transport deposits (MTDs) and the formation of turbidites, and minimum VII1/2 for the development of massive slope failures and megaturbidites (Moernaut et al., 2007; Van Daele et al., 2015; Vanneste et al., 2018). Systematic turbidite-paleoseismological approaches have been successful in several regions that meet these criteria, like in Cascadia (Goldfinger, 2011; Leithold et al., 2019,1), New-Zealand (Howarth et al., 2014,2), Mediterranean (Badhani et al., 2020; Ratzov et al., 2015), Southwest Iberian margin (Collico et al., 2020; Gràcia et al., 2010), Alaska (Praet et al., 2017,2), European Alps (Chapron et al., 2016; Daxer et al., 2022; Kremer et al., 2015; Schnellmann et al., 2005; Strasser et al., 2020) and Chile (Chapron et al., 2006; Moernaut et al., 2018; Völker et al., 2012; Wils et al., 2020) as well as in other regions (Inouchi et al., 1996; Nayak et al., 2021).

A connection between water-level fluctuations and MTDs has already been proposed for different settings (ten Brink et al., 2016), such as in Patagonia (Anselmetti et al., 2009), East Africa (Moernaut et al., 2010), New Jersey continental margin (McHugh et al., 2002), and the Dead Sea (Waldmann et al., 2009), the latter of which has a tectonic strike-slip fault context similar to that of Lake Towuti (Bartov and Sagy, 2004). For the Dead Sea, a link between climate-controlled lake-level fluctuations (Bartov et al., 2002; Bookman et al., 2006; Goldstein et al., 2020) and the occurrence of submarine mass failures has been documented (Belferman et al., 2018; Closson et al., 2010; Dente et al., 2021; Lu et al., 2021b). Lowstands from 35 ka to 15 ka, may have caused slope erosion and decreased

the stability of the emerged areas around the lake (Lu et al., 2021a).

This study forms part of the International Continental Scientific Drilling Program (ICDP) co-funded Towuti Drilling Project (TDP, Russell et al. (2016,2)). Previous and ongoing investigations on piston cores from site surveys and cores from scientific drilling document that Lake Towuti is highly sensitive to record past changes in hydroclimate. Evidence from various sedimentological and geochemical indicators suggests the region has experienced substantial drying during the last glacial between ∼29 and 16 kyr BP, roughly coincident with marine isotope stage (MIS) 2 and broadly consistent with other reconstructions from the region (De Deckker et al., 2003; Konecky et al., 2016; Krause et al., 2019; Ma et al., 2022; Partin et al., 2007; Reeves et al., 2013; Windler et al., 2020). Drying during the last glacial led to lake-level lowstands with basinward progradation of major deltas (Morlock et al., 2019; Vogel et al., 2015), opening of the local forest vegetation (Hamilton et al., 2019; Russell et al., 2014; Wicaksono et al., 2017), reduced terrestrial runoff (Morlock et al., 2019,2; Russell et al., 2020b,1) and deep mixing and oxygenation of the water column (Costa et al., 2015; Tamuntuan et al., 2015). These climatically driven environmental and depositional changes are likely to influence the sensitivity of Lake Towuti and, more broadly similar tropical sites, to record past earthquakes. Lake Towuti may therefore represent the ideal site to explore the interplay of climatic and depositional processes on the sensitivity of lacustrine settings to document the impact of past earthquakes.

Here we aim at generating an event stratigraphy based on seismic reflection and sediment-core data from Lake Towuti. The correlation of these analyses permits us to: (1) understand depositional processes occurring within and across the different stratigraphic and seismic units, (2) identify earthquake-related structures and deposits and their temporal relationships, (3) contribute to creating a paleoseismic record for the Malili Lakes region of East-Sulawesi, and (4) explore the effect of (hydro-) climate changes and associated lake-level fluctuations on the sensitivity to record past earthquakes in tropical settings.

2 Regional setting

The Island of Sulawesi (Fig. 2.1), in eastern Indonesia, comprises four elongated arms with a diverse geology that includes volcanic extrusives underlain by metamorphic rocks to the west, outcropping metamorphic rocks in the central part and ophiolites that are

partly covered with sedimentary rocks to the east (Villeneuve et al., 2002). The obduction of the East Sulawesi Ophiolite (ESO) is related to the interaction of the Eurasia, Indo-Australia and Pacific plates forming a triple junction since the Late Mesozoic to Oligocene (Kadarusman et al., 2004; Villeneuve et al., 2002).
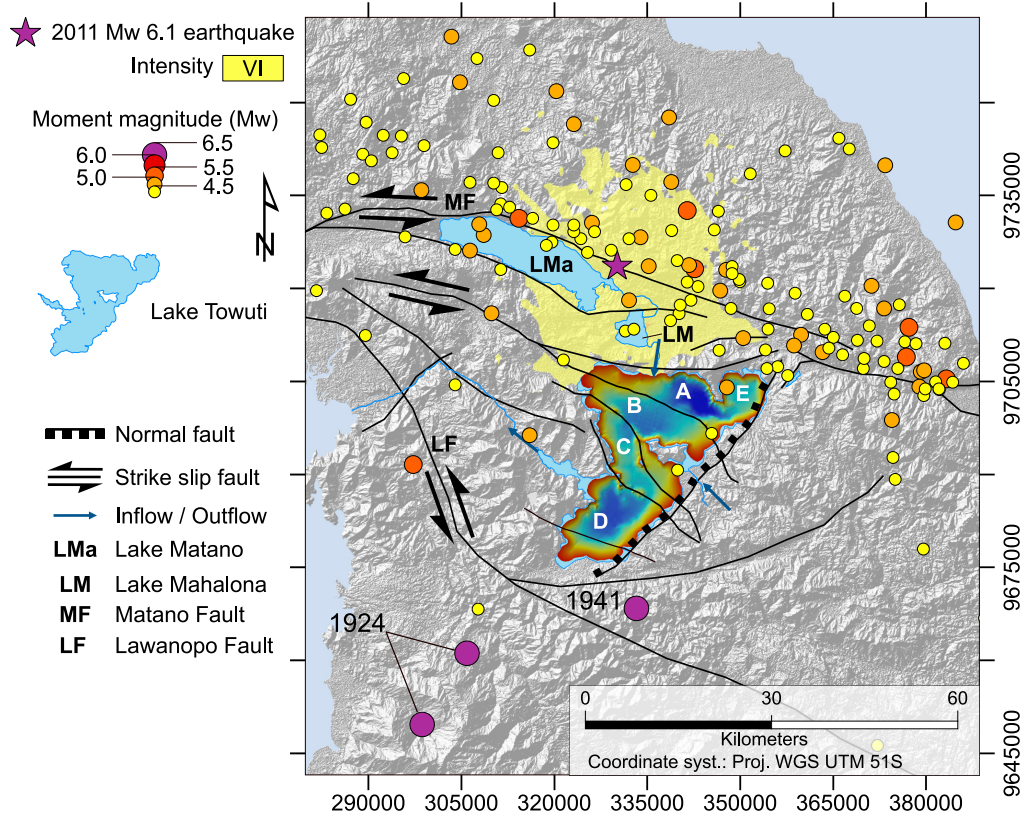
Figure 2.2: Map of the Malili system and the Matano and Lawanopo faults (from Watkinson et al., 2017) showing historical earthquakes. The earthquake catologue originates from the International Seismological Center (ISC), with only events of magnitude $\geq$ 4, depth $\leq$ 35 km, between 1924 and 2021 shown (Supplementary Material Table S2). The majority of the seismic events are located along the Matano Fault. The 2011 Mw 6.1 earthquake (purple star) affected the northern shoreline of Lake Towuti with an intensity of VI (Shakemap by USGS Earthquake Hazards Program: https://earthquake.usgs.gov/earthquakes/eventpage/usp000huje/shakemap/intensity, modified acceseed in Feb. 2022). The labels A–E are the five basins delineated by the faults

The Malili Lakes are located within Sulawesi's southeast arm forming a drainage basin that is tectonically active and characterized by major strike-slip faults with oblique components (Fig. 2.2). The three largest lakes of the Malili system (Matano, Mahalona and Towuti) are interconnected while the two other lakes (Lontoa and Masapi) are presently not connected. The formation of this ancient lake system is thought to have taken place 1 to 4 Ma ago (Russell et al., 2020b) following the activation of transform faults in the Early Miocene (Hall and Wilson, 2000), with Lake Matano thought of being the oldest lake (Vaillant et al., 2011). The catchment is predominantly composed of ultramafic bedrock (harzburgite peridotite and lherzolite; Hasberg et al. (2019)) with minor associations of more mafic rocks (Costa et al., 2015). These mafic and ultramafic rocks are interspersed with Mesozoic limestones or Tertiary sandstones and shales (Hamilton, 1972). Bedrock in the catchment is transformed to thick lateritic soils, which supply the lake with substrates high in redox-sensitive metals such as iron, nickel, and chromium (Crowe et al., 2008).

Lake Towuti formed around 1 Ma ago within a transtensional basin created by the predominant strike-slip motion along the MF (Russell et al., 2020b). The lake has a maximum depth of 203 m, lies at 319 m a.s.l. and represents the most downstream lake in the Malili Lake system. Lake Towuti is hydrologically open with a surface area covering 560 km^2 and a watershed comprising 1145 km2 (Morlock et al., 2019). The Mahalona River drains 25% of the Lake Towuti watershed dominated by Quaternary alluvial deposits (Hasberg et al., 2019; Morlock, 2018). To the east of the lake, the Loeha River partly drains metasedimentary rocks and supplies felsic minerals to the lake. To the south, three rivers drain 10% of the watershed composed of ultramafic rocks. The remaining shoreline to the north and west is dominated by steep slopes and dense vegetation, without permanent rivers. Lake Towuti has an average annual temperature of 25.7 °C, with monthly variations lower than 1 °C (Vogel et al., 2015). The maximum precipitation is in April and the minimum in August, for an annual average of 2540 mm. The annual cross-equatorial movement of the Intertropical Convergence Zone (ITCZ) and the Australo-Indonesian Summer Monsoon (AISM) control most of the seasonal rainfall distribution. The lake is also affected by El-Nino events, which can induce a decrease in lake level, such as the 3—5 m decrease during the 1997e1998 event (Tauhid and Arifian, 2000).

The three strike-slip faults are highly active, with displacements of ∼30—50 mm/year for the PKF (Bellier et al., 2006; Stevens et al., 1999; Watkinson and Hall, 2017). Displacement rates for the MF and LF are not as accurately documented as for the PKF, but the geomorphic features and their conjugated position in relation to the PKF point to

a similar rate in the order of tens of mm/year (Costa et al., 2015). These fault structures induce the formation of transtensional basins, like Lake Towuti, which are common features in a strike-slip faulting context (Ballance and Reading, 1980). This conjugated strike-slip fault system is responsible for most of the earthquakes in the region. Since the early 20th century, 150 earthquakes with Mw $\geq$ 4.5 and depths $\leq$ 35 km have occurred along the main strand of the MF and LF in the Malili Lakes area (Fig. 2.2, Willemann and Storchak (2001)). Amongst these events, the 2011 Mw 6.1 earthquake, with its epicenter on the MF, damaged the only hospital within a 100 km radius (Watkinson and Hall, 2017) near Lake Matano.

3 Material and methods

3.1 Seismic reflection survey

In 2007 in preparation of the TDP, more than 250 km of highresolution seismic lines (CHIRP) were acquired with an Edgetech$^{\text{TM}}$ 3200 with SB-424 (Russell and Bijaksana, 2012; Vogel et al., 2015) to characterize the sediment architecture of the basin and identify suitable sites for paleoclimate research. The data were acquired using a length of the source signal of 46 μs, a frequency of 3—15 kHz, and a shot time interval of 1 s, corresponding to shot spacing of approximately 1.74 m. Coordinates were continuously recorded using a Furano$^{\text{TM}}$ GPS. The data were converted to SEG-Y files that were then imported into the seismo-stratigraphic interpretation software Kingdom 2020 provided by IHS Markit. No bandpass filters were used but small bulk shifts were applied prior to data visualization and export of the seismic sections. The seismic horizons were traced along high-amplitude reflections in the acoustic signals, thus forming virtual lines allowing the definition of different seismic units. Within these units, acoustic facies were identified and described, and their characteristics were associated with specific depositional processes documented in the literature (Adams et al., 2001; Gasperini et al., 2020; Gilli et al., 2004; Maitituerdi et al., 2022; Moernaut and De Batist, 2011; Praet et al., 2017; Sammartini et al., 2021; Schnellmann et al., 2005). Airgun data were also collected to understand basin evolutionary processes and for detailed TDP drill site characterization (Russell and Bijaksana, 2012; Russell et al., 2020b), totalling~1200 km of seismic lines. In this study, airgun data was only used for the generation of a bathymetric map along with the CHIRP data. For details on the generation of the airgun data, we refer to Russell et al. (2020b). For the generation of a bathymetric map, the lake-floor horizon was picked prior to applying a

time-depth conversion with a constant acoustic velocity of 1450 m/s for the water column. Interpolation of the seismically-derived lake-floor data was performed in ArcGIS 10.8 using a natural neighbour interpolation method, which resulted in the bathymetric map of Lake Towuti presented here (Fig. 2.1B).

3.2 Sediment piston-coring

In 2010, the 19.8-m-long Co1230 piston core was collected in∼200 m water depth in the northern Basin A of Lake Towuti (Fig. 2.1B, 2°42'019"S, 121°35'033"E). The coring site is located a few kilometres downstream of the Mahalona River inlet, towards the distal part of its delta but not directly on the proximal deltaic deposits (Fig. 2.1). The base of Co1230 is dated to 28.8 cal ka BP (Vogel et al., 2015). The cores IDLE-TOW10-9 B-1K (2°43'012"S, 121°31'032"E; hereafter TOW9) and IDLE-TOW10-6 A-1K (2°43'057"S, 121°30'058"; hereafter TOW6) are 11.5- and 11.2-m-long piston cores recovered from the northern Basin B (Fig. 2.2) at 154 m and 158 m water depth (Fig. 2.1B), respectively. The location in the centre of the basin distal to the steep slopes and protected from deltaic deposition by bedrock highs results in the deposition of fine-grained, primarily pelagic sediments (Russell et al., 2020b). The base of TOW9 is dated to ∼60 ka (Russell et al., 2014). Cores IDLE-TOW10-7 B-1K (2°48'054"S, 121°30'016"E; hereafter TOW7) and IDLE-TOW108B-1K (2°50'040"S, 121°28'003"E; hereafter TOW8), are the only available piston cores from the southern Basins C and D (Figs. 2.1B and 2.2). The 11.0-m-long core TOW7 is located in the middle part of the lake at 140 m water depth, between Loeha Island and a bedrock ridge, which splits the southern part into two basins (Basins C and D, Figs. 2.1 and 2.2). Core TOW8 (11.2-m-long) was recovered in the deepest part of the southern Basin D at 174 m water depth.

3.3 Petrophysical analyses and radiocarbon dating

Whole core Gamma Ray density (GRAPE) and magnetic susceptibility (MS) measurements were performed on all cores with a resolution of 0.5 cm, using a Geotek Multisensor Core Logger (MSCL) equipped with a Bartington MS2E loop sensor. Split core high-resolution linescan images were brightness corrected using the same parameters for all core sections.

Radiocarbon dates (20 bulk organic carbon and 3 terrestrial macrofossil ages) from Russell et al. (2014) for core TOW9 were projected onto TOW6, TOW7 and TOW8.

These projections are based on clearly distinguishable stratigraphic features present in magnetic susceptibility, gamma-ray density data, and changes in lithology at all sites (Fig. 2.3 and Supplementary Material Fig.S1). Upon transfer of radiocarbon ages, age models were calculated using the IntCal20 calibration curve (Reimer et al., 2020) for cores TOW6, TOW7, and TOW8. The R package CLAM v.2.3.9 (Blaauw, 2010) was used to generate age-depth models using a smooth spline interpolation. For core TOW9 we relied on the age-depth model presented in Russell et al. (2014) and for core Co1230 on the one presented in Vogel et al. (2015).
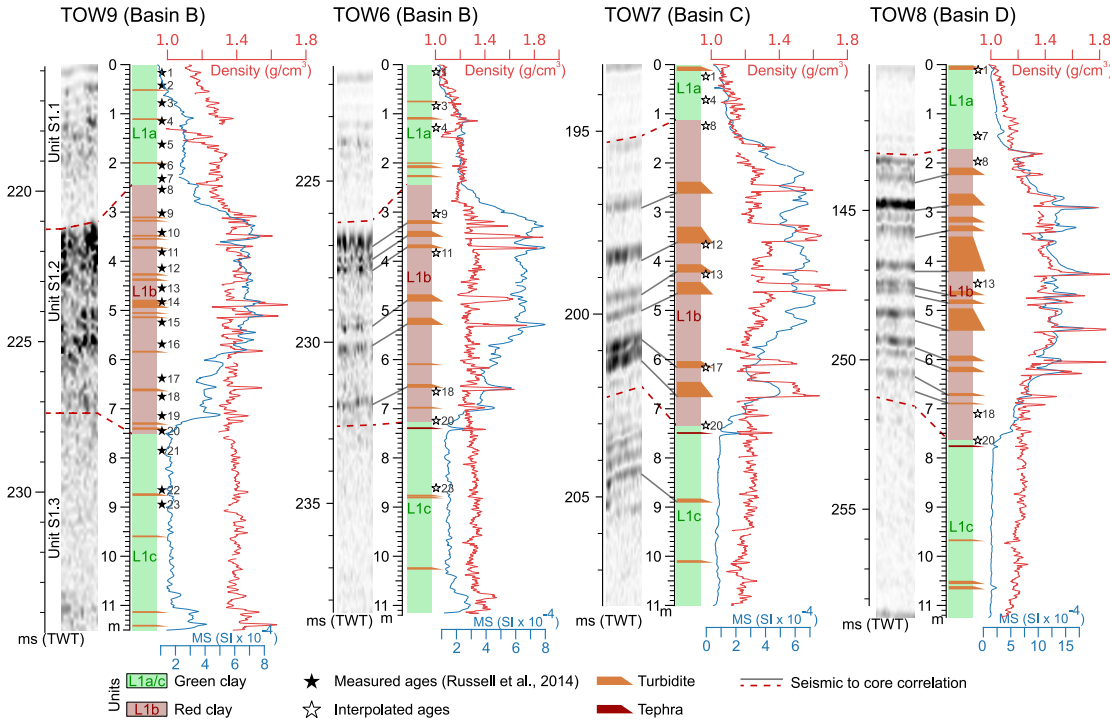
Figure 2.3: Core logs (lithological units, turbidites, Gamma ray density and magnetic susceptibility) aligned with respective windows of chirp seismic lines (two-way-travel-time, in ms). Differentiation of green and red clays was done using core images and magnetic susceptibility data. Ages measured on core TOW9 (Russell et al., 2014) are interpolated on the other cores with the matching patterns in MS variations.

3.4 Intensity prediction equation

Earthquake intensities in the surroundings of Lake Towuti are only available for strong events. However, a considerable number of smaller earthquakes are located at sufficient distances to reach the shores of the lake with an intensity $\geq$ VI. The Intensity Prediction Equation IPE in Leonard (2015) was used to estimate the Modified Mercalli Intensity MMI for additional events listed in Supplementary Table S2:

$$MMI = C_0 + C_1 * M_w + C_2 * ln(\sqrt{R^2 + (1 + C_3 * exp(M_w - 5))^2})$$

where R is the minimum/shortest distance to the shore of Lake Towuti, M_w, the moment magnitude of the event, and C_0, C_1, C_2, and C_3, are constants, equal to 3.5, 1.05, –1.09, 1.1 respectively.

4 Results

4.1 Bathymetry

The bathymetric map indicates five basins of variable depth separated transversely by bedrock ridges (Figs. 2.1 and 2.4) and fault structures (Fig. 2.2). The deepest basin to the north (A) receives the majority of direct sediment input from the Mahalona River, which forms a delta that progrades southeastward towards the Basin A center. Owing to its topographic confinement, slopes bordering Basin A are steep, often exceeding >15°. The lake-floor morphology of the two Basins B and C is rather flat, with water depths ranging between ~120 and ~160 m (Fig. 2.4). Basin B is characterized by gently inclined slopes to the NW and SE, while slopes from the bordering ridges to the N and S are generally steeper, particularly slopes originating off the Loeha Island (~12°). Basin C shows a more complex morphology with gradual slopes towards the north and south sills and steepest slopes to the west and east. The southern Basin D is characterized by an expansive relatively flat surface with a nearly constant water depth of ~160 m. The slopes bordering Basin D are gently inclined at 3° and 5° along the shoreline but are much steeper (max.18°) at its northern end, marked by a prominent ridge. Basin E is isolated in the northeast of the lake, featuring a circular shape and a depth of ~140 m.

4.2   Seismic stratigraphy

Single and multi-channel airgun seismic data reveal two clearly distinguishable seismic units for Lake Towuti (Russell et al., 2020b). The upper Unit 1, reaching a maximum thickness of nearly 150 m (using a seismic velocity of 1500 m/s) in the southern Basin D, is acoustically well stratified with alternations of parallel and continuous low- and high-amplitude reflections across all basins. The lower Unit 2 varies from ∼10 to ∼150 m in thickness and generally shows a chaotic appearance with limited areas of continuous and discontinuous sub-parallel high-amplitude reflections. These two seismic units correlate well with substantial lithological changes in the sediment cores obtained from the 2015 TDP deep drilling boreholes. The sediment succession is comprised of predominantly fine-grained lacustrine sediments in the upper part (Unit 1) and predominantly coarser grained fluvio-lacustrine sediments interspersed with occasional peats in the lower part (Unit 2) (Russell et al., 2020b).

Using the high-resolution CHIRP data, we delineated the seismic stratigraphy of the uppermost strata within Unit 1 into 5 seismic sub-units (youngest Unit S1.1 to oldest S1.5, Table 2.1, Fig. 2.4). This sub-classification is based on differences in the amplitude and frequency of reflections (seismic facies) and their overall geometry. However, in the depocenters, where sediment deposits are thickest, and near the major deltas where coarser sediments prevail, the CHIRP data lack signal strength to image the entire Unit 1 down to the Unit 1/Unit 2 boundary. Correlation of the seismic units between the different basins is not always straightforward as bedrock ridges separate the different basins. In this study, we therefore focus only on the three uppermost seismic sub-units (named Unit S1.1 to S1.3), which are also covered by sediment piston-cores (Fig 2.3).

Unit S1.1

Unit S1.1 reaches an average thickness of 11 ms two-way travel time (TWT, ∼8 m using a constant seismic velocity of 1500 m/s, Fig. 2.4) and is characterized by parallel and continuous reflections, with a general succession of higher amplitudes at the base to lower amplitudes at the top of the unit (Table 2.1). Some of the reflections terminate in onlaps at the slopes. At sites proximal to the delta, the lower limit of Unit S1.1 is more difficult to determine because gas rich sediments hamper the visualization of the reflections due to dissipation of energy at depth.

In Basin A, Unit S1.1 is substantially thicker than in the other basins. This
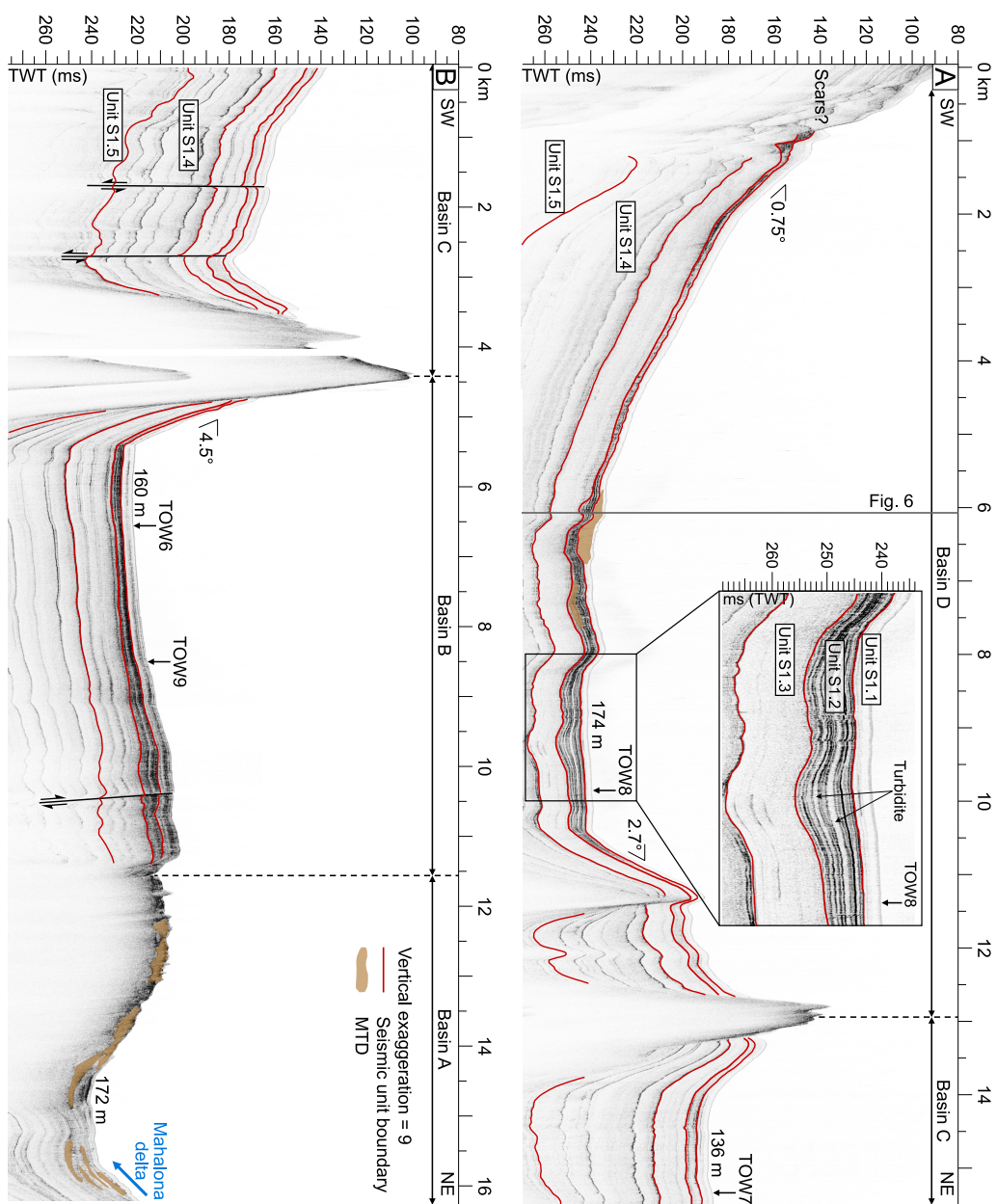
Figure 2.4: CHIRP seismic profiles crossing Lake Towuti from southwest to northeast. Core locations are projected onto the seismic sections. See Fig. 1 for locations of cores and seismic sections.

is because steep slopes and the great water depth direct the suspended load from the Mahalona River and its delta towards the Basin A depocenter (Fig. 2.1, Vogel et al. (2015)). The amplitudes of the reflections in this deep basin are weak to moderate, with transparent seismic facies at the base of the slopes. Unit S1.1 in Basin B, which is located farther away and protected by E-Wtrending bedrock highs from delta sediments, is much thinner ($\sim$5 ms TWT, $\sim$3.5 m) but spread over a large area compared to Basin A. It is acoustically well-stratified, with horizontally continuous and parallel low-to moderate-amplitude reflections over the entire Basin B. In Basin C, Unit S1.1 exhibits a generally constant thickness with parallel and continuous reflections of moderate amplitude (Fig. 2.4). Its thickness is similar to that in Basin B, except for the western littoral part where it tends to become thinner. The reflections of Unit S1.1 in Basin D are parallel and continuous with low amplitudes and an average thickness of 3 ms TWT ($\sim$2.3 m). A few thick and acoustically transparent acoustic strata, identified as MTDs are locally identifiable, especially towards the northwestern shore of the basin.

Table 2.1: Description of CHIRP seismic units of Lake Towuti with respective thicknesses in different basins A-D using a constant seismic velocity of 1500 m/s for time-depth conversion.

Unit	preview	description	maximal thickness			
			A	B	C	D
S1.1		Parallel, continuous, high-(base) to low-amplitude (surface) in Basin A. Acoustically well-stratified, with horizontally continuous and parallel reflections in Basins B, C and D	8 m	3.5 m	3.5 m	2 m
S1.2		High-amplitude, continuous and sub-parallel in Basin A. Succession of acoustically high-amplitude, parallel, continuous and homogeneous reflections in Basin B. Medium- to high-amplitude, semi-continuous, with ruptures (irregularities and discontinuities) in Basin C. Medium- to high-amplitude, continuous and parallel in Basin D	Undefined (loss of energy)	3.5 m	4.5 m	8.25 m
S1.3		Not imaged in Basin A. Thinly acoustically alternated reflections of low- and very low-amplitude, with high frequency, globally homogeneous and continuous, parallel with some minors deformation and disruption in Basin B, C and D		12 m	10.5 m	9.5 m
S1.4		Several high-amplitude reflections associated to tephra layers (Russell et al., 2020). Parallel and sub-parallel disrupted low-amplitude reflections in Basins B, C and D		35 m	20 m	33 m
S1.5		Succession of acoustically low- to very low-amplitude reflections, parallel and sub-parallel, continuous and homogeneous in Basin B, C and D	Undefined (loss of energy)			

Unit S1.2

The boundary between Units S1.1 and S1.2 is defined by a high-amplitude reflection visible across almost the entire sedimentary subsurface of Lake Towuti. This reflection
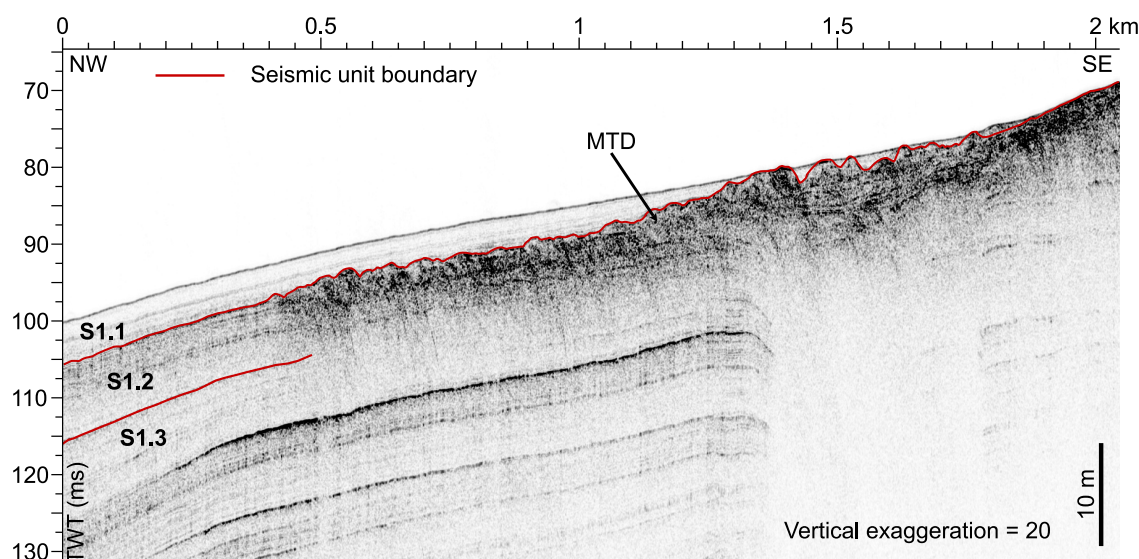
Figure 2.5: NW to SE CHIRP seismic profile close to the eastern shoreline of Basin B, showing a large MTD with an irregular surface.

is the first of a succession of high-amplitude reflections, which together form Unit S1.2 (Table 2.1). In the deep Basin A, the lower boundary of Unit S1.2 is not visible on the CHIRP data, but the thickness reaches at least 14 m (~19 ms TWT) in the deeper part. Unit S1.2 reflections are high in amplitude in the upper part, but appear less pronounced in the lower parts likely due to energy dissipation with depth. The decimetre-scale high- and low-amplitude alternations are continuous and sub-parallel. Variation in thickness is observed, with divergent stratification in the southern part of the Basin A depocenter. Most reflections terminate with onlaps onto frontally emergent subaquatic landslides at the toe of the slopes. Unit S1.2 is not visible in the CHIRP data in proximity to the Mahalona River delta (Fig. 2.4).

In Basin B, Unit S1.2 is comparably thin (~5 ms TWT, ~3.5 m) with ~8 clearly discernible, continuous, homogeneous, and high-amplitude reflections. The alterations become less distinct in the depocenter located to the north of the Loeha Island and are interspersed with acoustically transparent facies of varying thicknesses. To the east of this basin, chaotic facies appear with some reflections preserved close to the shoreline (Fig. 2.5), identified as a MTD.

Unit S1.2 in Basin C appears less continuous and is relatively thin. Some medium- to high-amplitude reflections are parallel over longer distances, but often show

discontinuous reflection patterns with irregularities (Fig. 2.4). These patterns occur in particular in the eastern part of Basin C, where a thick (up to 12 ms TWT, ∼9 m) megaturbidite covering a large area is observed, increasing the thickness of the unit to 25 ms TWT or almost 18 m (Supplementary Material Fig. S2).

The reflections in Unit S1.2 in Basin D show medium- to high-amplitudes and are generally continuous and parallel. Within this unit, several alternations of high-amplitude reflections and transparent seismic strata occur. Although the packages of high-amplitude reflections are of nearly uniform thickness in this basin, the transparent strata pinch out towards the shorelines and increase in thickness towards the basin center to ∼1 m. Mediumamplitude reflections appear very locally, sometimes with identifiable geometric structures, thickening in the center, with onlap terminations, transparent and with a very irregular surface (Fig. 2.6).

Unit S1.3

Similar to the transition from Unit S1.1 to S1.2, the boundary between Units S1.2 and S1.3 is marked by a strong contrast in reflection amplitude with the lowest high-amplitude reflection marking the unit boundary. Unit S1.3 is characterized by thinlyspaced reflections with amplitudes lower than those in unit S1.2. In Basin A, Unit S1.3 is not imaged by CHIRP data due to limited acoustic penetration. In Basins B, C, and D, it is homogeneous with thicknesses of ∼16, 14 and 13 ms TWT (∼11, 10, and ∼9 m), respectively. The reflections are of low-to very low-amplitude (Table 2.1), they are continuous across the basins, parallel and show only minor undulations. Within Basins B and C, two groups of mediumamplitude and evenly-spaced reflections are observable. These two groups appear as a single strong reflector in Basin D.

Units S1.4 and S1.5

Unit S1.4 is bounded at the top with a strong reflector. It is thick (∼70 ms TWT, ∼50 m) and widely transparent, including several high-amplitude reflections, associated with cm-to dm-thick tephra layers (Russell et al., 2020b). Unit S1.5 begins at its top with a higher number of discernible reflections of low-to very low-amplitudes, probably caused by the loss of energy with depth due to geometric spreading. These two units are characterized by parallel and sub-parallel and often non-continuous reflections (Table 2.1).
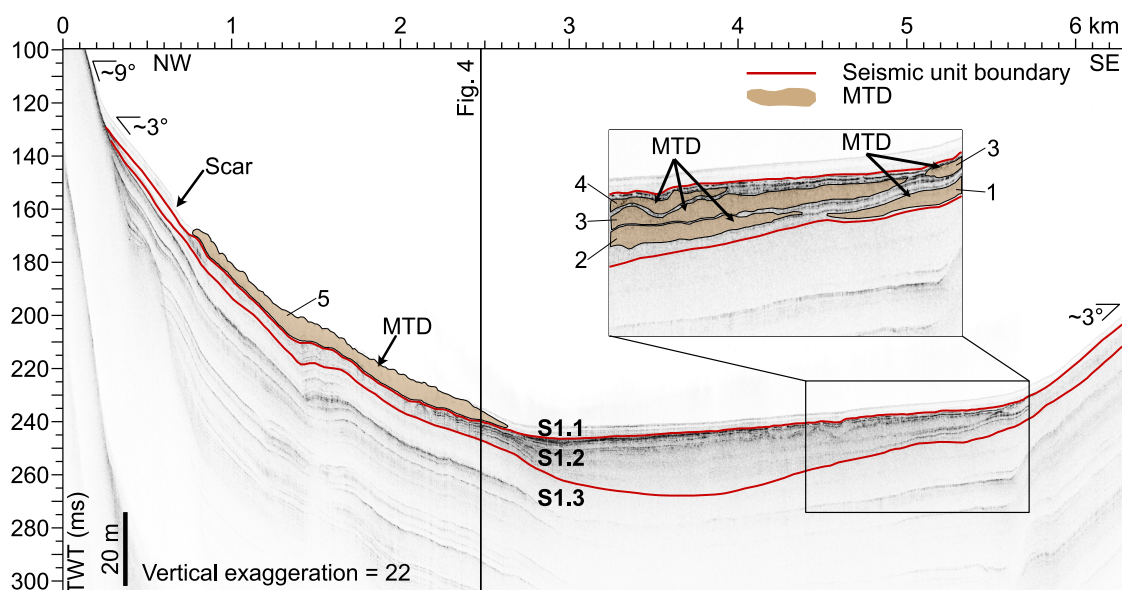
Figure 2.6: NW to SE CHIRP seismic profile through the depocenter of Basin D (see Fig. 1 for location). Seismic unit boundaries for S1.1 to S1.2, and S1.2 to S1.3 are delineated by the red lines. The MTDs, triggered on opposing slopes of the lake, are highlighted in brown. The numbers 1 to 5 correspond to the succession of MTDs from the oldest (1) to the youngest (5).

4.3   Lithostratigraphy of sediment cores

Sediment cores recovered from Lake Towuti's deeper basins show lithologies dominated by fine-grained pelagic muds with variable but generally low contents of organic matter and siderite (Russell et al., 2020b). Classifications introduced by Russell et al. (2020b,1) and Vogel et al. (2015) comprise alternations of green organic matter-rich and reddish sideritic clays. These alternations are a result of climate-induced changes in water-column oxygenation and lake level with the reddish-sideritic clays being deposited during colder and drier climates (glacials, stadials) with lake-level lowstands and deep oxygenation of the water column. In contrast, green clays are deposits that formed during wetter and warmer climate conditions (interglacials, interstadials) with lakelevel highstands and a stratified partly anoxic water column (Russell et al., 2020b).

The fine-grained muds are occasionally interrupted by turbidites, consisting of coarser-grained beds with a characteristic coarse-grained/sand-sized normal graded base overlain by a more homogenous silt-dominated succession occasionally showing cross-

bedding towards the top and typically capped by a several millimetre-thick clay bed (Fig. 2.7). The coarse base of these layers has grain sizes >100 μm and is clearly distinguishable from surrounding sediments by high GRAPE values (Figs. 2.3 and 2.7). We attribute the occurrence of abundant plant macrofossils, mainly occurring in the homogenous silt-sized sequence of some turbidites, to be a source indicator for deltaic material. Hence, these types of turbidites are very numerous in the deep Basin A where they have been described in detail and have been assigned to seismically triggered Mahalona Delta slope collapses (Vogel et al., 2015). We also find these features in the turbidites deposited at the TOW 7 site, where they probably originate from the slopes of the Loeha Delta. Turbidites lacking abundant plant macrofossils, which represent the majority at distal coring sites, are likely originating from mass wasting of hemipelagic slopes that experience little direct river sediment deposition. Color differences of the coarse base and the upper homogenous turbidite succession are likely the result of bedrock differences in sediment-source areas. The Mahalona River primarily delivers sediments with abundant serpentine minerals (Morlock et al., 2019; Vogel et al., 2015) explaining the dark-green colored base of these turbidites. In contrary, sediments supplied by the Loeha River show a more felsic composition (Morlock et al., 2019) likely leading to the lighter colored sediments in turbidites at site TOW 7 (Fig. 2.7).

Here we introduce a new and detailed account of turbidite occurrence, thickness, and chronological context (Fig. 2.3) in the form of a Towuti turbidite catalogue (Supplementary Material Table S1). Centimeter to decimeter-thick turbidites are abundant across the entire lake but most common in the deep Basin A (Co1230) in which units L1a and L1b are predominantly composed of these beds (Vogel et al., 2015). Basins B-D show substantially fewer turbidites, especially within Unit L1a. Overall, 23 turbidites were observed in core TOW9 (Basin B), with an average thickness of 3.1 cm (from 1 to 5 cm). Cores TOW6 (basin B) and TOW8 (Basin D) comprise 16 turbidites each, but the average thickness is 4 cm in TOW6 and 16 cm in TOW8. In core TOW7 (Basin C), only 9 turbidites are observed with an average thickness of 15.5 cm.

Alternations coinciding with the occurrence of green or redsideritic clays are present across all petrophysical and geochemical datasets obtained for cores from Lake Towuti including TOW6, 7, 8, and 9 (Fig. 2.3) as well as Co1230 (Vogel et al., 2015). Based on these major changes in lithology we suggest a sub-unit classification scheme for the upper ~10 m in the piston cores, based on the seismic and lithological unit classification introduced by Russell et al. (2020b). For the purpose of correlating lithologies between the
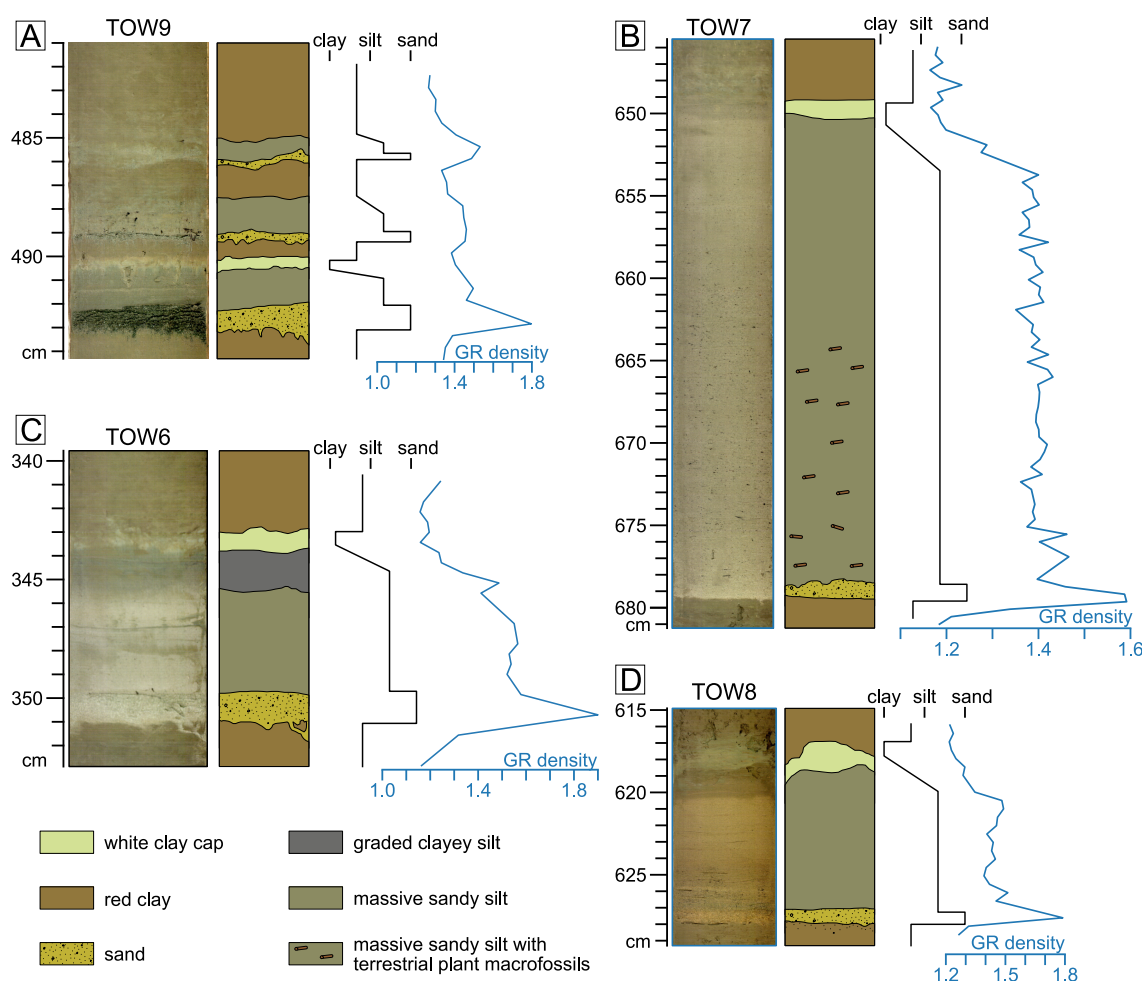
Figure 2.7: Core section images with lithological and petrophysical characteristics of typical turbidites observed in the cores.

different basins and for core-to-seismic correlation, we rely mostly on the MS and GRAPE data. MS is elevated in red sideritic clay and low in the green clay lithologies (Tamuntuan et al., 2015). MS therefore serves as an ideal dataset to correlate lithologies between the different cores and basins. GRAPE is particularly elevated in coarser/denser lithologies but also shows subtle changes at the transition of the fine-grained pelagic lithologies due to differences in sedimentary iron contents and interspersed sandy layers, often observed at the base of turbidites. GRAPE therefore serves as an ideal dataset to correlate turbidites between core and seismic data.

Three lithostratigraphic Units L1a, L1b and L1c can be identified and correlated

between cores TOW6, TOW7, TOW8, and TOW9 based on visual appearance and by matching prominent features of the MS data. The thickness of Unit L1a ranges from 113 (TOW7) to 240 cm (TOW9) in Basins B, C, and D, and reaches 640 cm thickness in the deep Basin A (TOW4 and Co1230). Unit L1a is composed of light green clay interspersed with cm-thick brownish to dark green beds. MS data shows some variability in Unit L1a but values are relatively low. One remarkable feature of Unit L1a, present in all the cores from the different basins, is a 7–17-cm-thick deposit characterized by a massive mottled siderite-bearing silty clay with elevated GRAPE values at the transition to Unit L1b, likely related to sediment remobilisation from onshore slopes induced by the lakelevel rise and subsequent formation of siderite concretions (Vuillemin et al., 2019). Unit L1b has a relatively constant thickness across the entire lake (between 506 and 622 cm). This unit is composed mainly of light to dark brownish red clay, sometimes tending towards light orange-red. MS variability is strong with high average values (>3 SI 10^{-4}). Unit L1c is the lowermost identifiable lithologic unit in the piston cores. Its total thickness cannot be determined because the unit was not sampled entirely in the piston cores. The description provided here is based on the upper ∼3 m of this unit collected in the piston cores. Unit L1c is composed of dark green clay interspersed with lighter colored clay. This unit is wellstructured with bedding in the mm – cm range.

This new unit and event deposit framework in combination with the projected chronology allows us to construct a depositional and event history of Towuti's different basins. The three lithological units (L1a–L1c) can be discerned in all piston cores from Basins B, C, and D. The boundary between Units L1a and L1b is dated to ∼12.3 ± 0.13 ka and the transition between Units L1b and L1c is dated to ∼40.8 ± 0.64 ka. In unit L1c MS-based core-to-core correlation is hampered by the muted data variability and the lack of reliable radiocarbon dates in cores TOW 7 and 8. Sedimentation in Unit L1c appears fairly constant with estimated rates of up to 15 cm/ ka in all of the sediment cores. Therefore, we here focus on the last ∼40 kyr BP where chronological constraints are most robust also due to the identified tephra marker layer, clearly visible in cores TOW6, TOW7 and TOW8, and dated to ∼41 ka (Fig. 2.3). Sedimentation rates, calculated by considering turbidites as instantaneous (constant ages), vary between lithological units and cores from different basins. In contrast, Unit L1b shows a variable sedimentation rate, with a prominent peak in all cores but particularly pronounced in TOW9 with 35 cm/ka around 560 cm (∼28.8 ka) and TOW7 with 38 cm/ka at 325 cm (∼21 ka). This increase in sedimentation rate in the Unit L1b red clays is followed by a slight decline and stabilization at 10–20 cm/ka towards the top of Unit L1a (Fig. 2.8) in all cores.

Of all the turbidites recorded in the cores, more than half occur in the red clay Unit L1b. Both the abundance and thickness of turbidites (Fig. 2.9) is increased between ∼10 and ∼35 ka relative to preceding and following periods. Turbidites constitute between 10.4% (TOW9) and 41% (TOW8) of the entire Unit L1b succession. The thickness of background sediments not including turbidites of Unit L1b differs between the basins (Table 2.2) with 348 cm in Basin D (core TOW8), 457 cm (core TOW9) and 429 cm (core TOW6) in Basin B, and 486 cm (core TOW7) in Basin C. Therefore, a significant overall increase in sedimentation rate in the red clays in Basin C relative to the other basins and in particular to Basin D is observed.
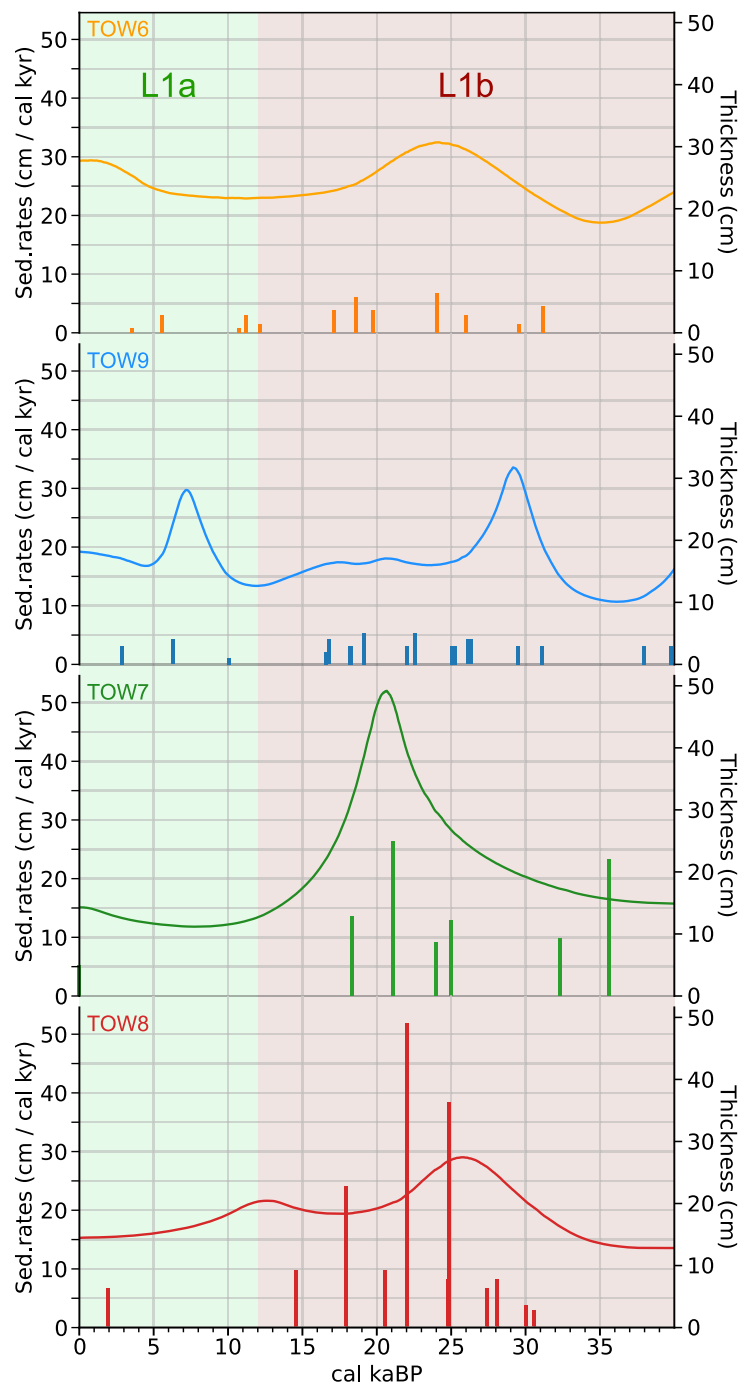
Figure 2.8: Comparison of event free sedimentation rates (curves) and turbidite thicknesses
(bars, in cm) on cores TOW6 and TOW9 (Basin B), TOW7 (Basin C) and TOW8 (Basin
D). For visual purposes, these data are based on smoothed age models. The data are
plotted for the last 40 kyrs due to extrapolations beyond that time interval being not very
coherent.

4.4 Sediment core–to–seismic correlation

In general, a strong correspondence between lithological and seismic facies is observed. This is particularly well demonstrated by the strong relationship of density with amplitude changes in seismic reflection data (Fig. 2.3). Low-amplitude reflections in seismic Unit S1.1 coincide well with lithologic Unit L1a, which is characterized by green clays and infrequent occurrence of coarser turbidites or MTDs, as is also evident by the overall low density. Likewise, the transition between seismic Units S1.1 and S1.2 coincides with the lithological Unit L1a to L1b transition as it is characterized by an increase in amplitude and sediment density, respectively. Individual turbidites are clearly resolved in seismic data for cores TOW6, 7, and 8 where these deposits reach thicknesses of several decimetres. On the contrary, turbidite thickness in TOW 9 is not sufficient to provide a clear distinction between individual deposits in seismic data but the increase in turbidite frequency leads to an overall increase in sediment density and thereby seismic reflection amplitude. A sudden decrease in seismic reflection amplitude marks the seismic Unit S1.2 to S1.3 transition and matches broadly with the change in lithology from high-density red clays of lithologic Unit L1b to lower density green clays of Unit L1c. Thick turbidites creating high-amplitude reflections in seismic data are largely absent in Units S1.3/L1c.

5 Discussion

5.1 Interpretations on sediment thicknesses

The thickness of seismic and lithologic units differs greatly between the basins. Lithological Units L1a and L1b in Basin A are 3–6 times thicker than in the other basins of the lake. The Mahalona River leads to a significant discharge of sediment directed primarily towards the deep Basin A (Costa et al., 2015; Hasberg et al., 2019; Morlock et al., 2019; Vogel et al., 2015), and the slopes surrounding the basin are steep with angles reaching up to 30°. This morphology results in an effective trap for sediments supplied by the Mahalona River (Vogel et al., 2015). Notable spatial variations in thickness are also observed elsewhere in the lake, albeit with much smaller magnitudes. Lithological Unit L1a is relatively thin in Basin D (∼170 cm) and very thin in Basin C (∼110 cm) compared to Basin B (∼240 cm, Figs. 2.3 and 2.4). We interpret these thickness variations of Unit L1a primarily as a result of spatial differences in sediment supply from rivers and by basin proximity to the Mahalona River inlet, which is the main source of suspended sediment loads to

Climate-controlled sensitivity of lake sediments to record earthquake-related mass
wasting in tropical Lake Towuti during the past 40 kyr
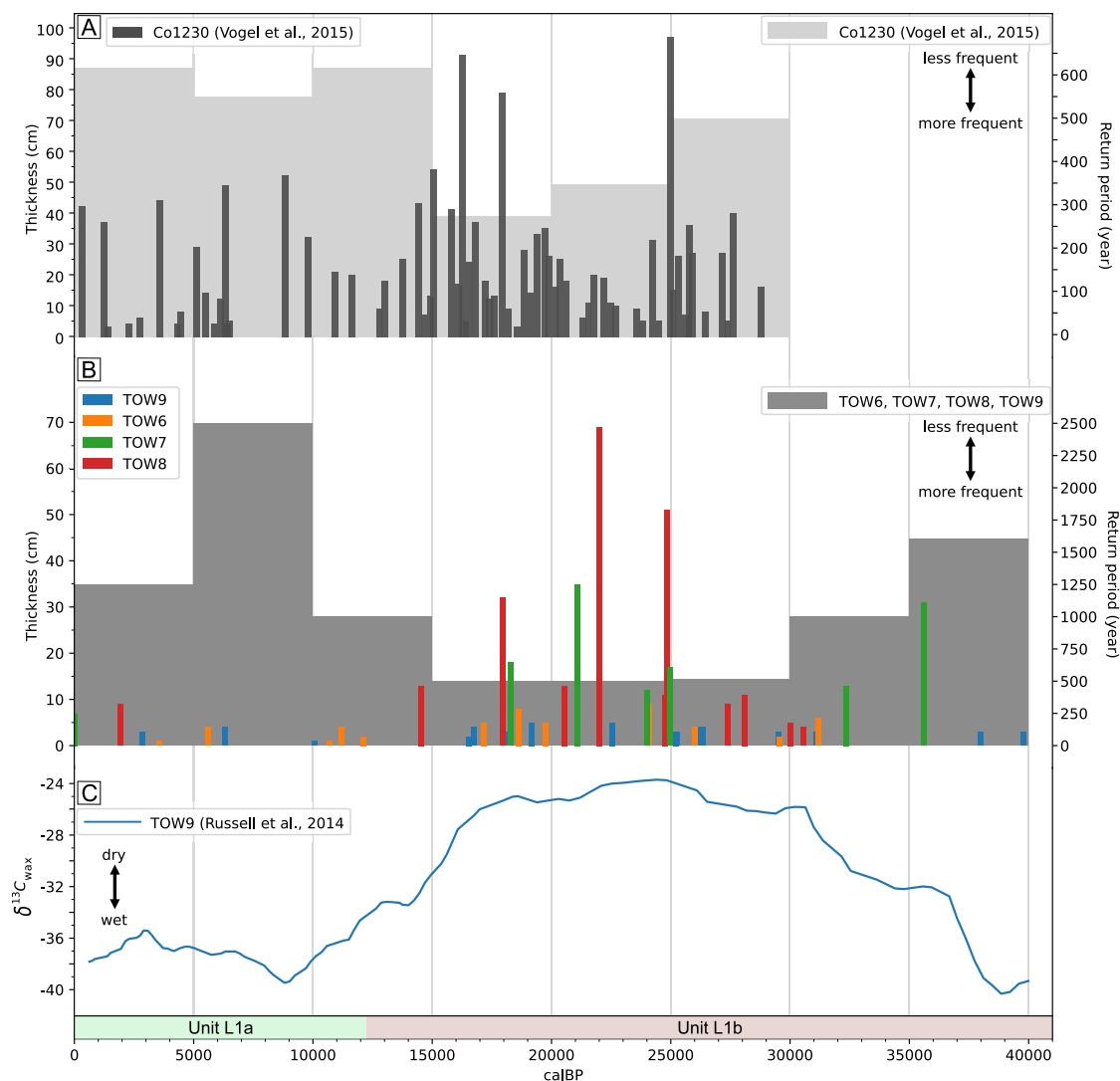
Figure 2.9: Comparison of event free sedimentation rates (curves) and turbidite thicknesses
(bars, in cm) on cores TOW6 and TOW9 (Basin B), TOW7 (Basin C) and TOW8 (Basin
D). For visual purposes, these data are based on smoothed age models. The data are
plotted for the last 40 kyrs due to extrapolations beyond that time interval being not very
coherent.

the entire lake but particularly to Basins A and B. In contrast, the southern Basins C
and D receive sediment supply by smaller rivers with the largest being the Loeha River
entering Basin C (Figs. 2.1 and 2.2). However, the sediment input from the Loeha River is
probably, to a large extent, also diverted to the northern basins by the Loeha island and the

associated NW – SE trending bedrock ridge (Fig. 2.1B) clearly visible in the bathymetric data. Additional submerged bedrock ridges surrounding Basin C also contribute to a lower thickness of Unit L1a in this southern basin.

Table 2.2: Comparison of lithostratigraphic Unit L1b thicknesses with and without turbidites. The turbidite proportion is relative to entire Unit L1b (100%).

Thickness Unit L1b (cm)	TOW9 - Basin B	TOW6 - Basin B	TOW7 - Basin C	TOW8 - Basin D
with turbidites	510	484	623	592
without turbidites	457	429	486	348
turbidite proportion (% Unit L1B)	10.4	11.4	22	41.2

5.2 Earthquakes as triggers of slope failure in Lake Towuti

Available data for recent earthquakes on Sulawesi and more specifically for the vicinity of Lake Towuti, based on the USGS (Shakemap by USGS Earthquake Hazards Program; https://earthquake.usgs.gov/earthquakes/eventpage/usp000huje/shakemap/intensity) and IPE show 12 earthquakes with MMI $\geq$ VI (Supplementary Material Table S2), sufficient to trigger sublacustrine slope failures (Moernaut et al., 2007; Van Daele et al., 2015). As an example, the 2011 Mw 6.1 earthquake with its epicenter 18 km to the north of Lake Towuti along the MF induced ground shaking with an intensity of VI along Towuti's northern shore (Fig. 2.2). In 1941, a Mw 6.2 earthquake was recorded with an epicenter 8 km to the southeast of Lake Towuti, with an estimated MMI intensity of VII calculated on the shoreline. We suggest that this event is responsible for the surficial MTD deposited on the western slope in the southern Basin D (Fig. 2.6). Basinward, the MTD is associated with a moderate-to high-amplitude surface reflection caused by the deposition of coarse material in a turbidite. This 4 cm thick turbidite is recovered in core TOW8, only 1 cm below the sediment-water interface (Supplementary Material Fig. S3). A more robust age determination using for example short-lived radionuclides is hampered by the extremely low sedimentation rate of around 0.1 mm per year. Nevertheless, we suggest that this deposit is a potential candidate for mass wasting related to the 1941 earthquake (Supplementary Material Fig. S3) when applying the above-mentioned sedimentation rate.

To better assess the return periods of earthquakes causing macroseismic intensities $\geq$ VI and $\geq$ VII at the lake shore we used the IPE (Leonard, 2015) and earthquake events with Mw $\geq$ 4.5 from the ISC catalogue, 2021. These data suggest return periods of ~8

years for $\geq$ VI and $\sim$32 years for $\geq$ VII intensities, based on 12 events covering the last 100 years (Supplementary Material Table S2). However, turbidites recorded in the cores of Lake Towuti are far less frequent compared to the number of earthquakes that can generate intensities $\geq$ VI at Lake Towuti. This is likely a result of insufficient sensitivity at Lake Towuti to record each individual seismic event with a triggered slope instability due to the overall low sedimentation rate in the different basins.

Before interpreting the seismic origin of turbidites, potential hydrological events must be excluded. An earthquake can cause destabilization of a slope, triggering a mass movement that will transition into a turbidity current (Kremer et al., 2017; Sabatier et al., 2022). In contrary, heavy precipitation induced processes such as floods and mudstreams (Wils et al., 2021a) cause a more steady flow of suspended sediment into the lake at the river mouths, inducing an increase in the capacity to erode and transport sediment along its path (Wilhelm et al., 2022). Many studies have focused on discerning earthquake- and flood-triggered turbidites (Kremer et al., 2015; Lauterbach et al., 2012; Praet et al., 2020; Vandekerkhove et al., 2020). Typically a sharp coarse-grained base overlain by a fining upward section is characteristic of turbidites related to a rapidly increasing energy, such as floods, spontaneous slope failure, or earthquake-induced slope failure (Sabatier et al., 2022; Talling, 2021; Vandekerkhove et al., 2020; Wilhelm et al., 2017). Flood-generated turbidites are often characterized by angular-shaped grains and often show several normal graded intervals and sometimes also reverse grading in one event as a result of changes in runoff volumes during flooding and a generally prolonged period (hours-days) of peak flow (St-Onge et al., 2004; Sturm and Matter, 1978; Vogel et al., 2015; Wilhelm et al., 2017). On the contrary, turbidites originating from slope failures typically show a normal graded base immediately followed by a thick and more homogenous sediment succession with an overlying clay cap as a result of the mobilization and fluidization of a large volume of sediment in a short time (Beck, 2009; Vandekerkhove et al., 2020). Sediment components such as abundant macrofossils are often indicative for a riverine source but are not suitable to differentiate between flood versus delta slope-failure sourced turbidites because macrofossils would also be mobilized and deposited in primarily riverine-sourced delta sediments. Based on their broadly basinwide consistent characteristic features with a graded coarsegrained base followed by a homogenous succession sometimes showing cross-bedding towards the top and a clay cap in combination with frequent large magnitude earthquakes in the region, we follow the interpretation by Vogel et al. (2015) suggesting turbidites in Towuti originate primarily from earthquake-triggered and slope-failure-induced mass-movement processes. The absence of flood turbidites at the coring

51

sites studied here can be explained by the morphology of the lake that constrains the propagation of flood-generated underflows and turbidity currents from the major inlets (Russell et al., 2020b). Several ridges in Towuti constitute effective hydrologic obstacles, especially in Basins B and D(Fig. 2.1), where the sediment input from rivers is already quite low.

Mass movements occur when the gravitational force exerted on the slope sediments exceeds their resisting force. This balance is influenced by several parameters, such as slope inclination (Sultan et al., 2004), sediment thickness and sedimentation rate (Wilhelm et al., 2016b), gas hydrate destabilization (Haq, 1998), pore pressures (Urlaub et al., 2015) and existence of weak layers (Strupler et al., 2017). Gas-hydrate stability, pore-pressure changes and activation of weak layers can be affected by seismic shaking contributing to slope instability and failure. For example, during an earthquake and the associated ground motions, pore-water escape can induce large-scale sediment liquefaction or pore-water overpressure, thereby reducing the sediment's shear strength (Biscontin et al., 2004). While spontaneous subaquatic or rainfall-induced onshore slope failures cannot be ruled out completely, we suggest these to be rather rare events considering the low sedimentation rates leading to slow slope charging in combination with frequent seismic shaking. Frequent seismic shaking may, in addition, also lead to so-called seismic strengthening through enhanced sediment compaction and efficient removal of surficial sediments (Molenaar et al., 2019).

The major parameters that control the formation of a turbidite triggered by an earthquake are the slope angle, the thickness and geotechnical properties of the sediment package emplaced on the slope, as well as the intensity of the seismic shaking (Molenaar et al., 2021; **?**). The slope angle as well as the thickness of the sediment package and its rheology are factors determining the stability of the sediments and thus the sensitivity to generate a failure (Hansen et al., 2016; Strasser et al., 2011,0; Van Daele et al., 2015; Wiemer et al., 2015; Wilhelm et al., 2016b). In case of Basin A with a high supply of suspended sediments from the Mahalona River, we assume that the slope angles and the sediment package are rather sensitive to seismic shaking as witnessed by a larger number of turbidites compared to the other basins (Russell et al., 2020b; Vogel et al., 2015). However, turbidite return periods of > 200 years in Basin A are still well below the return periods of earthquakes leading to intensities of $\geq$ VI and $\geq$ VII (Supplementary Material Fig. S4). The slopes in Basin B originating from the Loeha Island are similarly steep, with up to 10° in areas where mass movements occur (Supplementary Material Fig. S5) but lack

the steady supply of sediment from major rivers. This is emphasized by the presence of frequent but rather thin turbidites at coring sites TOW6 and TOW9. In contrast, slopes are generally much more gently inclined in the southern Basins C and D (<4°). This permits accumulation of a thicker sediment package over time that is less prone to failure. Turbidites in the southern basins are consequently less frequent but generally thicker than in Basin B (Figs. 2.3 and 2.9B), as also evidenced by the presence of large slope failure related MTD's observed on seismic data (Fig. 2.6). Hence, the less frequent but thick turbidites suggest a lower sensitivity of slopes to fail during moderate earthquakes, and therefore imply a lower sensitivity to ground shaking. Consequently, we propose that high-intensity shaking is required to cause slope failures in the southern Towuti basins. We suggest that such strong events must have triggered the large MTDs clearly visible in seismic units S1.1 and S1.2 and in cores TOW7 and TOW8. In Basin D, several MTDs are recorded on the CHIRP data, including some deposits within Unit S1.2 that appear to have been generated during the same event but on different/opposing slopes (Fig. 2.6 and Supplementary Material Fig. S6) thereby fulfilling the synchronicity criterium for an earthquake trigger as suggested by Schnellmann et al. (2002).

Owing to the ridges separating the basins, hampering the tracing of individual reflections, and age uncertainties, correlation of individual turbidites in the different basins remains rather vague. Dating these turbidites to estimate the age of an earthquake is very challenging, as radiocarbon dates are extrapolated from TOW9 and errors often exceed the recurrence intervals of major events (Talling, 2021). Nevertheless, the general increase in occurrence of turbidites in Unit L1b (Figs. 2.3 and 2.9B–C) clearly shows increased mass-movement activity during the dry Last Glacial between ~15 and 30 ka at Lake Towuti. This pattern suggests a potential aseismic influence related to regional changes in hydroclimate and Lake Towuti's associated lake level on the sensitivity towards seismic triggering of MTDs.

5.3 Climate-induced changes in sensitivity of slope failures

Based on previous studies in different settings, the link between lake or sea-level changes with the frequency of subaqueous mass failures has raised a controversial and ongoing debate. Some studies conclude that an increase in slope sensitivity towards failure occurs during a highstand phase (Brothers et al., 2013; Lu et al., 2021a; Neves et al., 2016) due to higher sedimentation rates, as well as due to immersion of steep banks, which destabilize the cohesion of sediments when they are loose and/or coarse. On the contrary, other

studies report an increase in slope failures during lowstands due to the (i) more significant erosion of emerged shelves resulting in higher sedimentation rates on the slopes (McHugh et al., 2002) eventually leading to sediment overloading and decreasing slope stability; and/or (ii) lowstand-induced pore-fluid overpressure (Anselmetti et al., 2009; Blumberg et al., 2008; Lee et al., 1996) possibly closely restricted to the phase when the lake-level is dropping (Moernaut et al., 2010). A higher frequency of turbidite deposition in the late Pleistocene and a lower frequency during the Holocene was observed at all latitudes (Anselmetti et al., 2009; Blumberg et al., 2008; Brothers et al., 2013; Lee et al., 1996; Wien et al., 2006) similar to Lake Towuti. Despite the discrepancies between high and low water levels, it seems evident that slope stability is influenced strongly by climate-induced water-level changes.

Our study of Lake Towuti turbidite occurrence indicates increased slope sensitivity towards failure during a climatically driven lake-level lowstand (Fig. 2.9). Indeed, the difference in turbidite occurrence between Units L1a and L1b is probably not associated with a change in tectonic activity alone. Previous studies suggest changes in lithology to be related with changes in the regions hydroclimate with green clays (L1a) deposited during warm and humid periods, and red sideritic clays (L1b) during colder and drier climate conditions of MIS 2 (Konecky et al., 2016; Russell et al., 2014) with lower lake levels (Vogel et al., 2015) and deep mixing at Towuti (Costa et al., 2015). Accordingly, deposition of the green clays of L1a (∼Holocene) and L1c (MIS 3) took place under lake-level highstands and a permanently stratified water column with anoxia in bottom waters (Russell et al., 2020b). We suggest the increase in turbidites in L1b to be related to changes in the regions hydroclimate (Konecky et al., 2016; Russell et al., 2014; Wicaksono et al., 2017) and an associated up to 30 m lower lake-level (Vogel et al., 2015) between ∼29 and 15 kyr BP, coincident with the regionally drier last glacial. Although an overall drier climate does not rule out heavy precipitation events and increased flooding, the observed turbidite compositions at our distal coring sites do not indicate increased occurrences of flood-related turbidites. However, accumulation of sediment in the catchment in intermediate storages/ sinks that can be mobilized during single heavy precipitation events in combination with a change in style of erosion during dry phases (Morlock et al., 2019) may also contribute to rapid slope charging and thereby a higher susceptibility of slopes to fail during an earthquake.

Lake-level changes in Lake Towuti also affected the background sedimentation rate, a parameter that was already shown to play a considerable role in the occurrence

of MTDs in other basins (Leynaud et al., 2007; Owen et al., 2007). In fact, all cores recovered from Lake Towuti's different depocenters show almost a twofold increase in background sedimentation rates during the last glacial period between ∼41 and 15 ka BP (Fig. 2.8). The increase cannot be explained by the coincident changes in sediment composition alone with more abundant diagenetic siderite in glacial red clays compared to more organic-rich interglacial green clays (Russell et al., 2020b). While sedimentation rates in Towuti's depocenters remain relatively low overall, we suggest lowstand-forced sediment redeposition from the exposed shore and shelf areas to be the most important factor explaining the increase in event-free sedimentation rate. Slope-to-basin focusing is also supported by rather constant glacial-interglacial slope sedimentation rates relative to the substantially higher glacial versus interglacial sedimentation rates in the depocenters. In addition, the lowering in base level of the tributaries likely contributed to increased sediment redeposition by rivers eroding into their own delta deposits (Morlock et al., 2019; Vogel et al., 2015). Moreover, the discharge of river suspension moved lakeward and focused closer to the basin depocenters. We thus hypothesize that the lowstand-forced increase in sediment redeposition caused a notable increase in slope charging that, in turn, increased the susceptibility of slopes to fail due to seismic shaking. Seismic data, acquired to image the basin fills, did not reach shallower areas where paleoshorelines or erosional features would allow to better characterize and quantify the impact of past lake-level lowstands (Anselmetti et al., 2006). Nevertheless, collected evidence from Towuti clearly points to a close interplay between climate-induced lake-level changes and associated sedimentation rates with frequency and thickness of seismoturbidites (Figs. 2.8 and 2.9), an interference that needs to be taken into account when interpreting a seismic event catalogue based solely on the turbidite record.

6   Conclusion and perspectives

Correlation of sediment piston-core lithologies with seismic reflection data enabled us to establish a lithology-based high-resolution seismic stratigraphy of Lake Towuti. The particular morphology of the lake, with basins separated by tectonicallycontrolled bedrock ridges, induces a complex and heterogeneous sedimentation within the different basins, accentuated by their variation in depth.

Based on seismic reflection, lithological and petrophysical data, we established a detailed unit subclassification scheme for Lake Towuti's upper lacustrine sediment

fill (Unit 1 in Russell et al. (2020b)). This scheme is based on the appearance of different and alternating lithotypes comprising green clays and red sideritic clays with more abundant turbidites and coinciding seismic reflection data with higher amplitudes in the red versus the green clays. Turbidites are particularly abundant with thicknesses reaching several decimetres in some of the basins during a last glacial/MIS 2 lake-level lowstand phase. Analysis of lithological characteristics, petrophysical parameters alongside seismic reflection data suggest that these turbidites predominantly originate from mass-transport processes triggered by seismic shaking. Differences in the abundance and thickness of turbidites between the different lake basins indicate varying susceptibilities of slopes to failure, primarily due to differences in slope angle and sedimentation rate.

Comparison of the seismological catalogue since the beginning of the 20th century with the Towuti turbidite record suggests an overall low sensitivity of Lake Towuti to record moderate earthquakes as a result of low sedimentation rates and reduced slope charging in this tropical setting. Given the higher abundance of seismo-turbidites during the MIS 2 lowstand phase, we suggest a strong climatic influence on slope sensitivity to failure. Lake-level lowstands at Lake Towuti cause sediment remobilisation from the exposed shoreline and shelf onto the slope and into the basins' depocenters thereby increasing slope-charging rates and sensitivity to failure. This process is supported by overall higher background sedimentation rates in all of the lake basins during the lowstand phase when compared to the preceding and following highstand phases. The interplay of climate, sediment slopecharging, and mass-transport deposits at Lake Towuti may, while complicating the establishment of an accurate earthquake catalogue, serve as a valuable quantitative hydroclimate indicator. In the case of Lake Towuti, higher frequency turbidites indicates lakelevel lowstand phases and coinciding drier regional climate conditions. Additional studies from other regional settings are required to fully exploit this relationship for paleoclimate reconstructions but the basin-scale results provided here appear promising.

7 References

Adams, E. W., Schlager, W., and Anselmetti, F. S. (2001). Morphology and curvature of delta slopes in Swiss lakes: lessons for the interpretation of clinoforms in seismic data. *Sedimentology*, 48(3):661–679.

Anselmetti, F., Ariztegui, D., Hodell, D., Hillesheim, M., Brenner, M., Gilli, A.,

McKenzie, J., and Mueller, A. (2006). Late Quaternary climate-induced lake level variations in Lake Petén Itzá, Guatemala, inferred from seismic stratigraphic analysis. *Palaeogeography, Palaeoclimatology, Palaeoecology*, 230(1-2):52–69.

Anselmetti, F. S., Ariztegui, D., De Batist, M., Catalina Gebhardt, A., Haberzettl, T., Niessen, F., Ohlendorf, C., and Zolitschka, B. (2009). Environmental history of southern Patagonia unravelled by the seismic stratigraphy of Laguna Potrok Aike. *Sedimentology*, 56(4):873–892.

Ariztegui, D., Chondrogianni, C., Lami, A., Guilizzoni, P., and Lafargue, E. (2001). Lacustrine organic matter and the Holocene paleoenvironmental record of Lake Albano (central Italy). *Journal of Paleolimnology*, 26:283–292.

Avşar, U., Hubert-Ferrari, A., De Batist, M., Schmidt, S., and Fagel, N. (2015). Sedimentary records of past earthquakes in Boraboy Lake during the last ca 600 years (North Anatolian Fault, Turkey). *Palaeogeography, Palaeoclimatology, Palaeoecology*, 433:1–9.

Avşar, U., Jónsson, S., Avşar, Ö., and Schmidt, S. (2016). Earthquake-induced soft-sediment deformations and seismically amplified erosion rates recorded in varved sediments of Köyceğiz Lake (SW Turkey). *Journal of Geophysical Research: Solid Earth*, 121(6):4767–4779. Publisher: John Wiley & Sons, Ltd.

Badhani, S., Cattaneo, A., Collico, S., Urgeles, R., Dennielou, B., Leroux, E., Colin, F., Garziglia, S., Rabineau, M., and Droz, L. (2020). Integrated geophysical, sedimentological and geotechnical investigation of submarine landslides in the Gulf of Lions (Western Mediterranean). *Geological Society, London, Special Publications*, 500(1):359–376.

Ballance, P. F. and Reading, H. G., editors (1980). *Sedimentation in oblique-slip mobile zones*. Number no. 4 in Special publication of the International Association of Sedimentologists. Blackwell Scientific Publications ; Distributed in the U.S.A. by Halsted Press, Oxford [Oxfordshire] ; Boston, Mass. : New York.

Bao, H., Ampuero, J.-P., Meng, L., Fielding, E. J., Liang, C., Milliner, C. W. D., Feng, T., and Huang, H. (2019). Early and persistent supershear rupture of the 2018 magnitude 7.5 Palu earthquake. *Nature Geoscience*, 12(3):200–205.

Bartov, Y. and Sagy, A. (2004). Late Pleistocene extension and strike-slip in the

Dead Sea Basin. *Geological Magazine*, 141(5):565–572.

Bartov, Y., Stein, M., Enzel, Y., Agnon, A., and Reches, Z. (2002). Lake Levels and Sequence Stratigraphy of Lake Lisan, the Late Pleistocene Precursor of the Dead Sea. *Quaternary Research*, 57(1):9–21.

Beck, C. (2009). "Late Quaternary lacustrine paleo-seismic archives in north-western Alps: Examples of earthquake-origin assessment of sedimentary disturbances". *Earth-Science Reviews*, 96(4):327–344.

Belferman, M., Katsman, R., and Agnon, A. (2018). Effect of large-scale surface water level fluctuations on earthquake recurrence interval under strike-slip faulting. *Tectonophysics*, 744:390–402.

Bellier, O., Sebrier, M., Beaudouin, T., Villeneuve, M., Braucher, R., Bourles, D., Siame, L., Putranto, E., and Pratomo, I. (2001). High slip rate for a low seismicity along the Palu-Koro active fault in central Sulawesi (Indonesia). *Terra Nova*, 13(6):463–470.

Bellier, O., Sébrier, M., Seward, D., Beaudouin, T., Villeneuve, M., and Putranto, E. (2006). Fission track and fault kinematics analyses for new insight into the Late Cenozoic tectonic regime changes in West-Central Sulawesi (Indonesia). *Tectonophysics*, 413(3-4):201–220.

Biscontin, G., Pestana, J., and Nadim, F. (2004). Seismic triggering of submarine slides in soft cohesive soil deposits. *Marine Geology*, 203(3-4):341–354.

Blaauw, M. (2010). Methods and code for 'classical' age-modelling of radiocarbon sequences. *Quaternary Geochronology*, 5(5):512–518.

Blumberg, S., Lamy, F., Arz, H., Echtler, H., Wiedicke, M., Haug, G., and Oncken, O. (2008). Turbiditic trench deposits at the South-Chilean active margin: A Pleistocene–Holocene record of climate and tectonics. *Earth and Planetary Science Letters*, 268(3-4):526–539.

Boncio, P., Amoroso, S., Galadini, F., Galderisi, A., Iezzi, G., and Liberi, F. (2020). Earthquake-induced liquefaction features in a late Quaternary fine-grained lacustrine succession (Fucino Lake, Italy): Implications for microzonation studies. *Engineering Geology*, 272:105621.

Bookman, R., Bartov, Y., Enzel, Y., and Stein, M. (2006). Quaternary lake levels in the Dead Sea basin: Two centuries of research. In *New Frontiers in Dead Sea Paleoenvironmental Research*. Geological Society of America.

Brothers, D. S., Luttrell, K. M., and Chaytor, J. D. (2013). Sea-level–induced seismicity and submarine landslide occurrence. *Geology*, 41(9):979–982.

Chapron, E. (1999). *Contrôles climatique et sismo-tectonique de la sédimentation lacustre dans l'avant pays alpin (Lac du Bourget) durant le quaternaire récent. (Alpes françaises).* Memoire H.S., Université de Grenoble, Laboratoire de Géodynamique des Chaînes Alpines.

Chapron, E., Ariztegui, D., Mulsow, S., Villarosa, G., Pino, M., Outes, V., Juvignié, E., and Crivelli, E. (2006). Impact of the 1960 major subduction earthquake in Northern Patagonia (Chile, Argentina). *Quaternary International*, 158(1):58–71.

Chapron, E., Simonneau, A., Ledoux, G., Arnaud, F., Lajeunesse, P., and Albéric, P. (2016). French Alpine Foreland Holocene Paleoseismicity Revealed by Coeval Mass Wasting Deposits in Glacial Lakes. In Lamarche, G., Mountjoy, J., Bull, S., Hubble, T., Krastel, S., Lane, E., Micallef, A., Moscardelli, L., Mueller, C., Pecher, I., and Woelz, S., editors, *Submarine Mass Movements and their Consequences*, volume 41, pages 341–349. Springer International Publishing, Cham. Series Title: Advances in Natural and Technological Hazards Research.

Chassiot, L., Chapron, E., Di Giovanni, C., Lajeunesse, P., Tachikawa, K., Garcia, M., and Bard, E. (2016). Historical seismicity of the Mont Dore volcanic province (Auvergne, France) unraveled by a regional lacustrine investigation: New insights about lake sensitivity to earthquakes. *Sedimentary Geology*, 339:134–150.

Closson, D., Abou Karaki, N., and Hallot, F. (2010). Landslides along the Jordanian Dead Sea coast triggered by the lake level lowering. *Environmental Earth Sciences*, 59(7):1417–1430.

Collico, S., Arroyo, M., Urgeles, R., Gràcia, E., Devincenzi, M., and Peréz, N. (2020). Probabilistic mapping of earthquake-induced submarine landslide susceptibility in the South-West Iberian margin. *Marine Geology*, 429:106296.

Costa, K., Russell, J., Vogel, H., and Bijaksana, S. (2015). Hydrological connectivity and mixing of Lake Towuti, Indonesia in response to paleoclimatic changes over the last 60,000 years. *Palaeogeography, Palaeoclimatology, Palaeoecology*, 417:467–475.

Crowe, S. A., O'Neill, A. H., Katsev, S., Hehanussa, P., Haffner, G. D., Sundby, B.,

Mucci, A., and Fowle, D. A. (2008). The biogeochemistry of tropical lakes: A case study from Lake Matano, Indonesia. *Limnology and Oceanography*, 53(1):319–331.

Daryono, M. R., Kumarawarman, B., Muslim, I. H., Triwurjani, R., Permadi, R., Prihatmoko, S., Wibowo, S., and Tutuko, G. H. (2021). Two earthquake events on the Pamsoa Segment of the Matano Fault, Sulawesi. *IOP Conference Series: Earth and Environmental Science*, 873(1):012053.

Daxer, C., Ortler, M., Fabbri, S. C., Hilbe, M., Hajdas, I., Dubois, N., Piechl, T., Hammerl, C., Strasser, M., and Moernaut, J. (2022). High-resolution calibration of seismically-induced lacustrine deposits with historical earthquake data in the Eastern Alps (Carinthia, Austria). *Quaternary Science Reviews*, 284:107497.

De Deckker, P., Tapper, N., and van der Kaars, S. (2003). The status of the Indo-Pacific Warm Pool and adjacent land at the Last Glacial Maximum. *Global and Planetary Change*, 35(1-2):25–35.

Dente, E., Lensky, N. G., Morin, E., and Enzel, Y. (2021). From straight to deeply incised meandering channels: Slope impact on sinuosity of confined streams. *Earth Surface Processes and Landforms*, 46(5):1041–1054.

Field, M. E., Gardner, J. V., Jennings, A. E., and Edwards, B. D. (1982). Earthquake-induced sediment failures on a 0.25° slope, Klamath River delta, California. *Geology*, 10(10):542.

Gasperini, L., Marzocchi, A., Mazza, S., Miele, R., Meli, M., Najjar, H., Michetti, A. M., and Polonia, A. (2020). Morphotectonics and late Quaternary seismic stratigraphy of Lake Garda (Northern Italy). *Geomorphology*, 371:107427.

Gastineau, R., de Sigoyer, J., Sabatier, P., Fabbri, S. C., Anselmetti, F. S., Develle, A. L., Şahin, M., Gündüz, S., Niessen, F., and Gebhardt, A. C. (2021). Active Subaquatic Fault Segments in Lake Iznik Along the Middle Strand of the North Anatolian Fault, NW Turkey. *Tectonics*, 40(1):e2020TC006404. _eprint: https://agupubs.onlinelibrary.wiley.com/doi/pdf/10.1029/2020TC006404.

Gilli, A., Anselmetti, F. S., Ariztegui, D., Beres, M., McKenzie, J. A., and Markgraf, V. (2004). Seismic stratigraphy, buried beach ridges and contourite drifts: the Late Quaternary history of the closed Lago Cardiel basin, Argentina (49°S): Seismic stratigraphy of Lago Cardiel, Argentina. *Sedimentology*, 52(1):1–23.

Goldfinger, C. (2011). Submarine Paleoseismology Based on Turbidite Records. *Annual Review of Marine Science*, 3(1):35–66.

Goldstein, S. L., Kiro, Y., Torfstein, A., Kitagawa, H., Tierney, J., and Stein, M. (2020). Revised chronology of the ICDP Dead Sea deep drill core relates drier-wetter-drier climate cycles to insolation over the past 220 kyr. *Quaternary Science Reviews*, 244:106460.

Gràcia, E., Vizcaino, A., Escutia, C., Asioli, A., Rodés, Á., Pallàs, R., Garcia-Orellana, J., Lebreiro, S., and Goldfinger, C. (2010). Holocene earthquake record offshore Portugal (SW Iberia): testing turbidite paleoseismology in a slow-convergence margin. *Quaternary Science Reviews*, 29(9-10):1156–1172.

Guyard, H., Chapron, E., St-Onge, G., Anselmetti, F. S., Arnaud, F., Magand, O., Francus, P., and Mélières, M.-A. (2007). High-altitude varve records of abrupt environmental changes and mining activity over the last 4000 years in the Western French Alps (Lake Bramant, Grandes Rousses Massif). *Quaternary Science Reviews*, 26(19-21):2644–2660.

Hage, S., Hubert-Ferrari, A., Lamair, L., Avşar, U., El Ouahabi, M., Van Daele, M., Boulvain, F., Ali Bahri, M., Seret, A., and Plenevaux, A. (2017). Flow dynamics at the origin of thin clayey sand lacustrine turbidites: Examples from Lake Hazar, Turkey. *Sedimentology*, 64(7):1929–1956.

Hall, R. and Wilson, M. (2000). Neogene sutures in eastern Indonesia. *Journal of Asian Earth Sciences*, 18(6):781–808.

Hamilton, R., Stevenson, J., Li, B., and Bijaksana, S. (2019). A 16,000-year record of climate, vegetation and fire from Wallacean lowland tropical forests. *Quaternary Science Reviews*, 224:105929.

Hamilton, W. B. (1972). Tectonics of the Indonesian Region. Report 72-1978. Edition: -.

Hansen, L., Waldmann, N., Storms, J. E., Eilertsen, R. S., Ariztegui, D., Chapron, E., and Nesje, A. (2016). Morphological signatures of mass wasting and delta processes in a fjord-lake system: insights from Lovatnet, western Norway. *Norwegian Journal of Geology*.

Haq, B. U. (1998). Natural gas hydrates: searching for the long-term climatic and slope-stability records. *Geological Society, London, Special Publications*, 137(1):303–318.

Hasberg, A. K. M., Bijaksana, S., Held, P., Just, J., Melles, M., Morlock, M. A., Opitz, S., Russell, J. M., Vogel, H., and Wennrich, V. (2019). Modern sedimentation processes in Lake Towuti, Indonesia, revealed by the composition of surface sediments. *Sedimentology*, 66(2):675–698.

Howarth, J. D., Fitzsimons, S. J., Norris, R. J., and Jacobsen, G. E. (2014). Lake sediments record high intensity shaking that provides insight into the location and rupture length of large earthquakes on the Alpine Fault, New Zealand. *Earth and Planetary Science Letters*, 403:340–351.

Howarth, J. D., Orpin, A. R., Kaneko, Y., Strachan, L. J., Nodder, S. D., Mountjoy, J. J., Barnes, P. M., Bostock, H. C., Holden, C., Jones, K., and Cağatay, M. N. (2021). Calibrating the marine turbidite palaeoseismometer using the 2016 Kaikōura earthquake. *Nature Geoscience*, 14(3):161–167.

Hubert-Ferrari, A., Lamair, L., Hage, S., Schmidt, S., Çağatay, M. N., and Avşar, U. (2020). A 3800 yr paleoseismic record (Lake Hazar sediments, eastern Turkey): Implications for the East Anatolian Fault seismic cycle. *Earth and Planetary Science Letters*, 538:116152.

Inouchi, Y., Kinugasa, Y., Kumon, F., Nakano, S., Yasumatsu, S., and Shiki, T. (1996). Turbidites as records of intense palaeoearthquakes in Lake Biwa, Japan. *Sedimentary Geology*, 104(1-4):117–125.

Irsyam, M., Cummins, P. R., Asrurifak, M., Faizal, L., Natawidjaja, D. H., Widiyantoro, S., Meilano, I., Triyoso, W., Rudiyanto, A., Hidayati, S., Ridwan, M., Hanifa, N. R., and Syahbana, A. J. (2020). Development of the 2017 national seismic hazard maps of Indonesia. *Earthquake Spectra*, 36(1_suppl):112–136.

Kadarusman, A., Miyashita, S., Maruyama, S., Parkinson, C. D., and Ishikawa, A. (2004). Petrology, geochemistry and paleogeographic reconstruction of the East Sulawesi Ophiolite, Indonesia. *Tectonophysics*, 392(1-4):55–83.

Kempf, P., Moernaut, J., Van Daele, M., Pino, M., Urrutia, R., and De Batist, M. (2020). Paleotsunami record of the past 4300 years in the complex coastal lake system of Lake Cucao, Chiloé Island, south central Chile. *Sedimentary Geology*, 401:105644.

Konecky, B., Russell, J., and Bijaksana, S. (2016). Glacial aridity in central Indonesia coeval with intensified monsoon circulation. *Earth and Planetary*

Science Letters, 437:15–24.

Krause, C. E., Gagan, M. K., Dunbar, G. B., Hantoro, W. S., Hellstrom, J. C., Cheng, H., Edwards, R. L., Suwargadi, B. W., Abram, N. J., and Rifai, H. (2019). Spatio-temporal evolution of Australasian monsoon hydroclimate over the last 40,000 years. *Earth and Planetary Science Letters*, 513:103–112.

Kremer, K., Corella, J. P., Adatte, T., Garnier, E., Zenhäusern, g., and Girardclos, S. (2015). Origin of Turbidites In Deep Lake Geneva (France–Switzerland) In the Last 1500 Years. *Journal of Sedimentary Research*, 85(12):1455–1465.

Kremer, K., Wirth, S. B., Reusch, A., Fäh, D., Bellwald, B., Anselmetti, F. S., Girardclos, S., and Strasser, M. (2017). Lake-sediment based paleoseismology: Limitations and perspectives from the Swiss Alps. *Quaternary Science Reviews*, 168:1–18.

Lafuente, P., Arlegui, L. E., Liesa, C. L., Pueyo, Ó., and Simón, J. L. (2014). Spatial and temporal variation of palaeoseismic activity at an intraplate, historically quiescent structure: The Concud fault (Iberian Chain, Spain). *Tectonophysics*, 632:167–187.

Lauterbach, S., Chapron, E., Brauer, A., Hüls, M., Gilli, A., Arnaud, F., Piccin, A., Nomade, J., Desmet, M., von Grafenstein, U., and Participants, D. (2012). A sedimentary record of Holocene surface runoff events and earthquake activity from Lake Iseo (Southern Alps, Italy). *The Holocene*, 22(7):749–760.

Lee, H., Chough, S., and Yoon, S. (1996). Slope-stability change from late Pleistocene to Holocene in the Ulleung Basin, East Sea (Japan Sea). *Sedimentary Geology*, 104(1-4):39–51.

Leithold, E. L., Wegmann, K. W., Bohnenstiehl, D. R., Joyner, C. N., and Pollen, A. F. (2019). Repeated megaturbidite deposition in Lake Crescent, Washington, USA, triggered by Holocene ruptures of the Lake Creek-Boundary Creek fault system. *Geological Society of America Bulletin*, 131(11).

Leithold, E. L., Wegmann, K. W., Bohnenstiehl, D. R., Smith, S. G., Noren, A., and O'Grady, R. (2018). Slope failures within and upstream of Lake Quinault, Washington, as uneven responses to Holocene earthquakes along the Cascadia subduction zone. *Quaternary Research*, 89(1):178–200. Publisher: Cambridge University Press.

Leonard, M. (2015). Consistent MMI area estimation for Australian earthquakes.

In *Proceedings of the Tenth Pacific Conference on Earthquake Engineering Building an Earthquake-Resilient Pacific*, page 9, Sidney, Australia. Geoscience Australia.

Leynaud, D., Sultan, N., and Mienert, J. (2007). The role of sedimentation rate and permeability in the slope stability of the formerly glaciated Norwegian continental margin: the Storegga slide model. *Landslides*, 4(4):297–309.

Lu, Y., Moernaut, J., Bookman, R., Waldmann, N., Wetzler, N., Agnon, A., Marco, S., Alsop, G. I., Strasser, M., and Hubert-Ferrari, A. (2021a). A New Approach to Constrain the Seismic Origin for Prehistoric Turbidites as Applied to the Dead Sea Basin. *Geophysical Research Letters*, 48(3).

Lu, Y., Moernaut, J., Waldmann, N., Bookman, R., Alsop, G. I., Hubert-Ferrari, A., Strasser, M., Agnon, A., and Marco, S. (2021b). Orbital- and millennial-scale changes in lake-levels facilitate earthquake-triggered mass failures in the Dead Sea Basin. *Geophysical Research Letters*, e2021GL093391(n/a):24. _eprint: https://agupubs.onlinelibrary.wiley.com/doi/pdf/10.1029/2021GL093391.

Ma, T., Tarasov, P. E., Huang, K., Leipe, C., Man, M., and Zheng, Z. (2022). Intensified climate drying and cooling during the last glacial culmination (20.8–17.5 cal ka BP) in the south-eastern Asian monsoon domain inferred from a high-resolution pollen record. *Quaternary Science Reviews*, 278:107371.

Maitituerdi, A., Van Daele, M., Verschuren, D., De Batist, M., and Waldmann, N. (2022). Depositional history of Lake Chala (Mt. Kilimanjaro, equatorial East Africa) from high-resolution seismic stratigraphy. *Journal of African Earth Sciences*, page 104499.

McHugh, C. M., Damuth, J. E., and Mountain, G. S. (2002). Cenozoic mass-transport facies and their correlation with relative sea-level change, New Jersey continental margin. *Marine Geology*, 184(3-4):295–334.

Melles, M., Brigham-Grette, J., Minyuk, P. S., Nowaczyk, N. R., Wennrich, V., DeConto, R. M., Anderson, P. M., Andreev, A. A., Coletti, A., Cook, T. L., Haltia-Hovi, E., Kukkonen, M., Lozhkin, A. V., Rosén, P., Tarasov, P., Vogel, H., and Wagner, B. (2012). 2.8 Million Years of Arctic Climate Change from Lake El'gygytgyn, NE Russia. *Science*, 337(6092):315–320.

Moernaut, J. (2020). Time-dependent recurrence of strong earthquake shaking near plate boundaries: A lake sediment perspective. *Earth-Science Reviews*,

210:103344.

Moernaut, J., Daele, M. V., Fontijn, K., Heirman, K., Kempf, P., Pino, M., Valdebenito, G., Urrutia, R., Strasser, M., and Batist, M. D. (2018). Larger earthquakes recur more periodically: New insights in the megathrust earthquake cycle from lacustrine turbidite records in south-central Chile. *Earth and Planetary Science Letters*, 481:9–19.

Moernaut, J., Daele, M. V., Heirman, K., Fontijn, K., Strasser, M., Pino, M., Urrutia, R., and De Batist, M. (2014). Lacustrine turbidites as a tool for quantitative earthquake reconstruction: New evidence for a variable rupture mode in south central Chile. *Journal of Geophysical Research: Solid Earth*, 119(3):1607–1633.

Moernaut, J. and De Batist, M. (2011). Frontal emplacement and mobility of sublacustrine landslides: Results from morphometric and seismostratigraphic analysis. *Marine Geology*, 285(1-4):29–45.

Moernaut, J., De Batist, M., Charlet, F., Heirman, K., Chapron, E., Pino, M., Brümmer, R., and Urrutia, R. (2007). Giant earthquakes in South-Central Chile revealed by Holocene mass-wasting events in Lake Puyehue. *Sedimentary Geology*, 195(3-4):239–256.

Moernaut, J., Verschuren, D., Charlet, F., Kristen, I., Fagot, M., and De Batist, M. (2010). The seismic-stratigraphic record of lake-level fluctuations in Lake Challa: Hydrological stability and change in equatorial East Africa over the last 140kyr. *Earth and Planetary Science Letters*, 290(1-2):214–223.

Molenaar, A., Moernaut, J., Wiemer, G., Dubois, N., and Strasser, M. (2019). Earthquake Impact on Active Margins: Tracing Surficial Remobilization and Seismic Strengthening in a Slope Sedimentary Sequence. *Geophysical Research Letters*, 46(11):6015–6023.

Molenaar, A., Van Daele, M., Vandorpe, T., Degenhart, G., De Batist, M., Urrutia, R., Pino, M., Strasser, M., and Moernaut, J. (2021). What controls the remobilization and deformation of surficial sediment by seismic shaking? Linking lacustrine slope stratigraphy to great earthquakes in South–Central Chile. *Sedimentology*, 68(6):2365–2396.

Morlock, M. (2018). *Depositional modes and post-depositional mineral formation in a Pleistocene sediment record from Lake Towuti, Indonesia*. PhD Thesis,

Universität Bern, Bern.

Morlock, M. A., Vogel, H., Nigg, V., Ordoñez, L., Hasberg, A. K. M., Melles, M., Russell, J. M., and Bijaksana, S. (2019). Climatic and tectonic controls on source-to-sink processes in the tropical, ultramafic catchment of Lake Towuti, Indonesia. *Journal of Paleolimnology*, 61(3):279–295.

Morlock, M. A., Vogel, H., Russell, J. M., Anselmetti, F. S., and Bijaksana, S. (2021). Quaternary environmental changes in tropical Lake Towuti, Indonesia, inferred from end-member modelling of X-ray fluorescence core-scanning data. *Journal of Quaternary Science*, 36(6):1040–1051. _eprint: https://onlinelibrary.wiley.com/doi/pdf/10.1002/jqs.3338.

Natawidjaja, D. H., Daryono, M. R., Prasetya, G., Udrekh, Liu, P. L.-F., Hananto, N. D., Kongko, W., Triyoso, W., Puji, A. R., Meilano, I., Gunawan, E., Supendi, P., Pamumpuni, A., Irsyam, M., Faizal, L., Hidayati, S., Sapiie, B., Kusuma, M. A., and Tawil, S. (2020). The 2018 Mw7.5 Palu 'supershear' earthquake ruptures geological fault's multi-segment separated by large bends: Results from integrating field measurements, LiDAR, swath bathymetry, and seismic-reflection data. *Geophysical Journal International*, page ggaa498.

Nayak, K., Lin, A. T.-S., Huang, K.-F., Liu, Z., Babonneau, N., Ratzov, G., Pillutla, R. K., Das, P., and Hsu, S.-K. (2021). Clay-mineral distribution in recent deep-sea sediments around Taiwan: Implications for sediment dispersal processes. *Tectonophysics*, 814:228974.

Neves, M. C., Roque, C., Luttrell, K. M., Vázquez, J. T., and Alonso, B. (2016). Impact of sea-level rise on earthquake and landslide triggering offshore the Alentejo margin (SW Iberia). *Geo-Marine Letters*, 36(6):415–424.

Omira, R., Dogan, G. G., Hidayat, R., Husrin, S., Prasetya, G., Annunziato, A., Proietti, C., Probst, P., Paparo, M. A., Wronna, M., Zaytsev, A., Pronin, P., Giniyatullin, A., Putra, P. S., Hartanto, D., Ginanjar, G., Kongko, W., Pelinovsky, E., and Yalciner, A. C. (2019). The September 28th, 2018, Tsunami In Palu-Sulawesi, Indonesia: A Post-Event Field Survey. *Pure and Applied Geophysics*, 176(4):1379–1395.

Oswald, P., Moernaut, J., Fabbri, S. C., De Batist, M., Hajdas, I., Ortner, H., Titzler, S., and Strasser, M. (2021). Combined On-Fault and Off-Fault Paleoseismic Evidence in the Postglacial Infill of the Inner-Alpine Lake

Achensee (Austria, Eastern Alps). *Frontiers in Earth Science*, 9:670952.

Owen, M., Day, S., and Maslin, M. (2007). Late Pleistocene submarine mass movements: occurrence and causes. *Quaternary Science Reviews*, 26(7-8):958–978.

Partin, J. W., Cobb, K. M., Adkins, J. F., Clark, B., and Fernandez, D. P. (2007). Millennial-scale trends in west Pacific warm pool hydrology since the Last Glacial Maximum. *Nature*, 449(7161):452–455.

Pohl, F., Eggenhuisen, J., Cartigny, M., Tilston, M., de Leeuw, J., and Hermidas, N. (2020). The influence of a slope break on turbidite deposits: An experimental investigation. *Marine Geology*, 424:106160.

Praet, N., Moernaut, J., Van Daele, M., Boes, E., Haeussler, P. J., Strupler, M., Schmidt, S., Loso, M. G., and De Batist, M. (2017). Paleoseismic potential of sublacustrine landslide records in a high-seismicity setting (south-central Alaska). *Marine Geology*, 384:103–119.

Praet, N., Van Daele, M., Collart, T., Moernaut, J., Vandekerkhove, E., Kempf, P., Haeussler, P. J., and De Batist, M. (2020). Turbidite stratigraphy in proglacial lakes: Deciphering trigger mechanisms using a statistical approach. *Sedimentology*, 67(5):2332–2359.

Ratzov, G., Cattaneo, A., Babonneau, N., Déverchère, J., Yelles, K., Bracene, R., and Courboulex, F. (2015). Holocene turbidites record earthquake supercycles at a slow-rate plate boundary. *Geology*, 43(4):331–334.

Reeves, J. M., Bostock, H. C., Ayliffe, L. K., Barrows, T. T., De Deckker, P., Devriendt, L. S., Dunbar, G. B., Drysdale, R. N., Fitzsimmons, K. E., Gagan, M. K., Griffiths, M. L., Haberle, S. G., Jansen, J. D., Krause, C., Lewis, S., McGregor, H. V., Mooney, S. D., Moss, P., Nanson, G. C., Purcell, A., and van der Kaars, S. (2013). Palaeoenvironmental change in tropical Australasia over the last 30,000 years – a synthesis by the OZ-INTIMATE group. *Quaternary Science Reviews*, 74:97–114.

Reimer, P. J., Austin, W. E. N., Bard, E., Bayliss, A., Blackwell, P. G., Bronk Ramsey, C., Butzin, M., Cheng, H., Edwards, R. L., Friedrich, M., Grootes, P. M., Guilderson, T. P., Hajdas, I., Heaton, T. J., Hogg, A. G., Hughen, K. A., Kromer, B., Manning, S. W., Muscheler, R., Palmer, J. G., Pearson, C., van der Plicht, J., Reimer, R. W., Richards, D. A., Scott, E. M.,

Southon, J. R., Turney, C. S. M., Wacker, L., Adolphi, F., Büntgen, U., Capano, M., Fahrni, S. M., Fogtmann-Schulz, A., Friedrich, R., Köhler, P., Kudsk, S., Miyake, F., Olsen, J., Reinig, F., Sakamoto, M., Sookdeo, A., and Talamo, S. (2020). The IntCal20 Northern Hemisphere Radiocarbon Age Calibration Curve (0–55 cal kBP). *Radiocarbon*, 62(4):725–757.

Russell, J. M., Barker, P., Cohen, A., Ivory, S., Kimirei, I., Lane, C., Leng, M., Maganza, N., McGlue, M., Msaky, E., Noren, A., Park Boush, L., Salzburger, W., Scholz, C., Tiedemann, R., Nuru, S., and Consortium, t. L. T. S. D. P. T. (2020a). ICDP workshop on the Lake Tanganyika Scientific Drilling Project: a late Miocene–present record of climate, rifting, and ecosystem evolution from the world's oldest tropical lake. *Scientific Drilling*, 27:53–60.

Russell, J. M. and Bijaksana, S. (2012). The Towuti Drilling Project: Paleoenvironments, Biological Evolution, and Geomicrobiology of a Tropical Pacific Lake. *Scientific Drilling*, 14:68–71.

Russell, J. M., Bijaksana, S., Vogel, H., Melles, M., Kallmeyer, J., Ariztegui, D., Crowe, S., Fajar, S., Hafidz, A., Haffner, D., Hasberg, A., Ivory, S., Kelly, C., King, J., Kirana, K., Morlock, M., Noren, A., O'Grady, R., Ordonez, L., Stevenson, J., von Rintelen, T., Vuillemin, A., Watkinson, I., Wattrus, N., Wicaksono, S., Wonik, T., Bauer, K., Deino, A., Friese, A., Henny, C., Imran, Marwoto, R., Ngkoimani, L. O., Nomosatryo, S., Safiuddin, L. O., Simister, R., and Tamuntuan, G. (2016). The Towuti Drilling Project: paleoenvironments, biological evolution, and geomicrobiology of a tropical Pacific lake. *Scientific Drilling*, 21:29–40.

Russell, J. M., Vogel, H., Bijaksana, S., Melles, M., Deino, A., Hafidz, A., Haffner, D., Hasberg, A. K., Morlock, M., von Rintelen, T., Sheppard, R., Stelbrink, B., and Stevenson, J. (2020b). The late quaternary tectonic, biogeochemical, and environmental evolution of ferruginous Lake Towuti, Indonesia. *Palaeogeography, Palaeoclimatology, Palaeoecology*, page 109905.

Russell, J. M., Vogel, H., Konecky, B. L., Bijaksana, S., Huang, Y., Melles, M., Wattrus, N., Costa, K., and King, J. W. (2014). Glacial forcing of central Indonesian hydroclimate since 60,000 y B.P. *Proceedings of the National Academy of Sciences*, 111(14):5100–5105.

Sabatier, P., Moernaut, J., Bertrand, S., Van Daele, M., Kremer, K., Chaumillon,

E., and Arnaud, F. (2022). A Review of Event Deposits in Lake Sediments. *Quaternary*, 5(3):34.

Sammartini, M., Moernaut, J., Kopf, A., Stegmann, S., Fabbri, S., Anselmetti, F., and Strasser, M. (2021). Propagation of frontally confined subaqueous landslides: Insights from combining geophysical, sedimentological, and geotechnical analysis. *Sedimentary Geology*, 416:105877.

Schnellmann, M., Anselmetti, F. S., Giardini, D., and McKENZIE, J. A. (2005). Mass movement-induced fold-and-thrust belt structures in unconsolidated sediments in Lake Lucerne (Switzerland): Mass movement-induced deformation structures. *Sedimentology*, 52(2):271–289.

Schnellmann, M., Anselmetti, F. S., Giardini, D., McKenzie, J. A., and Ward, S. N. (2002). Prehistoric earthquake history revealed by lacustrine slump deposits. *Geology*, 30(12):1131.

Schwestermann, T., Huang, J., Konzett, J., Kioka, A., Wefer, G., Ikehara, K., Moernaut, J., Eglinton, T. I., and Strasser, M. (2020). Multivariate Statistical and Multiproxy Constraints on Earthquake-Triggered Sediment Remobilization Processes in the Central Japan Trench. *Geochemistry, Geophysics, Geosystems*, 21(6).

Shanahan, T. M., Overpeck, J. T., Wheeler, C. W., Beck, J. W., Pigati, J. S., Talbot, M. R., Scholz, C. A., Peck, J., and King, J. W. (2006). Paleoclimatic variations in West Africa from a record of late Pleistocene and Holocene lake level stands of Lake Bosumtwi, Ghana. *Palaeogeography, Palaeoclimatology, Palaeoecology*, 242(3-4):287–302.

Shiki, T., Kumon, F., Inouchi, Y., Kontani, Y., Sakamoto, T., Tateishi, M., Matsubara, H., and Fukuyama, K. (2000). Sedimentary features of the seismo-turbidites, Lake Biwa, Japan. *Sedimentary Geology*, 135(1-4):37–50.

Shinohara, H., Yoshikawa, S., and Miyabuchi, Y. (2015). Degassing Activity of a Volcanic Crater Lake: Volcanic Plume Measurements at the Yudamari Crater Lake, Aso Volcano, Japan. In Rouwet, D., Christenson, B., Tassi, F., and Vandemeulebrouck, J., editors, *Volcanic Lakes*, pages 201–217. Springer Berlin Heidelberg, Berlin, Heidelberg.

Silver, E. A., McCaffrey, R., and Smith, R. B. (1983). Collision, rotation, and the initiation of subduction in the evolution of Sulawesi, Indonesia. *Journal of*

Geophysical Research: Solid Earth, 88(B11):9407–9418.

Socquet, A., Simons, W., Vigny, C., McCaffrey, R., Subarya, C., Sarsito, D., Ambrosius, B., and Spakman, W. (2006). Microblock rotations and fault coupling in SE Asia triple junction (Sulawesi, Indonesia) from GPS and earthquake slip vector data. *Journal of Geophysical Research*, 111(B8):B08409.

St-Onge, G., Mulder, T., Piper, D. J., Hillaire-Marcel, C., and Stoner, J. S. (2004). Earthquake and flood-induced turbidites in the Saguenay Fjord (Québec): a Holocene paleoseismicity record. *Quaternary Science Reviews*, 23(3-4):283–294.

Stevens, C., McCaffrey, R., Bock, Y., Genrich, J., Endang, Subarya, C., Puntodewo, S. S. O., Fauzi, and Vigny, C. (1999). Rapid rotations about a vertical axis in a collisional setting revealed by the Palu Fault, Sulawesi, Indonesia. *Geophysical Research Letters*, 26(17):2677–2680.

Strasser, M., Berberich, T., Fabbri, S., Hilbe, M., Huang, J.-J. S., Lauterbach, S., Ortler, M., Rechschreiter, H., Brauer, A., Anselmetti, F., and Kowarik, K. (2020). Geomorphology and event-stratigraphy of recent mass-movement processes in Lake Hallstatt (UNESCO World Heritage Cultural Landscape, Austria). *Geological Society, London, Special Publications*, 500(1):405–426.

Strasser, M., Hilbe, M., and Anselmetti, F. S. (2011). Mapping basin-wide subaquatic slope failure susceptibility as a tool to assess regional seismic and tsunami hazards. *Marine Geophysical Research*, 32(1-2):331–347.

Strasser, M., Monecke, K., Schnellmann, M., and Anselmetti, F. S. (2013). Lake sediments as natural seismographs: A compiled record of Late Quaternary earthquakes in Central Switzerland and its implication for Alpine deformation. *Sedimentology*, 60(1):319–341.

Strasser, M., Stegmann, S., Bussmann, F., Anselmetti, F. S., Rick, B., and Kopf, A. (2007). Quantifying subaqueous slope stability during seismic shaking: Lake Lucerne as model for ocean margins. *Marine Geology*, 240(1-4):77–97.

Strupler, M., Hilbe, M., Anselmetti, F. S., Kopf, A. J., Fleischmann, T., and Strasser, M. (2017). Probabilistic stability evaluation and seismic triggering scenarios of submerged slopes in Lake Zurich (Switzerland). *Geo-Marine Letters*, 37(3):241–258.

Sturm, M. and Matter, A. (1978). Turbidites and Varves in Lake Brienz

(Switzerland): Deposition of Clastic Detritus by Density Currents. In *Modern
and Ancient Lake Sediments*, pages 147–168. John Wiley & Sons, Ltd. _eprint:
https://onlinelibrary.wiley.com/doi/pdf/10.1002/9781444303698.ch8.

Sultan, N., Cochonat, P., Canals, M., Cattaneo, A., Dennielou, B., Haflidason, H.,
Laberg, J., Long, D., Mienert, J., Trincardi, F., Urgeles, R., Vorren, T., and
Wilson, C. (2004). Triggering mechanisms of slope instability processes and
sediment failures on continental margins: a geotechnical approach. *Marine
Geology*, 213(1-4):291–321.

Talling, P. J. (2021). Fidelity of turbidites as earthquake records. *Nature Geoscience*,
14(3):113–116.

Tamuntuan, G., Bijaksana, S., King, J., Russell, J., Fauzi, U., Maryunani, K.,
Aufa, N., and Safiuddin, L. O. (2015). Variation of magnetic properties in
sediments from Lake Towuti, Indonesia, and its paleoclimatic significance.
Palaeogeography, Palaeoclimatology, Palaeoecology, 420:163–172.

Tauhid, Y. I. and Arifian, J. (2000). Pengamatan Jangka Panjang Kondisi Danau
Towuti. *Jurnal Sains & Teknologi Modifikasi Cuaca*, 1(1):93–100.

ten Brink, U., Andrews, B., and Miller, N. (2016). Seismicity and sedimentation
rate effects on submarine slope stability. *Geology*, 44(7):563–566.

Tohari, A., Dani Wardhana, D., Hanif, M., and Koizumi, K. (2021). Understanding
of subsurface conditions controlling flow liquefaction occurrence during the
2018 Palu earthquake based on resistivity profiles. *E3S Web of Conferences*,
331:03002.

Urlaub, M., Talling, P. J., Zervos, A., and Masson, D. (2015). What causes large
submarine landslides on low gradient (<2°) continental slopes with slow (~0.15
m/kyr) sediment accumulation?: LARGE SUBMARINE LANDSLIDES
ON LOW GRADIENTS. *Journal of Geophysical Research: Solid Earth*,
120(10):6722–6739.

Vaillant, J. J., Haffner, G. D., and Cristescu, M. E. (2011). The Ancient Lakes
of Indonesia: Towards Integrated Research on Speciation. *Integrative and
Comparative Biology*, 51(4):634–643.

Van Daele, M., Moernaut, J., Doom, L., Boes, E., Fontijn, K., Heirman, K.,
Vandoorne, W., Hebbeln, D., Pino, M., Urrutia, R., Brümmer, R., and
De Batist, M. (2015). A comparison of the sedimentary records of the 1960

and 2010 great Chilean earthquakes in 17 lakes: Implications for quantitative lacustrine palaeoseismology. *Sedimentology*, 62(5):1466–1496.

Vandekerkhove, E., Van Daele, M., Praet, N., Cnudde, V., Haeussler, P. J., and De Batist, M. (2020). Flood-triggered versus earthquake-triggered turbidites: A sedimentological study in clastic lake sediments (Eklutna Lake, Alaska). *Sedimentology*, 67(1):364–389.

Vanneste, K., Wils, K., and Van Daele, M. (2018). Probabilistic Evaluation of Fault Sources Based on Paleoseismic Evidence From Mass-Transport Deposits: The Example of Aysén Fjord, Chile. *Journal of Geophysical Research: Solid Earth*, 123(11):9842–9865. Publisher: John Wiley & Sons, Ltd.

Villeneuve, M., Gunawan, W., Cornee, J.-J., and Vidal, O. (2002). Geology of the central Sulawesi belt (eastern Indonesia): constraints for geodynamic models. *International Journal of Earth Sciences*, 91(3):524–537.

Vogel, H., Russell, J. M., Cahyarini, S. Y., Bijaksana, S., Wattrus, N., Rethemeyer, J., and Melles, M. (2015). Depositional modes and lake-level variability at Lake Towuti, Indonesia, during the past ~29 kyr BP. *Journal of Paleolimnology*, 54(4):359–377.

Völker, D., Geersen, J., Behrmann, J. H., and Weinrebe, W. R. (2012). Submarine Mass Wasting Off Southern Central Chile: Distribution and Possible Mechanisms of Slope Failure at an Active Continental Margin. In Yamada, Y., Kawamura, K., Ikehara, K., Ogawa, Y., Urgeles, R., Mosher, D., Chaytor, J., and Strasser, M., editors, *Submarine Mass Movements and Their Consequences*, pages 379–389. Springer Netherlands, Dordrecht.

Vuillemin, A., Wirth, R., Kemnitz, H., Schleicher, A. M., Friese, A., Bauer, K. W., Simister, R., Nomosatryo, S., Ordoñez, L., Ariztegui, D., Henny, C., Crowe, S. A., Benning, L. G., Kallmeyer, J., Russell, J. M., Bijaksana, S., Vogel, H., and the Towuti Drilling Project Science Team (2019). Formation of diagenetic siderite in modern ferruginous sediments. *Geology*, 47(6):540–544.

Waldmann, N., Stein, M., Ariztegui, D., and Starinsky, A. (2009). Stratigraphy, depositional environments and level reconstruction of the last interglacial Lake Samra in the Dead Sea basin. *Quaternary Research*, 72(1):1–15.

Watkinson, I. M. and Hall, R. (2017). Fault systems of the eastern Indonesian triple junction: evaluation of Quaternary activity and implications for seismic

hazards. *Geological Society, London, Special Publications*, 441(1):71–120.

Watkinson, I. M. and Hall, R. (2019). Impact of communal irrigation on the 2018 Palu earthquake-triggered landslides. *Nature Geoscience*, 12(11):940–945.

Wicaksono, S. A., Russell, J. M., Holbourn, A., and Kuhnt, W. (2017). Hydrological and vegetation shifts in the Wallacean region of central Indonesia since the Last Glacial Maximum. *Quaternary Science Reviews*, 157:152–163.

Wiemer, G., Moernaut, J., Stark, N., Kempf, P., De Batist, M., Pino, M., Urrutia, R., de Guevara, B. L., Strasser, M., and Kopf, A. (2015). The role of sediment composition and behavior under dynamic loading conditions on slope failure initiation: a study of a subaqueous landslide in earthquake-prone South-Central Chile. *International Journal of Earth Sciences*, 104(5):1439–1457.

Wien, K., Holz, C., Kölling, M., and Schulz, H. D. (2006). Age models for pelagites and turbidites from the Cap Timiris Canyon off Mauritania. *Marine and Petroleum Geology*, 23(3):337–352.

Wilhelm, Nomade, J., Crouzet, C., Litty, C., Sabatier, P., Belle, S., Rolland, Y., Revel, M., Courboulex, F., Arnaud, F., and Anselmetti, F. S. (2016a). Quantified sensitivity of small lake sediments to record historic earthquakes: Implications for paleoseismology: Lake sensitivity to record earthquakes. *Journal of Geophysical Research: Earth Surface*, 121(1):2–16.

Wilhelm, B., Amann, B., Corella, J. P., Rapuc, W., Giguet-Covex, C., Merz, B., and Støren, E. (2022). Reconstructing Paleoflood Occurrence and Magnitude from Lake Sediments. *Quaternary*, 5(1):9.

Wilhelm, B., Vogel, H., and Anselmetti, F. S. (2017). A multi-centennial record of past floods and earthquakes in Valle d'Aosta, Mediterranean Italian Alps. *Natural Hazards and Earth System Sciences*, 17(5):613–625.

Wilhelm, B., Vogel, H., Crouzet, C., Etienne, D., and Anselmetti, F. S. (2016b). Frequency and intensity of palaeofloods at the interface of Atlantic and Mediterranean climate domains. *Climate of the Past*, 12(2):299–316.

Willemann, R. J. and Storchak, D. A. (2001). Data Collection at the International Seismological Centre. *Seismological Research Letters*, 72(4):440–453.

Wils, K., Daryono, M. R., Praet, N., Santoso, A. B., Dianto, A., Schmidt, S., Vervoort, M., Huang, J.-J. S., Kusmanto, E., Suandhi, P., Natawidjaja, D. H., and De Batist, M. (2021a). The sediments of Lake Singkarak and

Lake Maninjau in West Sumatra reveal their earthquake, volcanic and rainfall history. *Sedimentary Geology*, 416:105863.

Wils, K., Deprez, M., Kissel, C., Vervoort, M., Van Daele, M., Daryono, M. R., Cnudde, V., Natawidjaja, D. H., and De Batist, M. (2021b). Earthquake doublet revealed by multiple pulses in lacustrine seismo-turbidites. *Geology*, 49(11):1301–1306.

Wils, K., Van Daele, M., Kissel, C., Moernaut, J., Schmidt, S., Siani, G., and Lastras, G. (2020). Seismo-Turbidites in Aysén Fjord (Southern Chile) Reveal a Complex Pattern of Rupture Modes Along the 1960 Megathrust Earthquake Segment. *Journal of Geophysical Research: Solid Earth*, 125(9):e2020JB019405. Publisher: John Wiley & Sons, Ltd.

Windler, G., Tierney, J. E., Zhu, J., and Poulsen, C. J. (2020). Unraveling Glacial Hydroclimate in the Indo-Pacific Warm Pool: Perspectives From Water Isotopes. *Paleoceanography and Paleoclimatology*, 35(12):17. Publisher: John Wiley & Sons, Ltd.

Wu, D., Ren, Z., Liu, J., Chen, J., Guo, P., Yin, G., Ran, H., Li, C., and Yang, X. (2021). Coseismic surface rupture during the 2018 Mw 7.5 Palu earthquake, Sulawesi Island, Indonesia. *GSA Bulletin*, 133(5-6):1157–1166.

8 Supplementary material
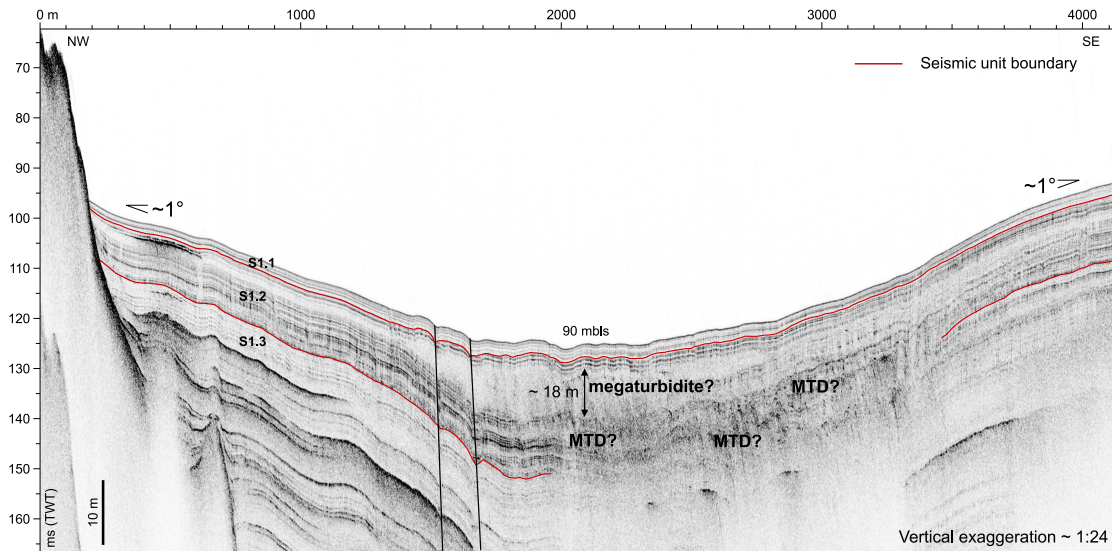
Figure S1: Seismic profile in the eastern part of basin C. At the edges of this profile, the seismic units S1.1, S1.2 and S1.3 are well defined. In the centre of this section, a wide ($\sim$ 2 km) and thick ($\sim$ 18 m) transparent facies occurs that may be interpreted as a mega turbidite. This CHIRP seismic profile is the only one in this part of the lake, and the bedrock highs that divide the lake into separate basins do not allow the event to be correlated to a piston core. The indicated faults and possible MTDs at the base of Unit S1.1 clearly indicate a tectonically active and sensitive zone.
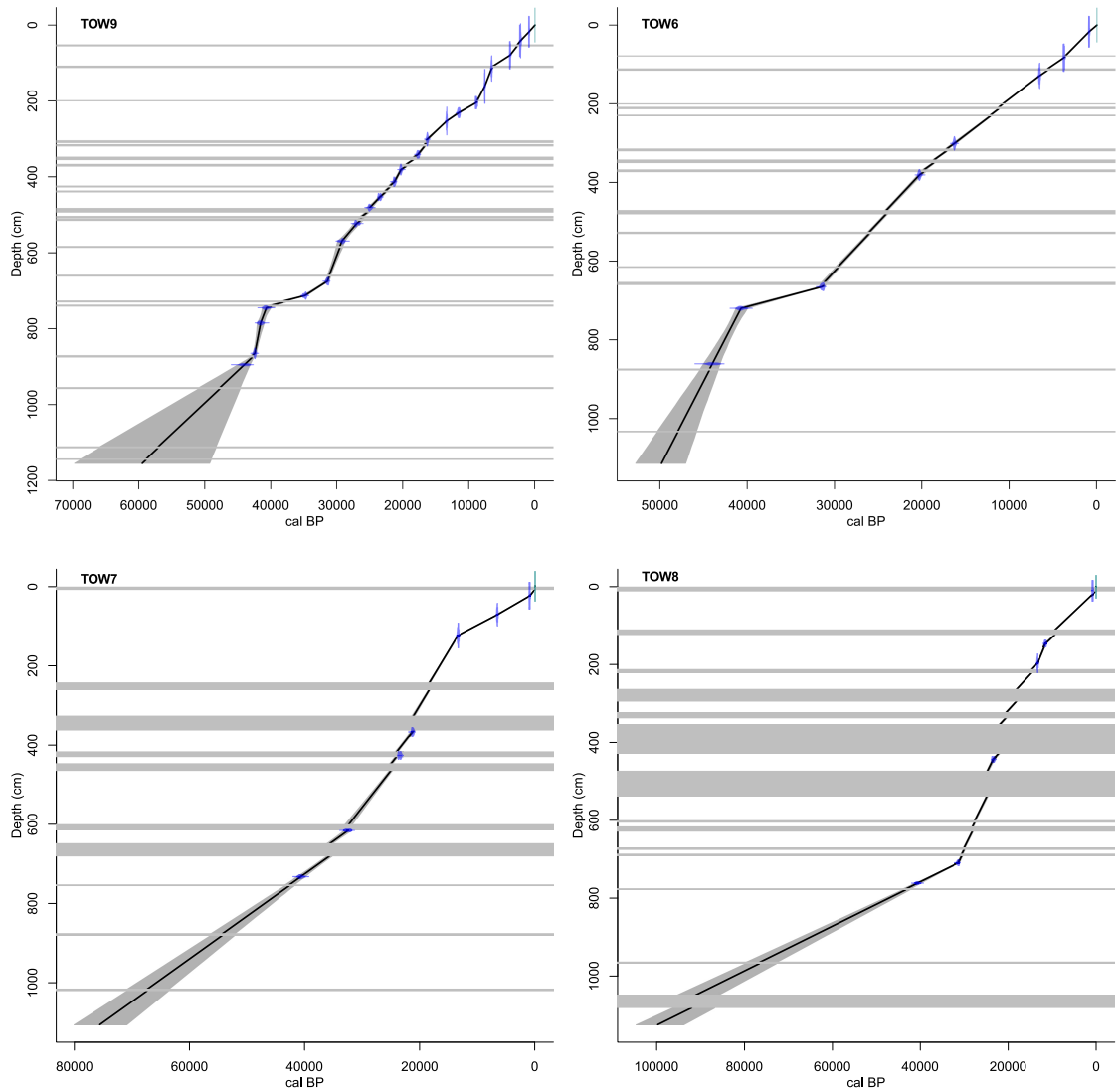
Figure S2: Age-depth models for cores TOW6, TOW7, TOW8 and TOW9 from Lake Towuti, using R package CLAM based on ages measured on core TOW9.
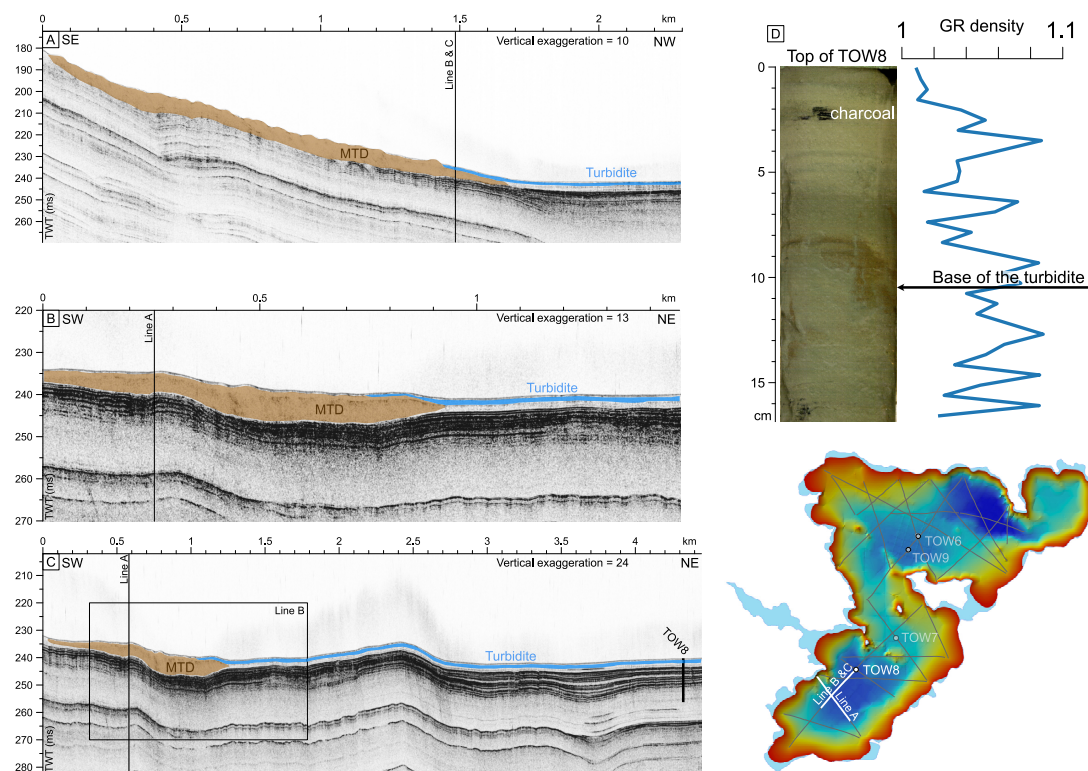
Figure S3: (A), (B) and (C) - CHIRP seismic profiles showing a recent MTD probably related to the historic 1941 earthquake. The seismic lines are indicated in white on the map. (D) Image and Gamma-Ray density of the top of core TOW8.
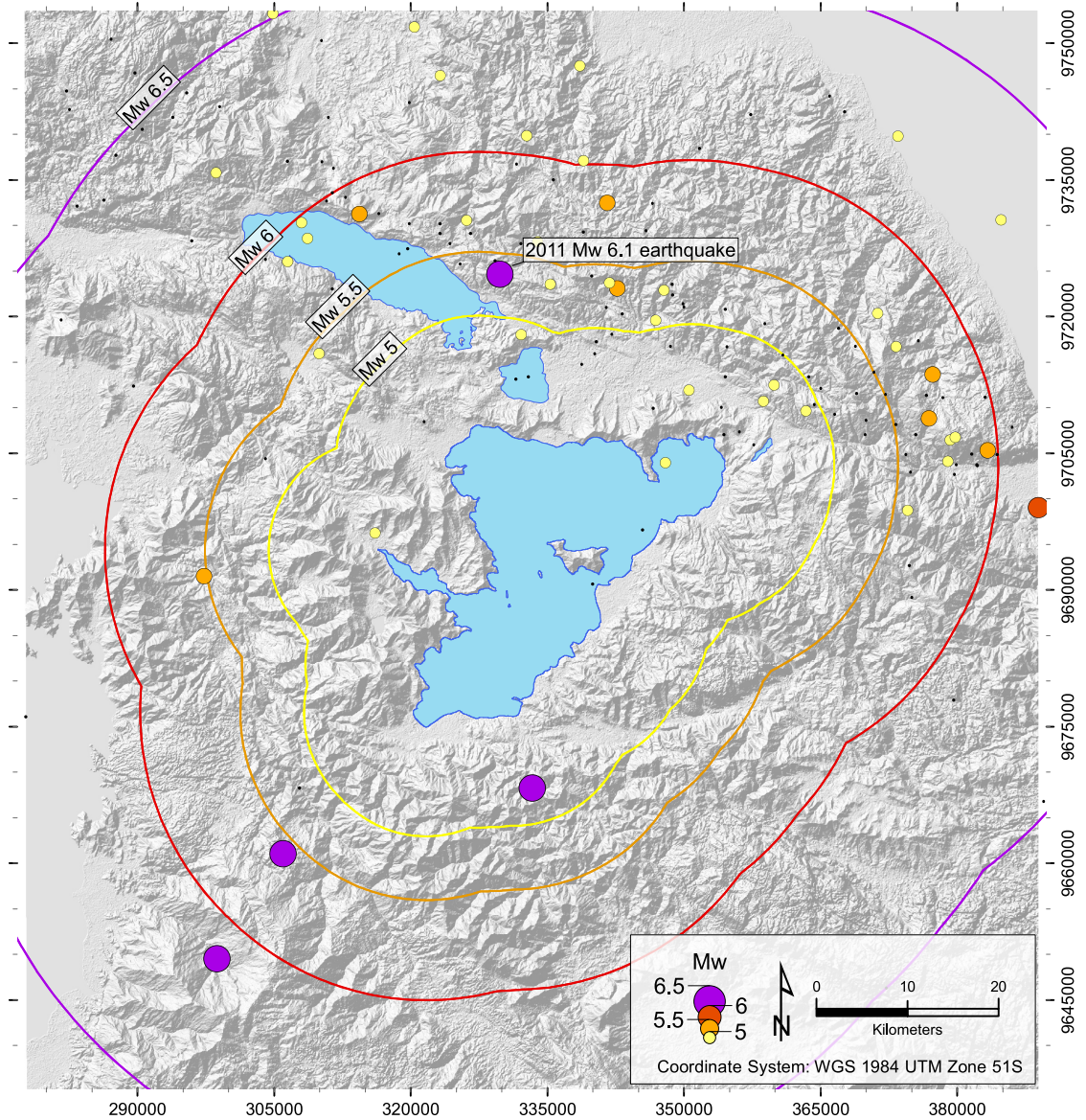
Figure S4: Map of the historical earthquakes from 1924 to 2022, with events of Mw ≥ 4.5 and depth ≤ 35 km. The buffer areas are estimated qualitatively, based on the 2011 Mw 6.1 earthquake which has reached the shoreline of Lake Towuti with an Intensity of VI.

Climate-controlled sensitivity of lake sediments to record earthquake-related mass wasting in tropical Lake Towuti during the past 40 kyr
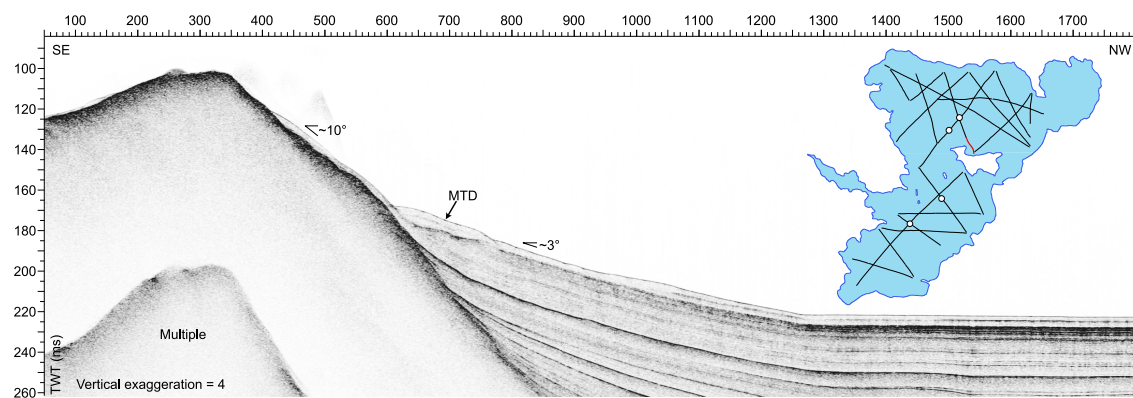
Figure S5: CHIRP seismic profile from Loeha Island to deep Basin B, showing sediment accumulation on slopes with different angles. The MTD at the base of the 10° slope angle suggests some slope charging.
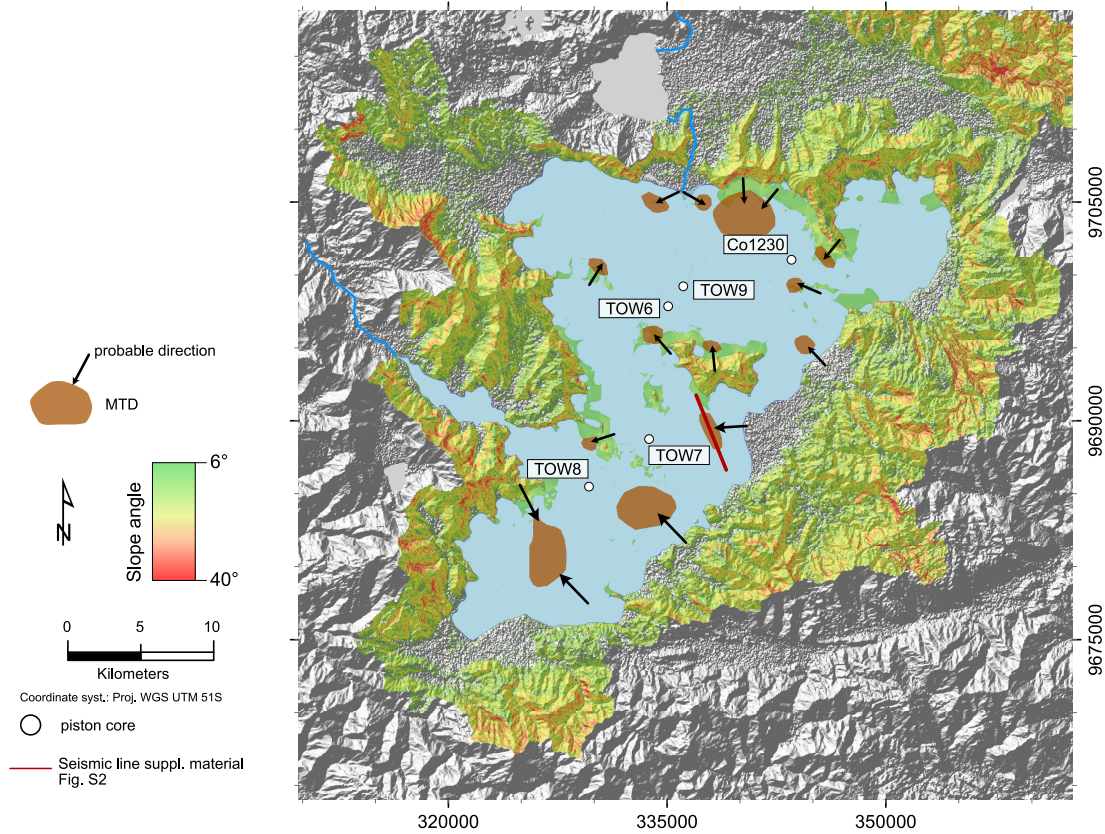
Figure S6: Slope map of the immediate catchment of Lake Towuti (terrestrial and subaqueous), with the MTD locations observed on the CHIRP and single channel seismic data. The black arrows indicate the probable direction of the sediment failure based on the slope inclination and direction as well as the morphology of the MTDs.

Climate-controlled sensitivity of lake sediments to record earthquake-related mass wasting in tropical Lake Towuti during the past 40 kyr

Table S1: Catalogue of turbidites identified on piston cores TOW9 (Basin B), TOW6 (Basin B), TOW7 (Basin C) and TOW8 (Basin D), based on macroscopic observations and gamma ray density data. Estimated ages of turbidites older than the base of core TOW9 are not included due to uncertainty in the extrapolation of sedimentation rates.

Core	Unit	depth top (cmblf)	thickness	Age_top
TOW9	L1a	52	3	2847
TOW9	L1a	108	4	6220
TOW9	L1a	199	1	10083
TOW9	L1b	305	5	16448
TOW9	L1b	315	4	16675
TOW9	L1b	348	3	18204
TOW9	L1b	352	3	18280
TOW9	L1b	367	5	19193
TOW9	L1b	424	3	21959
TOW9	L1b	437	3	22607
TOW9	L1b	483	2	25123
TOW9	L1b	487	2	25272
TOW9	L1b	490	3	25347
TOW9	L1b	504	4	26169
TOW9	L1b	511	4	26393
TOW9	L1b	583	3	29520
TOW9	L1b	659	3	31114
TOW9	L1b	727	3	37976
TOW9	L1b	738	3	39786
TOW9	L1c	871	4	42771
TOW9	L1c	955	3	47577
TOW9	L1c	1111	3	56228
TOW9	L1c	1143	2	57970
TOW6	L1a	78	1	3557
TOW6	L1a	112	3	5596
TOW6	L1a	200	1	10717
TOW6	L1a	209	4	11189
TOW6	L1a	229	2	12133
TOW6	L1b	315	4	17154
TOW6	L1b	343	8	18615
TOW6	L1b	368	5	19758
TOW6	L1b	471	10	24075
TOW6	L1b	526	6	26023
TOW6	L1b	614	2	29578
TOW6	L1b	654	6	31187
TOW6	L1b	689	9	35457
TOW6	L1c	874	1	44291
TOW6	L1c	876	1	44314
TOW6	L1c	1032	2	47928
TOW7	L1a	1	6	46
TOW7	L1b	243	17	18314
TOW7	L1b	327	35	21091
TOW7	L1b	417	12	24000
TOW7	L1b	447	17	24968

81

Table S1 (continued)

TOW7	L1b	600	14	32337
TOW7	L1b	649	31	35614
TOW7	L1c	876	4	54251
TOW7	L1c	1016	4	67315
TOW8	L1a	1	10	30
TOW8	L1b	212	13	14634
TOW8	L1b	262	32	18117
TOW8	L1b	327	14	20547
TOW8	L1b	355	69	22005
TOW8	L1b	425	1	22086
TOW8	L1b	427	1	22167
TOW8	L1b	474	11	24778
TOW8	L1b	487	53	24866
TOW8	L1b	596	9	27408
TOW8	L1b	616	12	28153
TOW8	L1b	670	5	30037
TOW8	L1b	686	5	30563
TOW8	L1c	964	3	76468
TOW8	L1c	1049	14	91135
TOW8	L1c	1067	14	91850

Chapter 3

Late Quaternary seismic stratigraphy and sedimentary borehole analysis of Lake Towuti

Picture of the TDP borehole platform on Lake Towuti (picture: Marina Morlock).

Late Quaternary seismic stratigraphy and sedimentary borehole analysis of Lake Towuti

Tournier, N.[1], Fabbri, S.C.[1], Anselmetti, F.S.[1], Cahyarini, S.Y.[2], Bijaksana, S.[3], Wattrus, N.[4], Russell, J.M.[5], Vogel, H.[1], TDP team

[1]Institute of Geological Sciences & Oeschger Centre of Climate Change Research, University of Bern, Baltzerstr. 1+3, 3012, Bern, Switzerland

[2]Research Centre for Climate and Atmosphere, National Research and Innovation Agency (BRIN), Indonesia

[3]Faculty of Mining and Petroleum Engineering, Institut Teknologi Bandung, 15 Bandung, 40132, Indonesia

[4]Large Lakes Observatory & Dept. of Earth and Environmental Sciences, University of Minnesota Duluth, Duluth, MN, 55812, USA

[5]Department of Earth, Environmental, And Planetary Sciences, Brown University, Box 1846, Providence, RI, 02912, USA

1 Introduction

Indonesia is located at the junction of the converged Great Pacific, Indo-Australian, Philippine, and Eurasian plates, making the tectonics of this area one of the most active in the world. As evidence, the biggest earthquakes, responsible for tsunamis and landslides, causing hundreds of thousands of fatalities, i.e. the 2004 Mw 9.1 Great Sumatra-Andaman Earthquake, triggered along the Sunda-Andaman trench system (Lay et al., 2005). The island of Sulawesi is bordered to the north and to the east by subduction zones (Fig. 3.1). The Tolo trust, to the east, is responsible for the formation of the island since the Oligocene (Robert and Bousquet, 2013) with the displacement moving the oceanic crust upward. Between these two subduction zones, the island is trough by a fast-slipping left-lateral strike-slip fault system, with the Palu-Koro Fault PKF, the Matano Fault MF and the Lawanopo Fault LF. Since the early 1900's, more than 200 magnitude M $\geq$ 5 earthquakes occurred along this strike-slip fault system ("International Seismological Centre", 2023). This system is responsible for the Mw 7.5 Palu "supershear" earthquake in 2018 in the northern part of the PKF (Bao et al., 2019; Natawidjaja et al., 2020; Socquet et al., 2019).

Before the invention of instrumental tools to record earthquakes, data on past events was lacking on the island of Sulawesi, which is considered one of the most tectonic places in the world. Therefore, the return period of major events is imprecise. The tropical setting, with high erosion and dense vegetation cover, makes the field expeditions difficult on land. However, Sulawesi contains 3 ancient lakes (Lake Matano, Lake Poso and Lake Towuti), and the lacustrine sediments are well known to record climate and environmental changes and tectonic activity (Costa et al., 2015; Crowe et al., 2008; Damanik et al., 2024; Morlock et al., 2019; Russell and Bijaksana, 2012). Previous studies clearly show that climate fluctuations induce modifications in the sediment composition, and the tectonic events destabilise the slope, triggering sediment collapse.

The method of correlating seismic stratigraphy with sediment core analysis is used and has been proven for decades over the world (Chapron et al., 2006; Colman et al., 2003; Daxer et al., 2022; Maitituerdi et al., 2022). In 2023, the sensitivity to record earthquakes of Lake Towuti has been studied over the last 40 kyr and highlights the influence of the climate on the capacity of the lake to generate earthquake-related turbidites (Tournier et al., 2023). This study extends this approach to the 1 Myr sediment drill core record and available airgun seismic data to differentiate between the climatic control and long-term tectonic processes on the paleoseismological record in the long-lived Lake Towuti
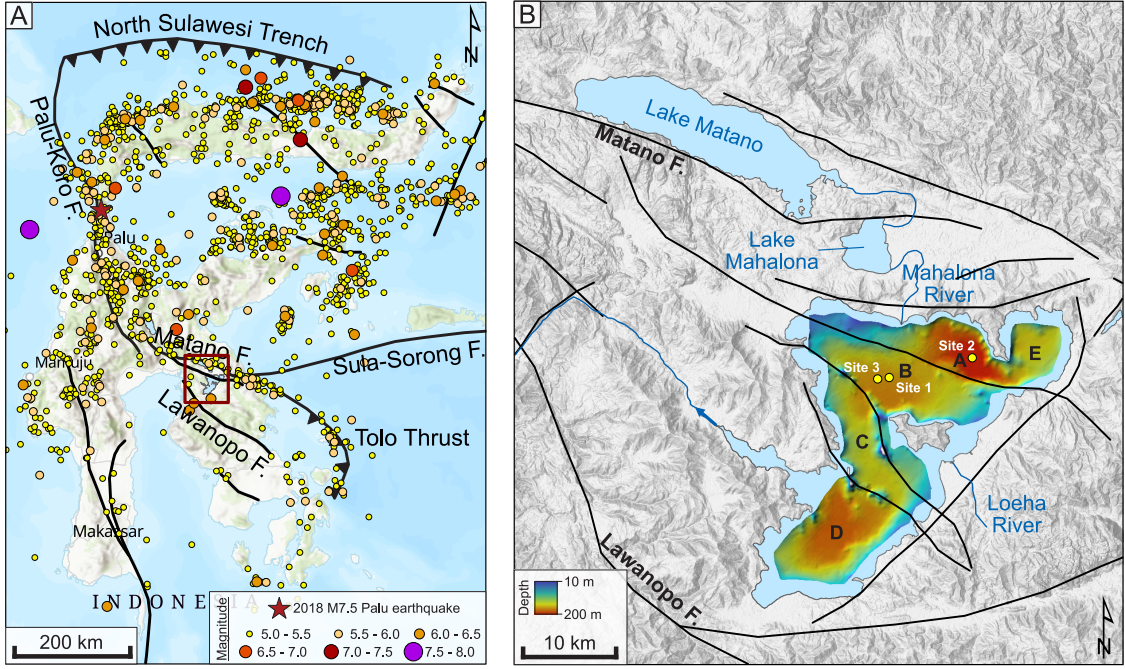
Figure 3.1: A. Tectonic map of the Island of Sulawesi with the M ≥ 5 earthquakes recorded since 1924 and depth < 35 km (source: USGS catalogue). B. Map of the Malili Lake system and the bathymetric data of Lake Towuti generated with the seismic data. The letters A-E are the names of the basins of Lake Towuti.

setting. Such an approach is thought to enable the detection of tectonic phases and earthquake evidence associated with the Sulawesi strike-slip fault system, which is still active nowadays.

2 Study site

2.1 Lake Towuti

Lake Towuti (2.75°S, 121.5°E) is located in central Sulawesi at 318 m above sea level. It is one of the largest lakes in Indonesia, second to Lake Toba. Previous studies in the framework of the Towuti Drilling Project (TDP) have already provided insight into depositional processes since the middle Pleistocene (Morlock et al., 2021; Russell et al., 2016; Sheppard et al., 2021; Ulfers et al., 2021; Vuillemin et al., 2020). The climate was drier during the Last Glacial Maximum (Wicaksono et al., 2015), with notably lower

lake levels (Vogel et al., 2015). During that phase, an increased turbidite deposition has
been reported in several piston cores in the lake, likely both climate- and seismic-induced
(Tournier et al., 2023).

2.2   Seismic settings

The earthquake catalogue around Lake Towuti contains only the events from 1924. The
intensity maps of only three events are available (USGS Shakemap). Nevertheless, the
Intensity Prediction Equation has been calculated, and buffer areas are defined around
Lake Towuti's edges to estimate the earthquakes that potentially reached the shoreline
with an intensity $\geq$ VI (Fig. 3.2), the minimum intensity estimate to generate a MTD
(Van Daele et al., 2015). We reported that height events since 1924 likely triggered
sufficient intensities to generate MTDs (Fig. 3.2).

2.3   Borehole descriptions

Macroscopic observations of the TDP boreholes' bedrock Unit 2 (Russell et al., 2020) show
tens of meters of peat formation and lithified mafic conglomerate paleosol. Overlying
this paleosol, a thin layer of coarse gravel suggests a transition from an open basin with
river channels and swamps to a deeper lacustrine basin during the early phases of basin
formation and subsidence.

After the initial subsidence, the low-energy environment of Lake Towuti induces
the deposition of clastic clay and silt sediment (Unit 1). The entire lacustrine succession
was deposited during the Pleistocene, with a base estimated at 1 Ma. However, the
mineralogy reveals significant changes in the source of the sediments and the depositional
conditions over the lake's history (Morlock, 2018). Changes in %Fe and %Siderite, from
high values at the base to low values at the top indicate the tectonic evolution of the lake
and the creation of accommodation space (Russell et al., 2020).

The lower Unit 1A (Fig. 3.3) is assimilated to the establishment of the permanent
lake. It is composed of high clay content and suggests a low transport energy at the coring
site. An increase in lake surface area induced a pulse of basin extension after the last peat
formation, shifting the coring site to a distal position in the lake.

Unit 1B is representative of a deep-water environment at Sites 1 and 3 without
major tectonic disturbance. Units 1A and 1B have sediment compositions indicating a very
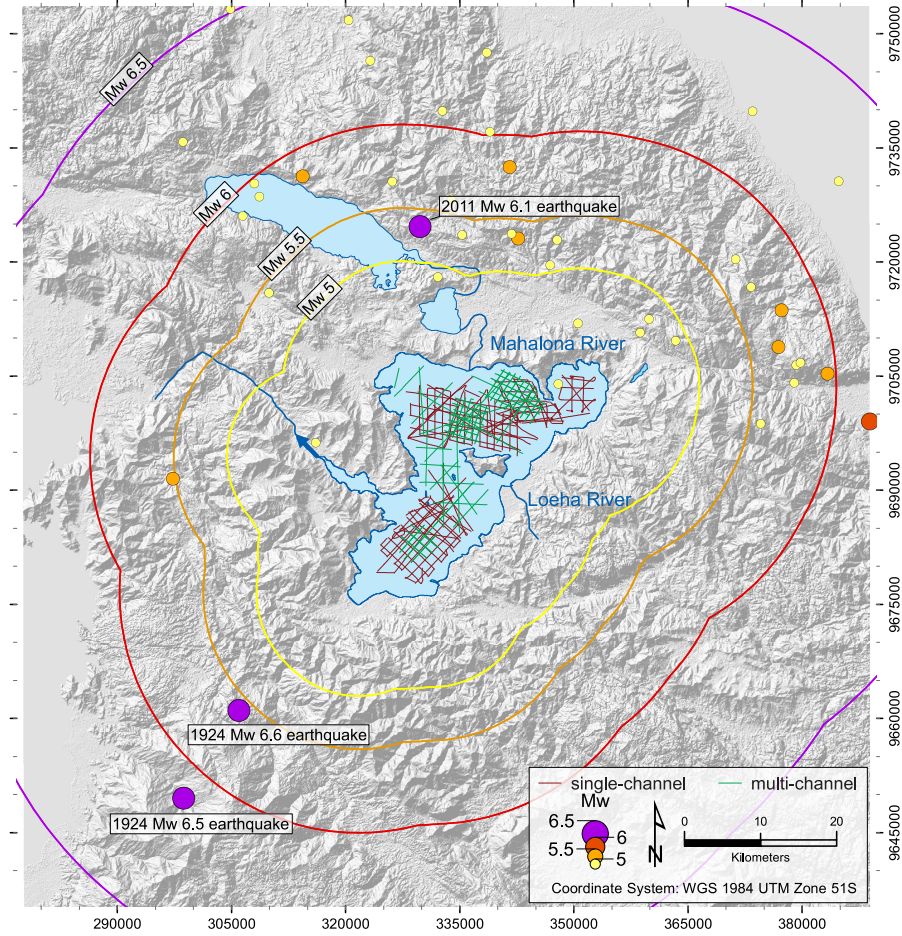
Figure 3.2: Digitalization of the earthquake magnitude's buffer areas to reach the edge of Lake Towuti with an Intensity $\geq$ VI. The single- and multi-channel survey grids are displayed on the lake.

reduced or absent influence of the Mahalona River, which delivers most Mg-serpentine-rich sediment to the lake at present (Morlock (2018), Fig. 3.3). Sediments are dominated by Si, suggesting the Loeha River is the main source of sediment (Hasberg et al., 2019).

Unit 1C shows fundamental changes in the hydrology of Lake Towuti. At 30 mcd (metre composite depth), the mineralogy changes abruptly to high serpentine and lower kaolinite content of the sediment. In this unit, the Mahalona River is the most important source of serpentine-rich material in the northern lake basin, indicated by the high amount of Mg (Fig. 3.3).
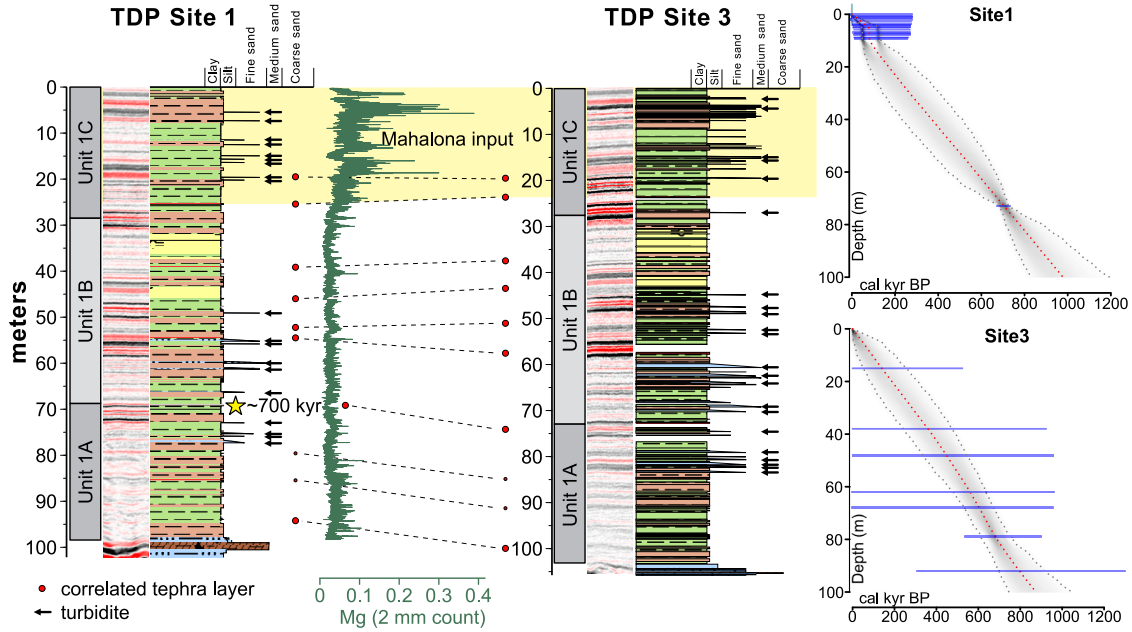
Figure 3.3: Stratigraphic logs of unit 1 of the boreholes Site 1 and Site 3. The Mg XRF data for Site 1 is representative of Mahalona River input. The yellow area shows the sections where the Mahalona River is the main source of sediment input. The age-depth models for both sites are displayed on the right. (from Russell et al. (2020)).

3 Material and methods

3.1 Seismic surveys

This study combines two airgun seismic datasets collected between 2010 and 2013 (Russell and Bijaksana, 2012; Russell et al., 2016) for a total of more than 1000 km of seismic lines (Fig. 3.2). The material used for the Single-Channel (hereafter SC) and the Multi-Channel (hereafter MC) is a Teledyne Bolt™ 600B equipped with 5 in3 chambers and a 150 m long Geometrics™ GeoEel Solid™ analogue streamer using 24-channel Geometrics™ Geode seismograph.

We used the seismo-stratigraphic interpretation software Kingdom™ (v.2022) provided by HIS Markit to analyse the SEGY files generated by the surveys. No Bandpass filter has been used for both SC and MC. The seismo-bathymetric map has been generated by tracing the sediment surface horizon on the SC, MC, and CHIRP data (3 − 15 kHz), described in Tournier et al. (2023). The thickness map has been generated by digitalising

the horizon of the Unit 2 – Unit 1 boundary and using the map calculator tool on Kingdom™. The difference between this horizon and the surface sediment, computed in seconds (two-way travel time), was converted to depth on ArcGIS Pro (v. 3.2.2) using a seismic velocity of 1500 m/s and extrapolated with the natural neighbor method.

3.2 Boreholes logging

Three sites were drilled during the Towuti Drilling Project (TDP) in 2015 (Russell et al., 2016). Site 1 (2°43'4" S, 121°30'53" E) with a terminal depth of 153 m and Site 3 (2°43'9" S, 121°30'13" E) with a terminal depth of 173 m are located in the northern basin of Lake Towuti, at respectively 157 m and 159 m water depth (Fig. 3.1). Site 2 (2°41'56" S, 121°35'39" E) with a terminal depth of 132 m is in the deep basin in 201 m of water depth.

XRF analysis has been processed for major element concentrations on dry and powder samples with an ITRAX core scanner (Cox Ltd., Sweden) equipped with a chromium anode X-ray tube (Cr-tube) at the University of Bern (Morlock et al., 2019). The parameters have been set to 30 kV, 50 mA, and 50 s integration time, with a resolution of 2 mm.

3.3 Chronology

Dates from piston core TOW9 (20 AMS 14C ages on bulk organic carbon + 3 ages measured on terrestrial macrofossils, Russell et al. (2020)) have been correlated to the borehole Site 1. In addition, ^{40}Ar/^{39}Ar dating on 2cm thick sanidine-bearing ash (tephra 18 – T18) at 72.95 mcd yielded an age of 797 ± 1.6 ka (Russell et al., 2020). Beyond the ^{14}C timescale, an extrapolation of the average sedimentation rate is used down to the tephra date, which functions as another tie point. Below the tephra, the ages have been extrapolated to the Unit 1/2 boundary.

Tephra layers between Sites 1 and 3 have been compared to get the best correlation (Fig. 3.3). The ages of these layers, estimated based on sedimentation rate interpolation and extrapolation at Site 1, were applied to the same layers on Site 3 to establish a sedimentation rate specific to each drilling site. Age-depth models (Fig. 3.3) were generated with the Bacon R package v.2.5.8 (Blaauw and Christen, 2011) using the SHCal20 calibration curve.

4 Results

4.1 Seismic stratigraphy

The thickness map of Unit 1 (Fig. 3.4) shows that basin B, where drill sites 1 and 3 are
located, has the thinnest lake sediment fill, with a thickness of around 100m. The other
basins show thicknesses of U1 of up to 130 m for Basin D, 140 m for Basin E, 145 m for
Basin A and 157 m for Basin C.
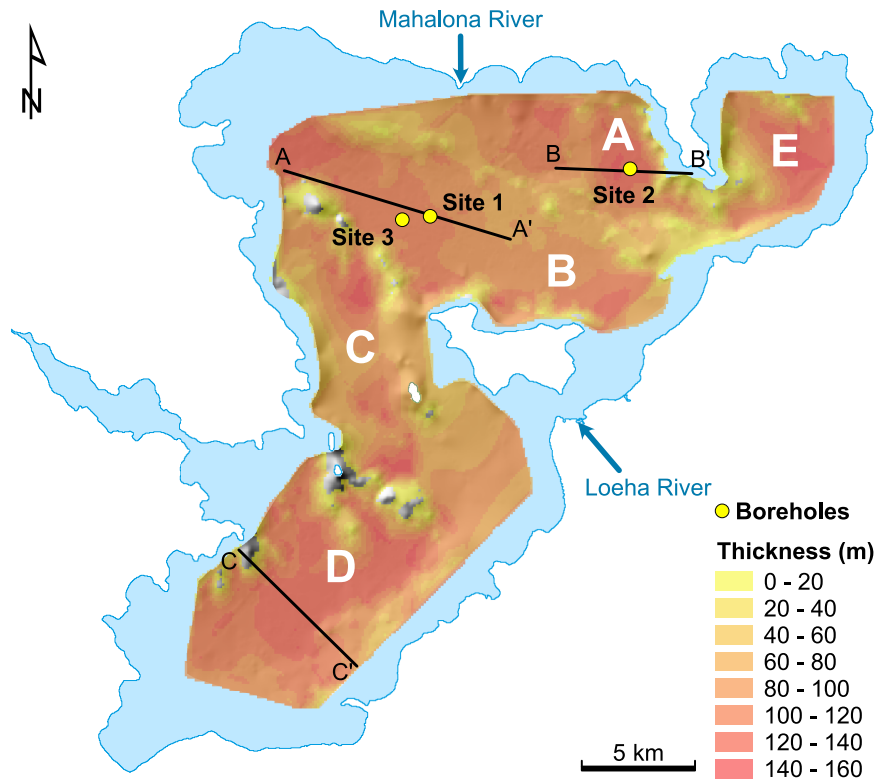
Figure 3.4: Thickness map of Unit 1. The white letters A-E are the basins, and the black
lines are the seismic profiles displayed in this study.

Analysis of single- and multi-channel seismic profiles reveals a complex
morphology of the whole basin of Lake Towuti. The bedrock is irregularly structured
with ridges, sometimes outcropping sediment (Fig. 3.4 and Fig. 3.5). These ridges divide
the lake into different basins with independent sedimentary fills (Morlock, 2018). Basins
B, C, D and E show broadly similar stratigraphy with medium-amplitude reflections.

Some cuts in the reflections are noticed in the lower part of the seismic Unit 1 of Basin B (Fig. 3.5).
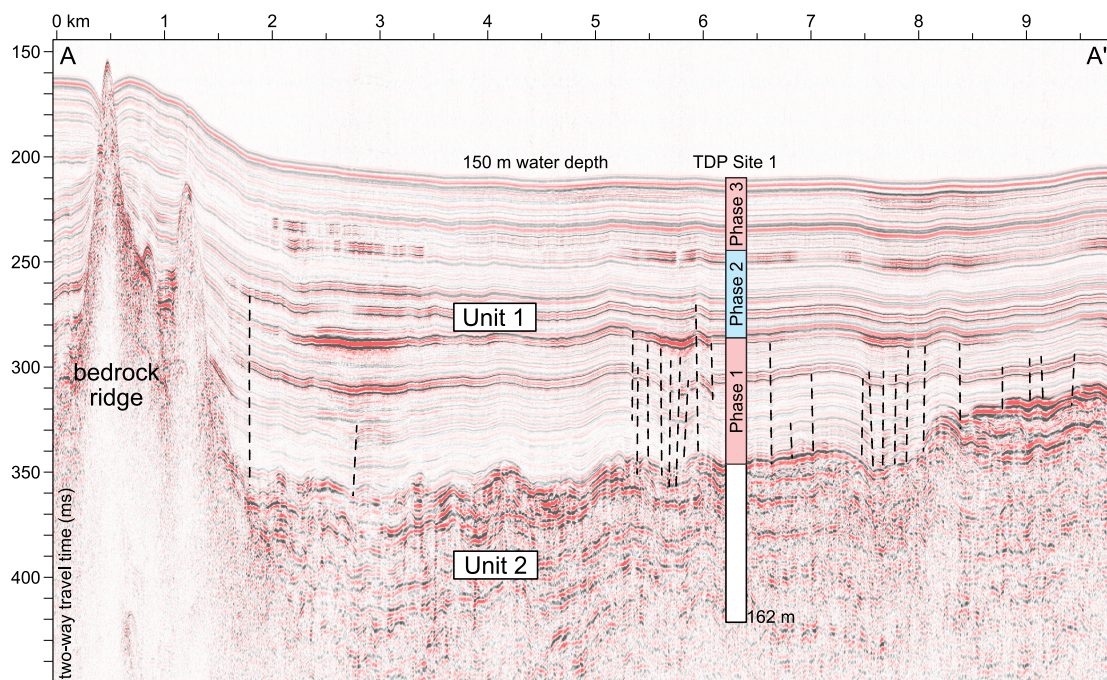
Figure 3.5: Single-channel line showing the seismic stratigraphy in Basin B of Lake Towuti near borehole Site 1. The location of the line is displayed in Fig. 3.4.

Deep basin A, on the other hand, has a distinctive seismic stratigraphy. The lacustrine Unit 1 is divided into two seismic sections. The lower section is ~92 ms TWT thick (~70 m) with medium-amplitude reflections draping the bedrock and composed of hemipelagic clay. The upper seismic section, with a similar thickness, shows high-amplitude reflections ending with onlaps (Fig. 3.6).

4.2 Turbidite catalogue

The turbidites identified in the boreholes of Site 1 and Site 3 are composed of a coarse base, topped by a layer with a grading that becomes finer towards the top. Turbidites on Site 2 are not included in this study, as the morphology of the deep basin makes it too sensitive to spontaneous delta collapse. In the lacustrine sediments of Unit 1, 19 turbidites are reported from Site 1 and 22 turbidites from Site 3 (Table 3.1). These deposits are dated by extrapolation of the sedimentation rate.
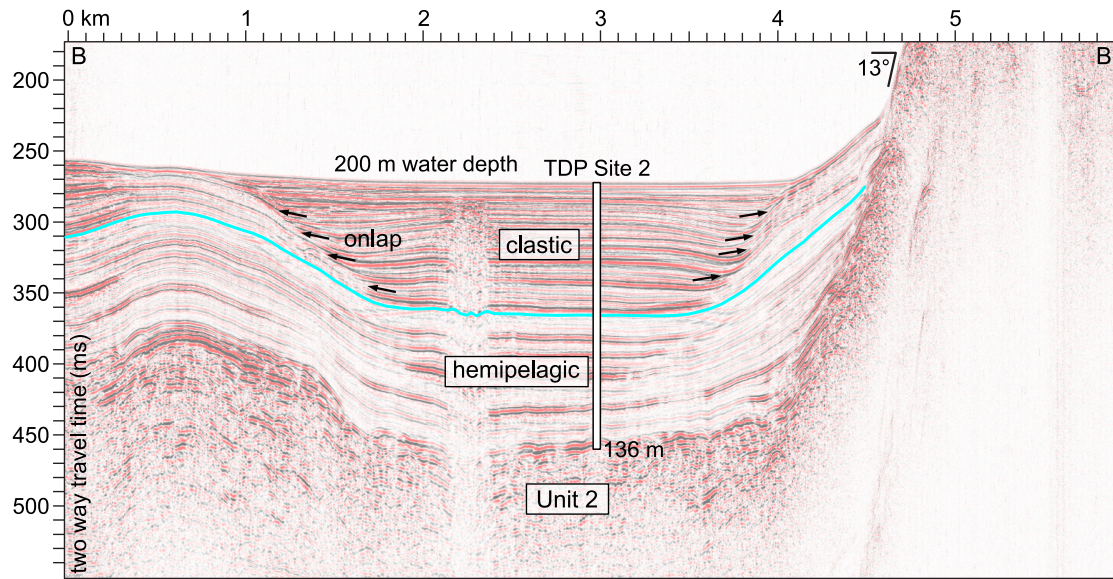
Figure 3.6: Seismic line crossing the deep basin A and the borehole TDP Site 2. Unit 1 is divided into two seismic sections (delineated by the turquoise line): a high-amplitude reflection section overlying the medium-amplitude reflection section. The location of the line is displayed in Fig. 3.4.

5 Discussion

At 1 Ma ago, sediment supply started from the Loeha River, the only major sediment source at that time, indicated by the high concentration of Si, Ca, Ti, K and Al (Hasberg et al., 2019). Subsequently, a change in the Lake Towuti catchment led to the input of Mg Serpentine-rich sediment from the Mahalona River at 230 ka (Fig. 3.3). Prior to this date, the area to the north of the lake had drained into Lake Mahalona and was not directly connected to Lake Towuti. The only possible explanation for this change in hydrology is a transformation of the catchment induced by tectonic movements of the Matano Fault. The gentle slope of the Mahalona River (Morlock, 2018) suggests that a slight variation in topography can induce significant modifications in the river's path.

The seismic stratigraphy of basins B, C and D does not reveal this hydrological change. However, the filling of the deep Basin A is influenced by this change due to its proximity to the Mahalona River delta and the steep slopes. Overlying the transition from hemipelagic sediment to sand to silt clastic sediment (Vogel et al., 2015), a high concentration of turbidites is reported after 230 ka (Fig. 3.6).

93

Table 3.1: Turbidite catalogue on boreholes Site 1 and Site 3 with the ages reported on each model.

Site 1		Site 3	
depth (mcd)	Age (kyr)	depth (mcd)	Age (kyr)
6	53	2	15
8	55	4	31
12	81	15	132
13	94	16	142
15	108	20	183
16	131	27	253
17	141	45	424
20	168	47	442
21	178	48	451
49	464	52	483
55	529	53	491
56	539	60	545
60	581	62	559
61	590	64	574
66	639	68	604
73	706	70	619
75	724	74	645
76	735	79	677
77	744	80	684
		81	693
		82	702
		83	715

The macroscopic analysis of the turbidites in the boreholes at Site 1 and Site 3 and interpretations of the seismic stratigraphy identified three phases (Fig. 3.7). From 740 ka to 420 ka, a first cluster of turbidites is reported, with an estimation of one turbidite every ∼12 kyr. The high concentration of turbidite and the faults observed in the seismic lines (Fig. 3.5) suggest a phase of active tectonic. From 420 ka to 180 ka, only one turbidite deposit occurs. This period could be considered a quiet phase without a major event deposit identified during that time. Then, from 180 ka to the present day, several turbidites have been reported to have a higher concentration in borehole Site 1 than in Site 3. Without clear evidence of faults in the seismic stratigraphy during that time, we suggest that this phase is associated with the catchment area change. The sediment supply from the Mahalona River, starting at 230 ka, induced Site 1 to be in a proximal location.

Also, as shown in the modern earthquake records, the events are mainly localised along the Matano fault, to the north of the lake.
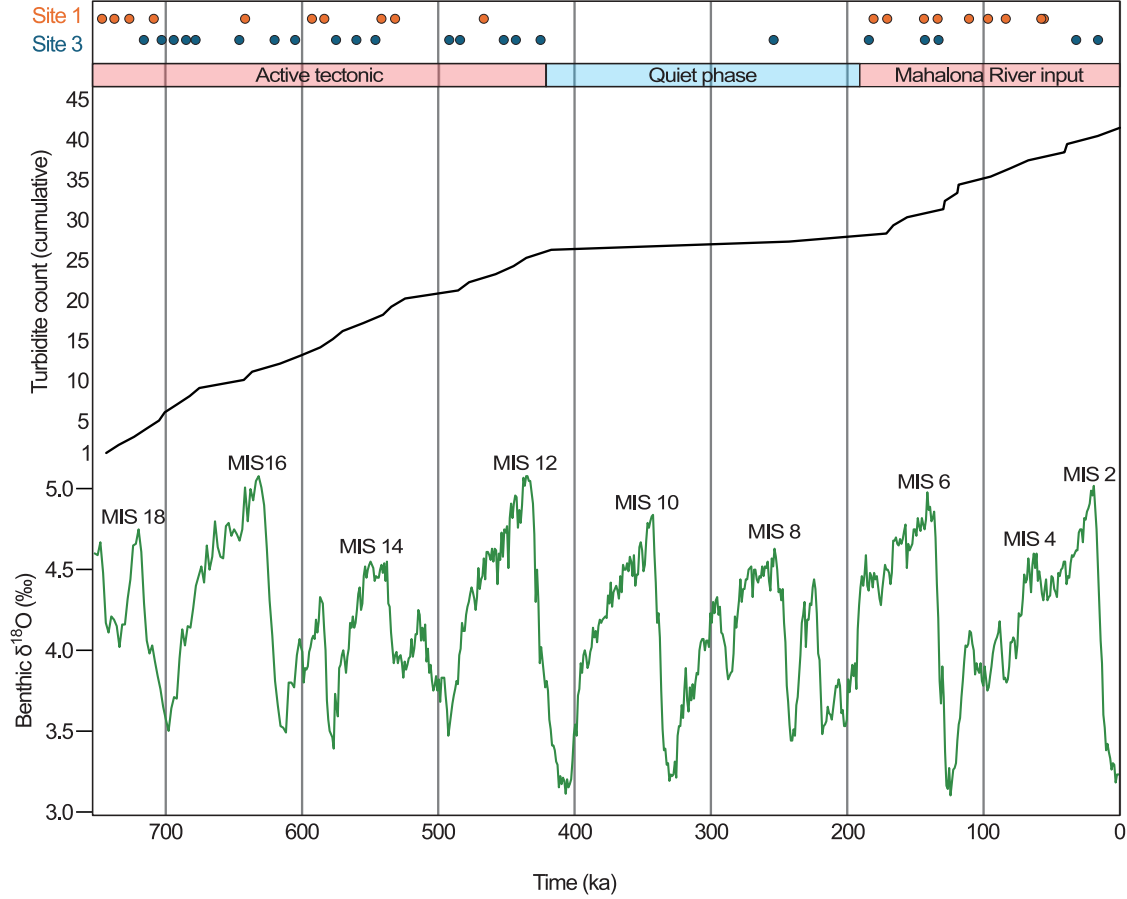
Figure 3.7: Identification of turbidites in the boreholes Site 1 (orange dots) and Site 3 (blue dots), dated with the age models. The accumulation of turbidites (black line) shows the sum of turbidites in both Site 1 and Site 3 over time. The green curve represents the variation of benthic $\delta^{18}O$ in the Oceans and is a global proxy for the Marine Isotope Stage (MIS) during the Quaternary (from Lisiecki and Raymo (2005)).

In order to compare these data with climatic fluctuations, the benthic $\delta^{18}O$ records are plotted in parallel and show much faster cycles. However, on a short geological timescale, we can identify the effect of climate on the recurrence of turbidites (Tournier et al., 2023). The comparison between seismic cycles and climatic fluctuation shows no correlation over the last 1 Ma. If the climate seems to have control in the turbidite formation at a short-time scale, we interpreted the absence of correlation at a long

timescale by the strength of the seismic cycle, dissipating the climate input.

6   Conclusion

The seismic stratigraphy of Lake Towuti provides an insight into the tectonic history of Central Sulawesi. The Matano and Lawanopo faults have profoundly deformed the bedrock and overlying sediments. Over the past 1 Ma, fault unconformity has led to the formation of basins in Lake Towuti, involving sedimentary isolation.

Three phases have been identified in the lacustrine sediment of Lake Towuti. From 740 ka to 420 ka, a high tectonic activity phase is defined by the turbidite concentration and the faults observed in the lake, followed by a quiet phase from 420 to 180 ka. Then, from 180 ka to the present day, the catchment area change modified the sediment input. The Mahalona River becomes the major sediment inlet and induces low stability in the delta and steep slopes of the deep basin.

By combining this survey with the study of the sensitivity of Lake Towuti, analysed with the piston cores and covering 40 kyr, we better understand how the lake reacts to its environment. It would appear that climate plays a significant role in the lake's sensitivity to record earthquakes during recent history. Variations in lake level will result in a different response depending on the magnitude of an earthquake. However, this is only verified on short-time scales with high-resolution analyses. On a long-time scale, the influence of climate is not visible because the seismic phases remain predominant.

7   References

Bao, H., Ampuero, J.-P., Meng, L., Fielding, E. J., Liang, C., Milliner, C. W. D., Feng, T., and Huang, H. (2019). Early and persistent supershear rupture of the 2018 magnitude 7.5 Palu earthquake. *Nature Geoscience*, 12(3):200–205.

Blaauw, M. and Christen, J. A. (2011). Flexible paleoclimate age-depth models using an autoregressive gamma process. *Bayesian Analysis*, 6(3):457–474.

Chapron, E., Ariztegui, D., Mulsow, S., Villarosa, G., Pino, M., Outes, V., Juvignié, E., and Crivelli, E. (2006). Impact of the 1960 major subduction earthquake in Northern Patagonia (Chile, Argentina). *Quaternary International*, 158(1):58–71.

Colman, S., Karabanov, E., and Nelson, C. (2003). Quaternary Sedimentation and Subsidence History of Lake Baikal, Siberia, Based on Seismic Stratigraphy and Coring. *Journal of Sedimentary Research*, 73(6):941–956.

Costa, K., Russell, J., Vogel, H., and Bijaksana, S. (2015). Hydrological connectivity and mixing of Lake Towuti, Indonesia in response to paleoclimatic changes over the last 60,000years. *Palaeogeography, Palaeoclimatology, Palaeoecology*, 417:467–475.

Crowe, S. A., O'Neill, A. H., Katsev, S., Hehanussa, P., Haffner, G. D., Sundby, B., Mucci, A., and Fowle, D. A. (2008). The biogeochemistry of tropical lakes: A case study from Lake Matano, Indonesia. *Limnology and Oceanography*, 53(1):319–331.

Damanik, A., Janssen, D. J., Tournier, N., Stelbrink, B., Von Rintelen, T., Haffner, G., Cohen, A., Yudawati Cahyarini, S., and Vogel, H. (2024). Perspectives from modern hydrology and hydrochemistry on a lacustrine biodiversity hotspot: Ancient Lake Poso, Central Sulawesi, Indonesia. *Journal of Great Lakes Research*, 50(3):102254.

Daxer, C., Ortler, M., Fabbri, S. C., Hilbe, M., Hajdas, I., Dubois, N., Piechl, T., Hammerl, C., Strasser, M., and Moernaut, J. (2022). High-resolution calibration of seismically-induced lacustrine deposits with historical earthquake data in the Eastern Alps (Carinthia, Austria). *Quaternary Science Reviews*, 284:107497.

Hasberg, A. K. M., Bijaksana, S., Held, P., Just, J., Melles, M., Morlock, M. A., Opitz, S., Russell, J. M., Vogel, H., and Wennrich, V. (2019). Modern sedimentation processes in Lake Towuti, Indonesia, revealed by the composition of surface sediments. *Sedimentology*, 66(2):675–698.

Lay, T., Kanamori, H., Ammon, C. J., Nettles, M., Ward, S. N., Aster, R. C., Beck, S. L., Bilek, S. L., Brudzinski, M. R., Butler, R., DeShon, H. R., Ekström, G., Satake, K., and Sipkin, S. (2005). The Great Sumatra-Andaman Earthquake of 26 December 2004. *Science*, 308(5725):1127–1133.

Lisiecki, L. E. and Raymo, M. E. (2005). A Pliocene-Pleistocene stack of 57 globally distributed benthic δ18O records. *Paleoceanography*, 20(1). Publisher: John Wiley & Sons, Ltd.

Maitituerdi, A., Van Daele, M., Verschuren, D., De Batist, M., and Waldmann, N.

(2022). Depositional history of Lake Chala (Mt. Kilimanjaro, equatorial East Africa) from high-resolution seismic stratigraphy. *Journal of African Earth Sciences*, page 104499.

Morlock, M. (2018). *Depositional modes and post-depositional mineral formation in a Pleistocene sediment record from Lake Towuti, Indonesia*. PhD Thesis, Universität Bern, Bern.

Morlock, M. A., Vogel, H., Nigg, V., Ordoñez, L., Hasberg, A. K. M., Melles, M., Russell, J. M., and Bijaksana, S. (2019). Climatic and tectonic controls on source-to-sink processes in the tropical, ultramafic catchment of Lake Towuti, Indonesia. *Journal of Paleolimnology*, 61(3):279–295.

Morlock, M. A., Vogel, H., Russell, J. M., Anselmetti, F. S., and Bijaksana, S. (2021). Quaternary environmental changes in tropical Lake Towuti, Indonesia, inferred from end-member modelling of X-ray fluorescence core-scanning data. *Journal of Quaternary Science*, 36(6):1040–1051. _eprint: https://onlinelibrary.wiley.com/doi/pdf/10.1002/jqs.3338.

Natawidjaja, D. H., Daryono, M. R., Prasetya, G., Udrekh, Liu, P. L.-F., Hananto, N. D., Kongko, W., Triyoso, W., Puji, A. R., Meilano, I., Gunawan, E., Supendi, P., Pamumpuni, A., Irsyam, M., Faizal, L., Hidayati, S., Sapiie, B., Kusuma, M. A., and Tawil, S. (2020). The 2018 Mw7.5 Palu 'supershear' earthquake ruptures geological fault's multi-segment separated by large bends: Results from integrating field measurements, LiDAR, swath bathymetry, and seismic-reflection data. *Geophysical Journal International*, page ggaa498.

Robert, C. and Bousquet, R. (2013). *Géosciences - La dynamique du système Terre*. Belin edition.

Russell, J. M. and Bijaksana, S. (2012). The Towuti Drilling Project: Paleoenvironments, Biological Evolution, and Geomicrobiology of a Tropical Pacific Lake. *Scientific Drilling*, 14:68–71.

Russell, J. M., Bijaksana, S., Vogel, H., Melles, M., Kallmeyer, J., Ariztegui, D., Crowe, S., Fajar, S., Hafidz, A., Haffner, D., Hasberg, A., Ivory, S., Kelly, C., King, J., Kirana, K., Morlock, M., Noren, A., O'Grady, R., Ordonez, L., Stevenson, J., von Rintelen, T., Vuillemin, A., Watkinson, I., Wattrus, N., Wicaksono, S., Wonik, T., Bauer, K., Deino, A., Friese, A., Henny, C., Imran, Marwoto, R., Ngkoimani, L. O., Nomosatryo, S., Safiuddin, L. O., Simister, R.,

and Tamuntuan, G. (2016). The Towuti Drilling Project: paleoenvironments, biological evolution, and geomicrobiology of a tropical Pacific lake. *Scientific Drilling*, 21:29–40.

Russell, J. M., Vogel, H., Bijaksana, S., Melles, M., Deino, A., Hafidz, A., Haffner, D., Hasberg, A. K., Morlock, M., von Rintelen, T., Sheppard, R., Stelbrink, B., and Stevenson, J. (2020). The late quaternary tectonic, biogeochemical, and environmental evolution of ferruginous Lake Towuti, Indonesia. *Palaeogeography, Palaeoclimatology, Palaeoecology*, page 109905.

Sheppard, R. Y., Milliken, R. E., Russell, J. M., Sklute, E. C., Dyar, M. D., Vogel, H., Melles, M., Bijaksana, S., Hasberg, A. K. M., and Morlock, M. A. (2021). Iron Mineralogy and Sediment Color in a 100 m Drill Core From Lake Towuti, Indonesia Reflect Catchment and Diagenetic Conditions. *Geochemistry, Geophysics, Geosystems*, 22(8).

Socquet, A., Hollingsworth, J., Pathier, E., and Bouchon, M. (2019). Evidence of supershear during the 2018 magnitude 7.5 Palu earthquake from space geodesy. *Nature Geoscience*, 12(3):192–199.

Tournier, N., Fabbri, S. C., Anselmetti, F. S., Cahyarini, S. Y., Bijaksana, S., Wattrus, N., Russell, J. M., and Vogel, H. (2023). Climate-controlled sensitivity of lake sediments to record earthquake-related mass wasting in tropical Lake Towuti during the past 40 kyr. *Quaternary Science Reviews*, 305:108015.

Ulfers, A., Hesse, K., Zeeden, C., Russell, J. M., Vogel, H., Bijaksana, S., and Wonik, T. (2021). Cyclostratigraphy and paleoenvironmental inference from downhole logging of sediments in tropical Lake Towuti, Indonesia. *Journal of Paleolimnology*, 65(4):377–392.

Van Daele, M., Moernaut, J., Doom, L., Boes, E., Fontijn, K., Heirman, K., Vandoorne, W., Hebbeln, D., Pino, M., Urrutia, R., Brümmer, R., and De Batist, M. (2015). A comparison of the sedimentary records of the 1960 and 2010 great Chilean earthquakes in 17 lakes: Implications for quantitative lacustrine palaeoseismology. *Sedimentology*, 62(5):1466–1496.

Vogel, H., Russell, J. M., Cahyarini, S. Y., Bijaksana, S., Wattrus, N., Rethemeyer, J., and Melles, M. (2015). Depositional modes and lake-level variability at Lake Towuti, Indonesia, during the past ~29 kyr BP. *Journal of Paleolimnology*,

54(4):359–377.

Vuillemin, A., Friese, A., Wirth, R., Schuessler, J. A., Schleicher, A. M., Kemnitz, H., Lücke, A., Bauer, K. W., Nomosatryo, S., von Blanckenburg, F., Simister, R., Ordoñez, L. G., Ariztegui, D., Henny, C., Russell, J. M., Bijaksana, S., Vogel, H., Crowe, S. A., Kallmeyer, J., and the Towuti Drilling Project Science team (2020). Vivianite formation in ferruginous sediments from Lake Towuti, Indonesia. *Biogeosciences*, 17(7):1955–1973.

Wicaksono, S. A., Russell, J. M., and Bijaksana, S. (2015). Compound-specific carbon isotope records of vegetation and hydrologic change in central Sulawesi, Indonesia, since 53,000 yr BP. *Palaeogeography, Palaeoclimatology, Palaeoecology*, 430:47–56.

Chapter 4

The large-magnitude earthquake potential of an active strike-slip fault system in Lake Poso, Central Sulawesi, Indonesia

Picture of the city of Tentena with Lake Poso in the background (personal collection).

The large-magnitude earthquake potential of an active strike-slip fault system in Lake Poso, Central Sulawesi, Indonesia

Tournier, N.[1], Fabbri, S.C.[1], Damanik, A.[1]; Anselmetti, F.S.[1], Wiguna T.[2]Cahyarini, S.Y.[2], Vogel, H.[1]

[1]Institute of Geological Sciences & Oeschger Centre of Climate Change Research, University of Bern, Baltzerstr. 1+3, 3012, Bern, Switzerland
[2]Research Centre for Climate and Atmosphere, National Research and Innovation Agency (BRIN), Indonesia

The large-magnitude earthquake potential of an active strike-slip fault system in Lake Poso, Central Sulawesi, Indonesia

Abstract

Earthquakes along the Ring of Fire are considered among the most destructive earthquakes on Earth. In Indonesia, 19 earthquakes with a magnitude greater than 7.5 have been recorded in the last 20 years, all causing devastating catastrophes. As witnessed by the 2018 magnitude 7.5 Palu earthquake, extensive areas on the island of Sulawesi are particularly prone to seismic hazards due to the converging Australian, Eurasian, Pacific, and Philippine tectonic plates. However, larger areas in the island's centre appear to be seismically inactive, as the instrumental record lacks indication for magnitude $\geq$ 7 earthquakes in the last century. The sedimentary subsurface of lakes serves as a natural archive for seismic events, allowing us to question the notion of absence of large-magnitude earthquakes in those areas. In 2022, we conducted a seismic and high-resolution bathymetric survey at Lake Poso to provide insight into seismic activity in Central Sulawesi beyond the instrumental record. Large subaquatic landslides and lake-bottom offsets indicate high-intensity earthquakes possibly related to an active local fault system. Our paleoseismological assessment suggests a recurrence of large-magnitude earthquakes every $\sim$1600 $\pm$ 1450 years over the last 11,000 years. Based on our subsurface observations, the evolution of the Poso tectonic basin indicates that the next high-magnitude earthquake could happen in the following decades. The consequences of such an event may be devastating for populations and infrastructures in less developed and underprepared areas of Sulawesi.

1   Introduction

Owing to the convergence of the Pacific, Philippine, Australian, and Eurasian plates, the island of Sulawesi in Indonesia is located in one of the most active tectonic regions in the world (Baillie and Decker, 2022; Hamilton, 1972; Patria et al., 2023; Titu-Eki and Hall, 2020). Most of the convergence is accommodated by a left-lateral strike-slip fault system, including the Palu-Koro Fault (PKF), the Matano Fault, and the Lawanopo Fault between the North Sulawesi Trench and the Tolo Thrust (Fig. 4.1). With an average displacement of 30 mm/year for the PKF (Watkinson and Hall, 2017), the seismic activity is high, as demonstrated by the 2018 Moment Magnitude (Mw) 7.5 Palu earthquake (Frederik, 2019) and several Mw $\geq$ 6 events along the strike-slip fault trace for the duration of the instrumental record (Fig. 4.1A). In recent years, several studies have

explored Sulawesi's tectonic evolution, fault systems, and the associated seismicity (i.e. Beaudouin et al. (2003); Hall (2009); Hutchings and Mooney (2021); Villeneuve et al. (2002)). However, the studies predominantly relied on instrumental and historical data and outcrop investigations (Watkinson and Hall, 2017). Only a few events have been instrumentally tracked (ISC and USGS) during the last 60 years (Fig. 4.1B), with the result that only areas that have been seismically active along the PKF during this period are included in the seismic hazard maps for Sulawesi (Irsyam et al., 2020). Consequently, these records are insufficiently long to identify the recurrence pattern of high-magnitude earthquakes, which may exceed 100 or 1000 years (Fig. 4.1C).
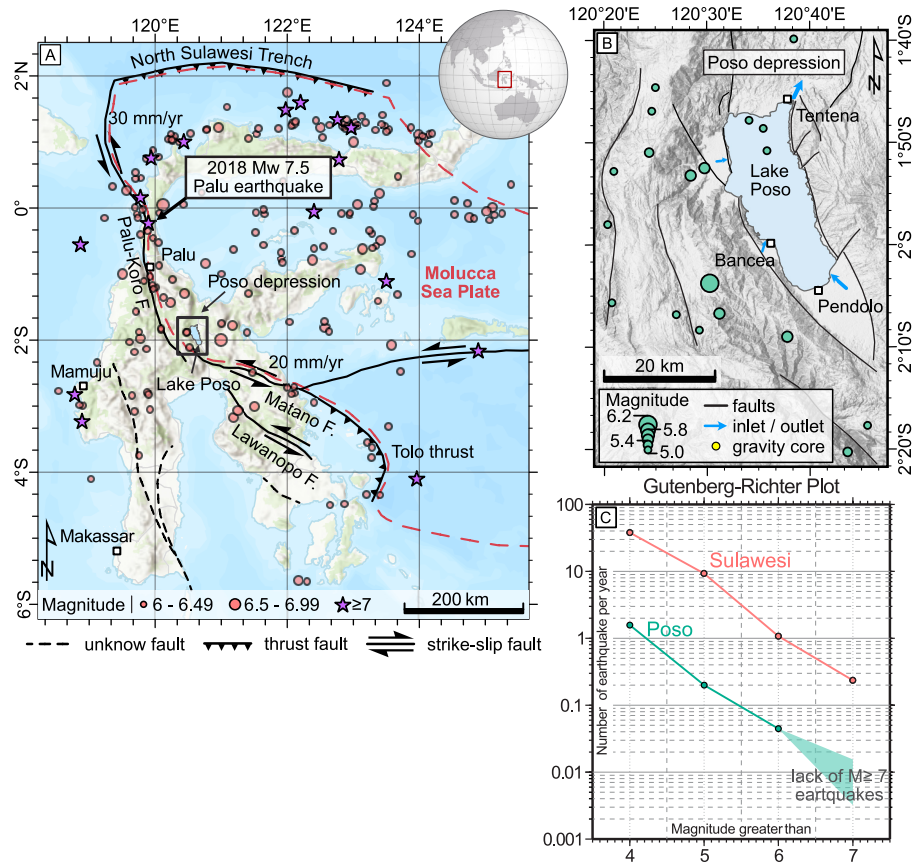

Figure 4.1: A. Tectonic map of the Island of Sulawesi showing earthquakes with a magnitude ≥ 6, depth ≤ 40 km since 1923 documented by USGS and ISC. B. Seismotectonic map of Lake Poso and its surroundings. C. Gutenberg-Richter plot illustrating the number of earthquakes per year for Sulawesi (red) and the Lake Poso area (green) based on instrumental records of the last 100 years.

In presently active seismic zones, such as the Sumatra subduction zone or the Molucca Sea (Hutchings and Mooney, 2021), the earthquake catalogue is fairly accurate and suitable for risk evaluation purposes (Pasari et al., 2021; Supendi et al., 2023) since the region showed significant seismic activity during the instrumentally recorded timespan. However, areas without significant seismic activity during the instrumental period may temporarily be dormant, implying a false sense of security and thus posing an underestimated threat (Galli et al., 2019; Rubin and Sieh, 1997; Schulz and Wang, 2014). Contrary to most regions on the island of Sulawesi, some areas lack instrumental evidence of larger magnitude earthquakes. One such region is the collision zone, where the western and eastern arms of Sulawesi converge (Nugraha et al., 2023), an area known as the Poso Depression (Fig. 4.1A and Fig. 4.1B), only ~50 km to the east of the seismically highly active PKF. In a 200 km radius surrounding the depression, earthquakes with magnitude M > 7 are lacking during the past 60 years (Fig. 4.1C). The absence of larger magnitude events in this area may be due to the lack of active tectonic structures generating these events. However, it may also result from a longer return period of ≥ 100 years, which is also supported by extrapolation of the instrumentally recorded events (Fig. 4.1C). Generally, large-magnitude earthquakes (M > 7) often leave traces in the form of surface ruptures or landslides (Galli et al., 2023; Ocakoğlu and Tuncay, 2023; Tiwari et al., 2021; Waldmann et al., 2011). However, in tropical settings where rainfall is on the order of several meters per year with high surface runoff, substantial erosion, and dense vegetation, uncovering surficial exposed earthquake traces is notoriously difficult (Bellier et al., 1998). Tectonic lakes, on the contrary, can offer an ideal erosion- and vegetation-free setting where traces of past earthquakes are recorded, either in the form of lake-bottom or subsurface ruptures along active faults as direct proof (on-fault) or seismically generated sedimentary structures and deposits as indirect evidence of active faulting (off-fault) (Gastineau et al., 2023; Ghazoui et al., 2019; Howarth et al., 2014; Inouchi et al., 1996; Kremer et al., 2017; Moernaut et al., 2007; Schnellmann et al., 2002; Wils et al., 2021).

The morphology of the lake floor's surface and subsurface can reveal direct evidence of tectonic activity in the form of lake bottom offsets, linear fault expressions and pull-apart basins or thrusting and uplift (Fabbri et al., 2021; Lozano et al., 2022; Ribot et al., 2021). Indirect evidence appears typically in the form of offset linear features such as subaquatic canyon shifts or offset paleoshorelines, which allow the delineation of a lateral or vertical displacement of a fault that otherwise shows no surface expression (Alsop et al., 2016). While such primary, on-fault evidence can often be directly linked to an active fault structure, off-fault evidence is typically only indicative of local shaking intensities

that are dependent on magnitude, epicentral distance, and local effects. Off-fault evidence becomes more significant when observed at multiple locations independently within the same lake basin or neighbouring sub-basins. Subaquatic mass movements and related turbidites are typical off-fault paleoseismic indicators caused by seismically triggered submerged slope failures (Moernaut et al., 2017). These deposits were successfully used as paleoseismological indicators in many studies worldwide (Adams, 1990; Gràcia et al., 2010; Lu et al., 2021a; Ratzov et al., 2015). During an earthquake, different locations receive different amounts of shaking, whereas a Modified Mercalli Intensity MMI of $\geq$ VI is often considered as a threshold to induce slope instabilities (Van Daele et al., 2015). In the case of a high-intensity earthquake, mobilised material occurs in larger areas as it can flow for kilometres through the water and as intensities reach high values also in large distances to the fault, making the evidence detectable also far away from its source. However, subaquatic sediment collapses can be triggered by multiple factors, such as climate due to fluctuations in lake level (Anselmetti et al., 2006; Lu et al., 2021b; Tournier et al., 2023; Vogel et al., 2015), excessive precipitation and flooding (Simonneau et al., 2012; Vandekerkhove et al., 2020; Wilhelm et al., 2022), and sediment overload, leading to a spontaneous collapse (Hilbe and Anselmetti, 2014; Sabatier et al., 2022). Therefore, the combination of multiple types of off- and on-fault seismic evidence, such as pockmarks (single and aligned), offset channels, mass transport deposits and head scars thereof, turbidites, and soft-sediment deformation structures in cores, is vital for a sound paleoseismological assessment. Ideally, on- and off-fault structures are combined and used to confirm independently the existence of an active fault zone, which is, however, rarely observed (Gastineau et al., 2021; Oswald et al., 2021).

Here, we apply these paleoseismological concepts to tectonic Lake Poso in Central Sulawesi to explore whether large-magnitude earthquakes have occurred in the past, in an area that is otherwise indicated as being a low-hazard zone. For this, we combined for the first time in one of the large SE Asian lakes detailed multibeam swath bathymetry and seismic reflection data spanning the entire lake area with sediment short cores to provide a thorough characterisation of the lake-floor morphology and subsurface sediment architecture. These combined datasets are then used to estimate the evolution of the seismic activity for the Poso Depression while also contributing to the region's seismic hazard awareness.

106

2 Geological Setting

The shape of the island of Sulawesi is a consequence of the collision of the Sula Platform with the northern Australia-New Guinea continental margin. The collision resulted in the rotation of the volcanic arc and the development of the North Sulawesi Trench (Parkinson, 1998; Silver et al., 1983). Lake Poso was formed by the extension of an asymmetric half-graben of the Poso Depression. The half-graben was initially open to the sea to the N, but an uplift during the Early Pleistocene connected East Sulawesi and West Sulawesi and resulted in the closed basin as of today (Nugraha et al., 2023). The region around Lake Poso in central Sulawesi therefore shows a distinct division into two metamorphic units. A Middle Cretaceous metamorphic basement is observed on the western part of the lake, and the eastern part is composed of Mesozoic and Cenozoic sediments (Villeneuve et al., 2002). The collision is accommodated by the Sulawesi strike-slip fault system and induced the obduction of an ophiolite formation to the East (Stevens et al., 1999).

Lake Poso is elongated SSE-NNW, ~33 km long and ~12 km wide. Its morphology is best described as a single tub-shaped basin with an extensive central depocenter with a maximum depth of 395 m (Fig. 4.2). Steep slopes (>20°) occur to the east and west and more gently inclined slopes (1-4°) to the north and south (Fig. 4.2).

3 Material and methods

3.1 Bathymetry acquisition

A 17-day bathymetric survey was conducted on Lake Poso in Nov. 2022, using a Kongsberg EM2040 multibeam echosounder (300 kHz, 1° x 1° beam width) combined with a Leica GX 1230+ GNSS receiver for positioning. The acoustic sound-velocity profiles were measured using a Valeport MiniSVP probe. The bathymetric raw data and the 5 m backscatter mosaics were processed and reviewed using Caris HIPS – SIPS 10.4 software. The maps were generated with ArcGIS pro (v. 3.1.1). The bathymetry point clouds were rasterised using a "swath angle surface" algorithm with a horizontal grid size of 4 m. The raster was interpolated to fill minor data gaps.
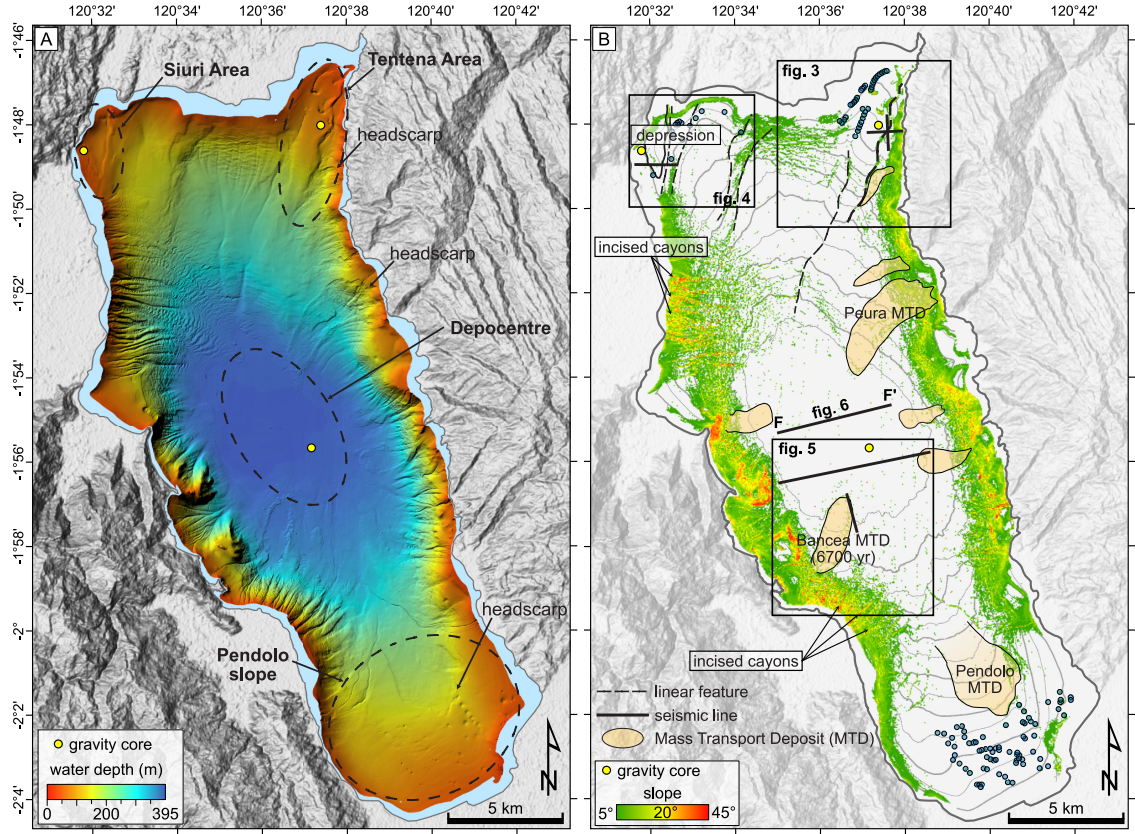
Figure 4.2: A. Bathymetric map of Lake Poso. B. Interpretation of the bathymetry highlighting the sediment-surface features and the slope-angle map. Blue dots are the reported pockmarks.

3.2   Seismic survey

A seismic acquisition survey was carried out with a single-channel 3.5 kHz Geoacoustic pinger source. A total of 576 km of seismic reflection profiles (Suppl. Fig. S1) were recorded to image the lake's subsurface using an independent GPS receiver (Garmin GPS 72H) for positioning. The data were processed with the IHS Markit Kingdom software (v. 2022). To remove noise, a bandpass filter was applied with low-cut and high-cut frequencies of 1500 Hz and 6700 Hz.

3.3   Coring and radiocarbon dating

In addition to the bathymetric and seismic surveys, three short (max. 99 cm long) sediment
cores were recovered from Tentena Area, Siuri Area, and the depocenter of Lake Poso
(Fig. 4.2) using an ETH-style gravity corer. After opening the cores lengthwise, linescan
images were taken, and a lithological description was performed. Radiocarbon dating was
performed on macrofossils at the AMS laboratory of the Department of Chemistry at
the University of Bern and ETH Zurich (Suppl. Table S1). Age-depth models (Fig. 4.3)
were generated with the Bacon R package v.2.5.8 (Blaauw and Christen, 2011) using the
SHCal20 calibration curve. The extrapolations of the sedimentation rates were calculated
using a velocity of seismic data of 1500 m/s and supposing a constant sedimentation rate
in the entire sections for each core.
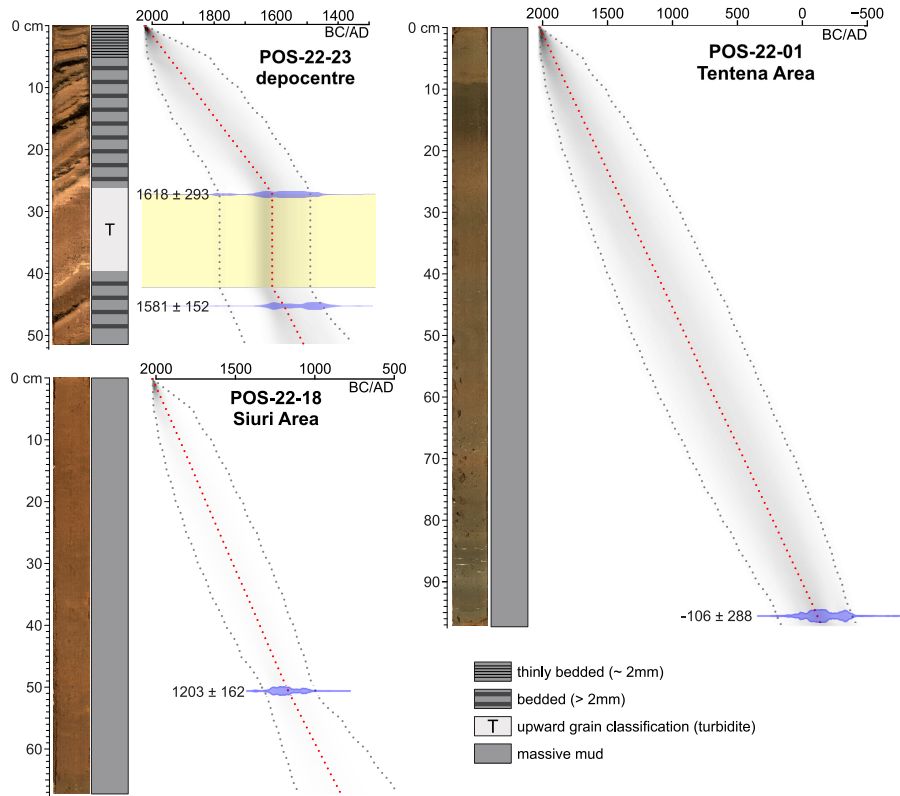

Figure 4.3: High-resolution images and simplified lithological description of the cores POS-
22-23 (top left; depocenter), POS-22-01 (right; Tentena area) and POS-22-18 (bottom left;
Siuri Area) with their respective age-depth models.

109

4 Results

4.1 On-fault evidence in Lake Poso

Tentena Area

Near the outflow, in the Tentena Area in the northeast part of the lake, the bathymetric data indicate a prominent SW-NE-trending sinuous and irregular canyon-like structure (Fig. 4.4). The offset between the topographic high to the west of the canyon-like structure and its thalweg is ∼20 m (Suppl. Fig. S2), extending along longitudinal NW-SE trending sections of up to 280 m in length. Backscatter-intensity data, indicating lake bottom hardness, exhibit extended areas with hard reflectors, interpreted as coarse-grained sediment or outcropping bedrock (indicated in bright yellow in Fig. 4.4B) and dark-blue areas (fine-grained sediment). The high backscatter intensity in the Tentena Area shows hard ground following the sinuous ridge.

The seismic data reveal the detailed morphology of the sediment strata helpful for the analysis of tectonic processes. We defined two seismic stratigraphic units (Ua below and Ub above) characterised by a similar seismic facies, with a medium-frequency and alternating between reflections of high- and low-amplitudes. The units are separated by a high-amplitude reflection, marking a sharp unconformity, and can be differentiated by the morphology of the reflections. The reflections of Ua are parallel and inclined to the NW (Fig. 4.4D), ending with toplaps at the unconformity. Ub is laterally continuous and often fills the irregular surface of the underlying Ua. At the base of the steep slopes, the seismic facies shows medium- to high-amplitude reflections, indicative of a seismic sequence jammed by the bedrock ridge. At greater depth, typically around 150 ms two-way travel time (TWT), gas-rich sediments often hampered seismic penetration, and the deeper sections could not be imaged. At the centre of the Tentena Area, the seismic data show a large body of acoustically transparent seismic facies, rising vertically from deep sections of the profiles to the lake floor with almost no sediment cover (Fig. 4.4). In accordance with the high-intensity backscatter signal and the laterally onlapping reflections, this structure is interpreted as bedrock (Suppl. Fig. S2).

Based on the bathymetry and seismic observations, we interpreted the sinuous SE-NW-trending feature with outcropping bedrock as a geomorphic expression of a strike-slip fault with a discernible oblique component. This interpretation is also supported by

110

the SE-NW alignment of pockmarks, delineating secondary faults in the same direction
(Fig. 4.2). We attributed the inclined layers within seismic Ua to a tectonic tilting
induced by active faulting and bedrock uplift. The overlying and substantially less
inclined sediments making up Ub are interpreted as a phase of fault inactivity. Plant
macrofossils were retrieved from 97 cm depth in core POS-22-01 (Fig. 4.4A and Suppl.
Table S1), revealing a radiocarbon age of 2326 $\pm$ 1749 cal year BP. This suggests an
average sedimentation rate of 0.40 mm/year for the uppermost sediments. Extrapolation
of the sedimentation rate to 10 ms TWT depth (7.5 m of sediment) yields an approximate
age of 16.8 kyr for the Ua-Ub boundary.

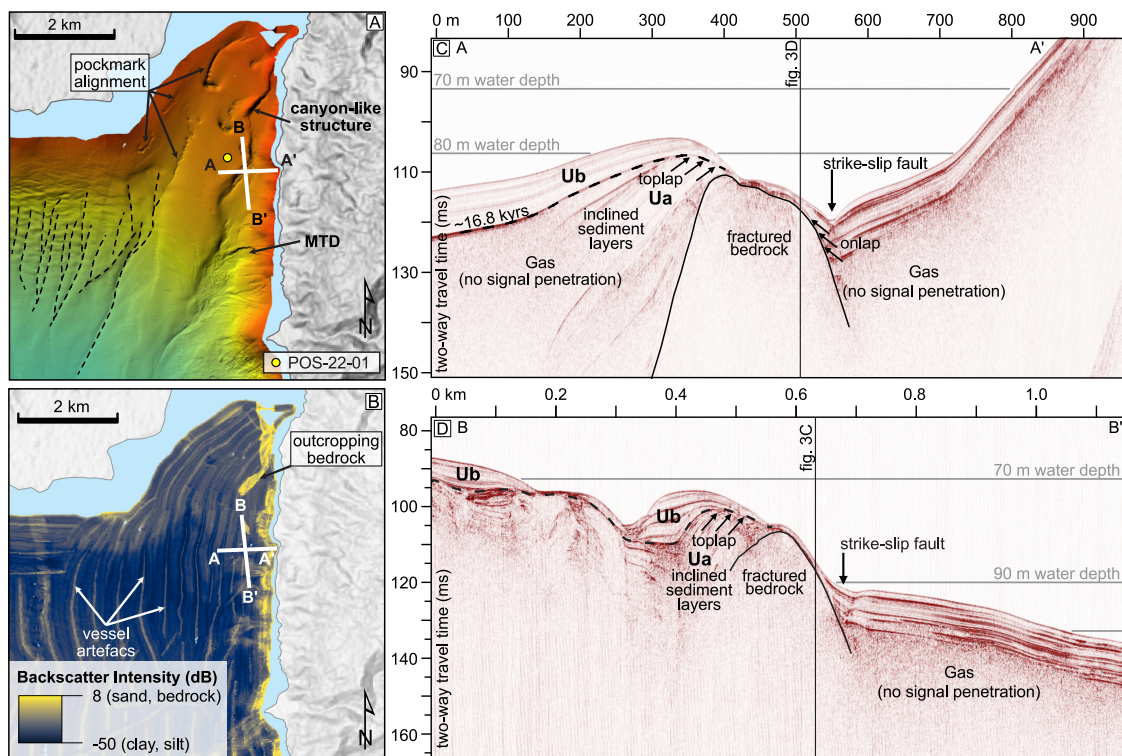Figure 4.4: A. Bathymetry of the northeastern part of Lake Poso. B. Backscatter-intensity
map. C. and D. Seismic sections crossing the sinusoidal fault.

Siuri Area

In the northwestern part of the lake, the lake bottom forms an up to 1-km-wide local
depression that is bounded by a topographic high to the east, the shoreline to the
northwest and a southeast trending cliff along its southwestern extent (Fig. 4.5B). The

depression aligns with a basin onshore bounded by a topographic high to the east and a prominent mountain range to the west. The clearly discernible limitations of the depression indicate that the feature is the result of active and localised tectonic subsidence bordered by normal faults to the W and E. The seismic data reveal mostly parallel high- and low-amplitude reflections (Fig. 4.5), interpreted as stratigraphic equivalent of Ub in the northeastern part of the lake. Deeper penetration in the centre of the depression is hampered by gas (Fig. 4.5). The reflections of Ub are not continuous near the depression area where decimetric offsets in the horizons along vertical cuts indicate faults with a normal component (Fig. 4.5C). The surface of the sediment is also cut by a fault, indicating a recent surface-rupturing tectonic event.
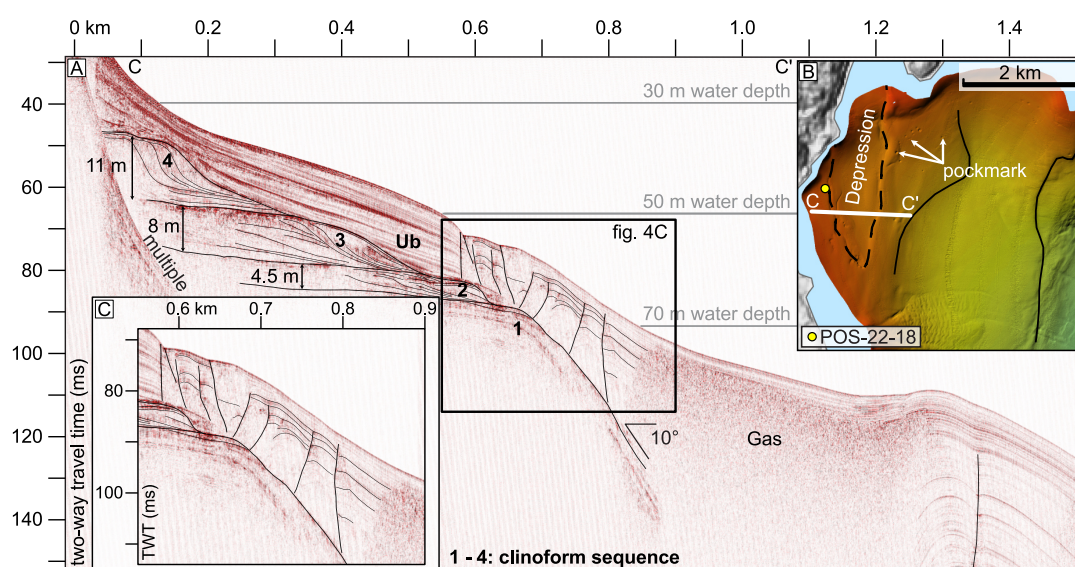
Figure 4.5: A. Seismic line across the depression in the Siuri Area. B. Bathymetric map of the Siuri Area. The seismic line (A) is displayed by the white line. C. Zoom on the faults cutting seismic unit Ub.

Seismic profile C — C' extending basinward from the western shoreline shows a vertical and lateral succession of four stacked clinoform sequences (1-4) below ∼10 m of continuously and acoustically stratified Ub strata. These clinoforms comprise thin horizontal topsets and well-developed foresets, but lack clearly distinguishable bottomsets, except for the topmost clinoform sequence 4, for which a thick bottomset unit can be clearly distinguished in the seismic data. Each individual clinoform sequence is interpreted as a prograding subaqueous delta, with the sequence comprising four vertically distinguishable deltas as the result of significant changes in relative lake level (Marin et al., 2017).

112

Differentiating between tectonic subsidence and climatically driven changes in shoreline is not straightforward in active tectonic and climate-sensitive settings such as Lake Poso. Extrapolating a radiocarbon date of a terrestrial macrofossil found at 52 cm depth in the 69 cm-long core POS-22-18, which yielded an age of 1019 $\pm$ 691 cal year BP (Fig. 4.3), indicates estimated ages of 25 kyr, 21.2 kyr and 17.5 kyr for the clinoform sequences 2, 3 and 4, respectively. Even when considering the uncertainty of the sedimentation rates, the ages fall broadly into the Last Glacial Maximum (LGM; 23 — 18 kyr BP). At nearby Lake Towuti, lake-level indicators (Tournier et al., 2023; Vogel et al., 2015), as well as runoff and dry-adapted vegetation indicators (Russell et al., 2014), suggest a significantly drier regional LGM with up to 30 m lower lake levels. Consequently, we suggest that the paleoshorelines at Lake Poso primarily result from drier climate conditions during the last glacial maximum.

Off-fault features

We find multiple geomorphic expressions of off-fault earthquake traces in Lake Poso, comprising Mass Transport Deposits (MTD), turbidites, fluid escapes and pockmarks. Based on their characteristic surface morphologies and distinctive seismic facies, eight large-volume MTDs (>3 Mm^3) were identified in different parts of Lake Poso (Fig. 4.2), flowing towards the depocentre. For the most recent MTD, slump headscarps are clearly visible upslope of the frontally emergent positive topography and the irregular, often blocky surface of the respective MTD. Three MTDs, hereafter named Bancea, Peura and Pendolo MTDs (Fig. 4.2), are the result of large-scale substantial slope failures.

Seismic reflection data of lines crossing the MTDs illustrate characteristic acoustically transparent seismic facies with a basal detachment surface and accumulation zones in the centre (Fig. 4.6); MTDs are either concave or convex. The internal sedimentary structures are not, or rarely partially, preserved in Lake Poso, as is also reported elsewhere (Frey-Martínez et al., 2006; Gamberi et al., 2011; Sammartini et al., 2021; Strasser et al., 2013). The estimated volumes of the Peura and Pendolo MTDs comprise $\sim$20 and $\sim$50 Mm^3, respectively. The Bancea MTD lacks a clearly visible headscarp, and the seismic data coverage is spatially insufficiently resolved for volume calculation. The seismic line E -– E' crossing the depocentre (Fig. 4.6) shows three large units of acoustically transparent facies, with the deepest one associated with the Bancea MTD. Interestingly, this MTD exhibits an unusual topography with a central depression and a topographically higher outer rim (Fig. 4.6A), as was also described for

113

MTDs in Wörthersee, Austria (Daxer et al., 2020), contrasting with the typical concave-up topography of MTDs (Clare et al., 2019; Moernaut and De Batist, 2011). The seismic line across the Bancea MTD (Fig. 4.6B) shows that the contact between the MTD's transparent seismic facies and the acoustically well-stratified strata, indicating pelagic background sediments, is disrupted along the MTD's outer rim by vertical, chimney-like transparent facies. These vertical chimney-like features with a similar seismic facies as within the MTD are interpreted as fluid escapes that formed because of the dewatering of the underconsolidated and fluid-rich sediment body of the MTD. A collapse of the MTD's body accompanied by fluid escapes along its outer rim would explain the peculiar reversed topography of the Bancea MTD. Fluid escape structures related to seismic shaking have also been described in two lakes in South Central Chile (Moernaut et al., 2009). Similar, albeit less frequent, fluid-escape structures intersecting the entire overburden are also apparent on top of other larger MTDs in Lake Poso (e.g. MTD, Fig. 4.6C). The prevalence of these fluid-escape structures in Lake Poso is interpreted as an indicator of frequent seismic shaking causing enhanced sediment compaction. In Lake Poso, not every fluid escape structure captured in the seismic data extends entirely through the overlying sediment. It remains uncertain whether this is due to variable intensity of different earthquake events or due to variable fluid release pressure and volume variations.

Some fluid-escape structures on the Bancea MTD seem to penetrate the overlying sediments but do not propagate through a high-amplitude reflection correlated with the upper MTD4. This suggests a possible correlation between the fluid escapes and the MTD4's slope-failure event. It remains, however, uncertain whether the fluid escape in the Bancea MTD resulted from seismic shaking triggering the MTD4 event or whether it originated from the impact of the sliding mass. However, the timing of fluid-escape structures on top of the older Bancea MTD with the emplacement of the MTD4 suggests these fluid escapes could be potential off-fault indicators of earthquakes in Lake Poso.

In addition to these fluid-escape structures associated with the MTDs, we find pockmarks with the highest spatial densities in the Tentena Area and the Pendolo Slope (Fig. 4.2). These pockmarks are not aligned in a systematic way that would allow correlation with underlying MTDs or fault structures but could also indicate fluid escape related to seismic events (Cojean et al., 2021; Hovland et al., 2002).

Six event deposits located in the depocentre (undefined MTDs or turbidites) in the seismic line F — F' (Fig. 4.7) have been identified. These are characterised by a transparent and homogeneous seismic facies, covering large areas with conformable
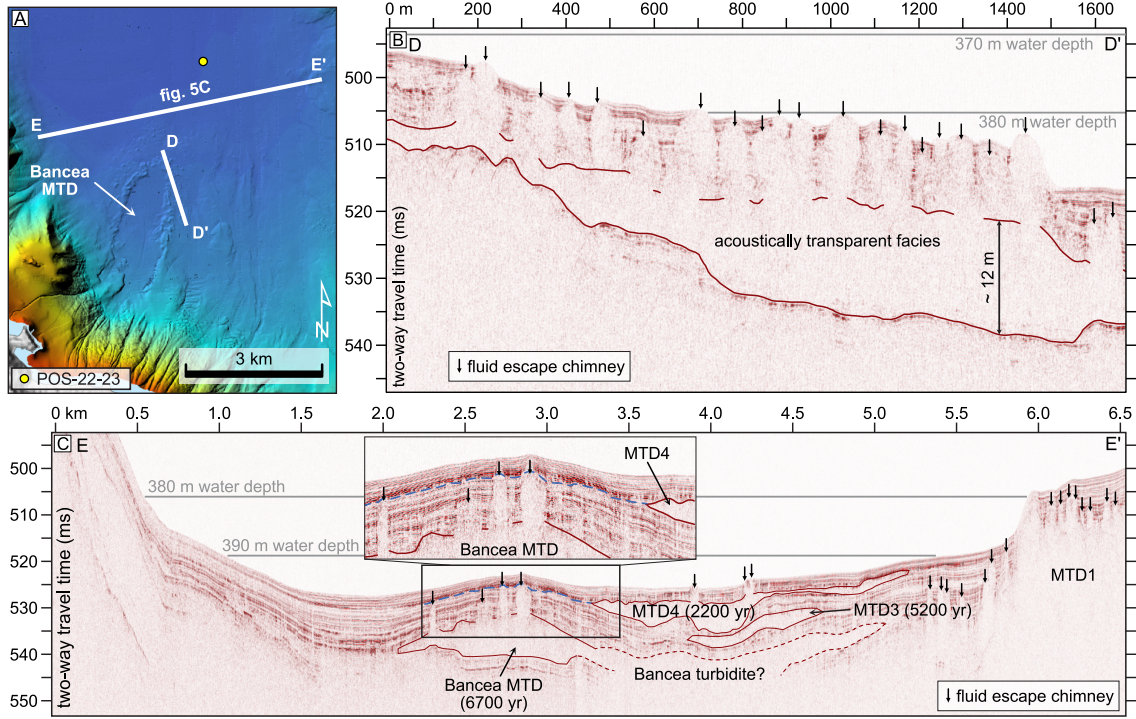
Figure 4.6: A. Seismic line across the 395 m depth depocentre showing mass movement deposits. B. Zoom of the western part of the lake, showing the depocentre and a massive MTD. C. Seismic line of the previously mentioned MTD.

boundaries. Their thicknesses vary from ∼10 cm (thinner layers are limited by the resolution of the seismic data) to slightly more than 1 m. The ages were estimated from the dating of core POS-22-23 and extrapolated to the deeper layers. The oldest turbidite 1 in our seismic data is dated at ∼11.4 ± 3.1 kyr.

5 Discussion

Lake Poso shows multiple on- and off-fault indicators for recent and sub-recent seismicity, including active faulting, mass transports, and fluid expulsions (Fig. 4.8). Despite the limitations in terms of the chronological succession of the events observed in our datasets, we attempt to provide interpretations of the observed on- and off-fault features likely associated with historical earthquakes and the chronostratigraphy of the events. Through the combination of the rough paleoseismological event chronostratigraphy with the available instrumental data, we provide a better estimate of earthquake magnitude

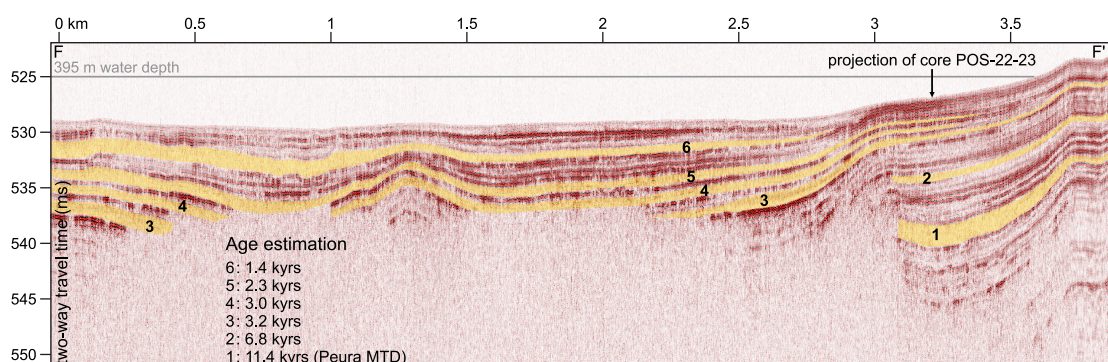Figure 4.7: Seismic line F-F' across the depocentre showing event deposit successions highlighted in yellow, with the estimated ages by extrapolation of the near core POS-22-23. The location of the line is shown in Fig. 4.2.

and recurrence in the Lake Poso region.

The chronostratigraphy of seismic events in Lake Poso (Fig. 4.8) is based on the extrapolation of sedimentation rates derived from the radiocarbon dating of terrestrial plant macrofossils and charcoal found in sediment short cores (Fig. 4.3). Sedimentation rates vary across the entire lake basin, with generally lower sedimentation rates in near-shore areas (0.45 mm/year on core POS-22-01) and highest sedimentation rates in the depocenter (1.00 mm/year on core POS-22-23). We used the bulk sedimentation rate without prior removal of event deposits for extrapolation purposes, as the only sizeable cm-thick event deposit was observed in core POS-22-23 (Fig. 4.3). This approach provides a somewhat representative sedimentation rate for extrapolation and age assignment of event deposits and structures, for which the sedimentation rates of the nearest cores to the seismic lines in which we identified the event deposits were used. Additionally, we took the seismic stratigraphy into consideration for extrapolation purposes.

The clinoform sequences 2 (∼25 kyr BP), 3 (∼21.2 kyr BP) and 4 (∼17.5 kyr BP) in the Siuri Area indicating past lake levels are the oldest structures, falling roughly into the LGM, we attempted to date based on our extrapolation of sedimentation rates. Owing to the clustering of these dates and the reconstructed drier climate with a more open landscape, reduced terrestrial runoff (Russell et al., 2014) and lower lake levels at nearby Lake Towuti (Tournier et al., 2023; Vogel et al., 2015) during this period, we suggest that these paleoshorelines are indicative of a climate-driven lake-level lowstand at Lake Poso rather than being the result of submergence due to tectonic subsidence.
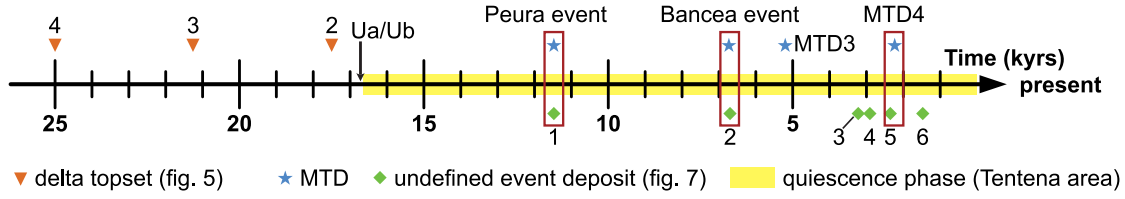
116

Figure 4.8: Time scale representing all the dated features in Lake Poso, likely related
to tectonic movement or earthquake evidence. The red rectangles indicate probable
correlations between MTDs and associated turbidites (Fig. 4.6) based on ages or
correlations of seismic reflections. The delta topsets (in the Siuri Area) are displayed
even if they are likely climate-induced because we cannot completely exclude a tectonic
influence and better visualise the lake's timeline.

In the Siuri Area, the limited penetration depth of the seismic data is restricted
to 60 ms TWT and, therefore, only captures the upper ∼45 m of the sediment fill. In
the depocenter, it does not exceed 20 ms TWT or ∼15 m of sediment. Nevertheless,
seismic penetration and the extrapolation of sedimentation rates are sufficient to provide
a chronostratigraphy for event deposition in the lake's depocentre. Four MTDs, clearly
distinguishable in both seismic and bathymetric data, are dated to ∼11.4 ± 3.2 kyr (Peura
MTD), ∼6.7 ± 2.5 kyr (Bancea MTD), ∼5.2 ± 2.3 kyr (MTD3) and ∼2.2 ± 1.7 kyr
(MTD4); Fig. 4.6). In addition, six MTDs or turbidites are dated to 11.4 ± 3.1 kyr, 6.8 ±
2.6 kyr, 3.2 ± 2.0 kyr, 3.0 ± 1.9 kyr, 2.3 ± 1.7 kyr and 1.4 ± 1.5 kyr (Fig. 4.7). The oldest
event 1 is likely a turbidite related to the Peura MTD (Suppl. Fig. S3). The Bancea MTD
can be correlated to the turbidite event 2 (Fig. 4.7). However, the other MTDs in the
depocenter, identified via bathymetric data, cannot be linked to the seismic line crossing
the depocentre due to the limited penetration of the seismic signal.

Providing accurate earthquake magnitudes for individual events is challenging
based on the available data. However, the observed on-fault features, especially the rupture
length of the strike-slip fault in the Tentena Area, can provide a rough estimate for a
minimal possible magnitude. The magnitude estimation for the fault in the Tentena Area
can be calculated using the regression of Mw on surface-rupture length (Stirling et al.,
2002) for a pre-instrumental event with the following equation:

$$M_w = a + b \log(L)$$

with Mw being the moment magnitude, a and b the regression parameters (5.89 and 0.79,
respectively) and L the fault length in km. Assuming that the entire section of the fault is

117

visible on the bathymetric data with a total length of 7 km and assuming it ruptured in a single event results in a minimum Mw of 6.6 ± 0.2. An overestimation of this magnitude is possible, considering that only a small section of the fault ruptures. Similarly, if the fault continues onshore beyond the reach of the bathymetric dataset or offshore, below the penetration capacity of the seismic data, an underestimation magnitude may be possible.

The constructed event catalogue suggests a return period for larger magnitude earthquakes of ∼1600 ± 1450 years over the last 11 ka. The standard deviation indicates a low confidence in the return period estimation. Nevertheless, the Coefficient of Deviation (CoV) is lower than 1 (CoV = 0.95), which indicates that we have a weak periodicity without considering the data as "bursty" (Salditch et al., 2020). Based on the instrumental record and considering the relationship between the magnitude and the total number of earthquakes in the region, M ≥ 6 earthquakes occur every ∼55 years. When extrapolating this relationship, M ≥ 7 earthquakes are expected to occur every ∼1350 ± 450 years.

A minimum intensity of VI is necessary to trigger a slope failure in a lake system (Van Daele et al., 2015). Nevertheless, it is essential to also consider the sensitivity of lakes to record earthquakes (Wilhelm et al., 2016). The sedimentation rate, the composition of the sediment and the slope angles influence the sediment stability and the failure potential, as demonstrated in Lake Towuti ∼130 km to the SE of Lake Poso (Tournier et al., 2023; Vogel et al., 2015). Since the beginning of the instrumental record, only one earthquake (2019 Mw 5.5, ∼3 km from the lake) reaching Lake Poso with an intensity > VI has been documented (Fig. 4.9). On- and off-fault traces of this event are absent in the 2022 seismic and bathymetric data from Lake Poso. Nevertheless, the local population living on the eastern shoreline testified that a large wave washed ashore that day. Therefore, we suggest that Lake Poso has a low sensitivity to record earthquakes in the form of mass-wasting events, which is also supported by the large gap between the number of high-magnitude earthquakes (i.e. one M ≥ 6 earthquake every ∼55 years) and the recurrence of event deposits reported here. Therefore, the lake seems insufficiently sensitive to respond to M ≥ 6 earthquakes but may, in turn, be a suitable recorder of strong (M > 7) local earthquakes with sufficient intensity to trigger slope failure in this setting.

Seismic hazards in coastal lake settings include tsunami threats (Nigg et al., 2021; Schnellmann et al., 2006). The massive MTDs in Lake Poso remobilised large volumes of sediment that likely have the potential to generate tsunami waves in Lake Poso. A seismic event similar to the one that triggered the Pendolo MTD could lead to a serious tsunami hazard for the town of Tentena and other coastal villages today. This hazard is
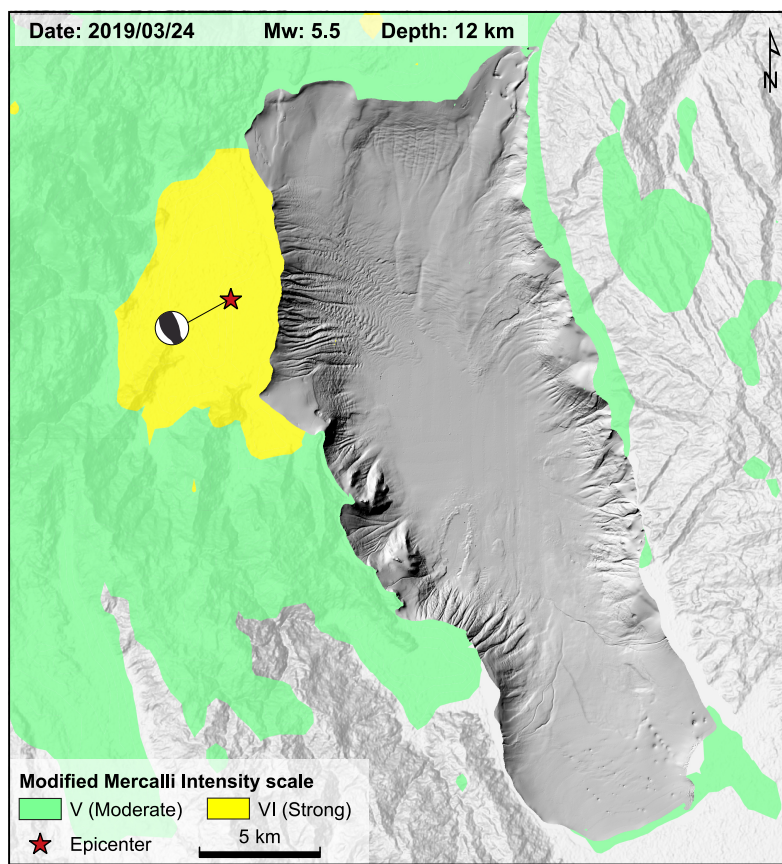
Figure 4.9: Intensity (MMI) map of the 2019 Mw 5.5 earthquake located 2 km to the western shoreline of Lake Poso. (Shakemap by USGS Earthquake Hazards Program; `https://earthquake.usgs.gov/earthquakes/eventpage/us1000jkv5/shakemap/intensity,modifiedaccessedinApr.2024`)

accentuated by the great depth of the lake, its large volume, and the steep slopes on the eastern and western flanks of the lake basin, which form a corridor for the propagation of a tsunami wave (Franco et al., 2021).

6   Conclusion

In the tropical setting of seismically active Central Sulawesi, where records of prehistoric earthquakes are otherwise scarce, Lake Poso's sediment record provides a well-needed archive of past seismic activity. Seismic events in Lake Poso are apparent through characteristic features in the lake-floor morphology (faults, pockmarks, slide scars) and

119

frequent mass-wasting deposits in the subsurface (Suppl. Fig. S4). Assuming that the 16.8 kyr BP rupture of the fault in the Tentena area was likely caused by a M $\geq$ 6.8 earthquake and considering the low sensitivity of Lake Poso's subaquatic slopes to fail during seismic shaking, we suggest that M $\geq$ 7 earthquakes are likely to occur in the region. Our event-based return period closely overlaps with the expected return period of M $\geq$ 7 earthquakes based on the Gutenberg-Richter law and the available instrumental record. Considering the uncertainty in the chronology of the estimated return period of larger magnitude events, these initial data provide a working hypothesis that can be tested in future studies at Lake Poso that allow for a more sophisticated chronological framework.

Owing to the scarcity of paleoseismological studies in lacustrine settings in the wet tropics, datasets presented here are considered of exploratory nature that will help access the information on past seismic events and to design future, more targeted research studies. The lack of detailed historical and instrumental records limits the accurate assessment of the seismic hazard. The need for more data on past earthquakes is partly compensated by our paleoseismological approach analysing on- and off-fault seismic evidence and the morphology of the faults underneath the lake, revealing active sub-recent Late Pleistocene tectonics. To achieve a more precise assessment of seismic hazard in the Lake Poso region, utilising sediment long-cores would enable us to quantify the frequency of significant earthquakes throughout the entire Quaternary period. This information could then be extrapolated to estimate future recurrence rates. Additionally, it would facilitate the analysis of Maximum Credible Earthquake (MCE) and tsunami hazard scenarios.

7   References

Adams, J. (1990). Paleoseismicity of the Cascadia Subduction Zone: Evidence from turbidites off the Oregon-Washington Margin. *Tectonics*, 9(4):569–583.

Alsop, G., Marco, S., Weinberger, R., and Levi, T. (2016). Sedimentary and structural controls on seismogenic slumping within mass transport deposits from the Dead Sea Basin. *Sedimentary Geology*, 344:71–90.

Anselmetti, F., Ariztegui, D., Hodell, D., Hillesheim, M., Brenner, M., Gilli, A., McKenzie, J., and Mueller, A. (2006). Late Quaternary climate-induced lake level variations in Lake Petén Itzá, Guatemala, inferred from seismic stratigraphic analysis. *Palaeogeography, Palaeoclimatology, Palaeoecology*, 230(1-2):52–69.

Baillie, P. and Decker, J. (2022). Enigmatic Sulawesi: The tectonic collage. *Berita Sedimentologi*, 48(1):1–30.

Beaudouin, T., Bellier, O., and Sebrier, M. (2003). Present-day stress and deformation field within the Sulawesi Island area (Indonesia) : geodynamic implications. *Bulletin de la Société Géologique de France*, 174(3):305–317.

Bellier, O., Beaudouin, T., Sebrier, M., Villeneuve, M., Bahar, I., Putranto, E., Pratomo, I., Massault, M., and Seward, D. (1998). Active faulting in central Sulawesi (Eastern Indonesia): a geological approch. Scient. Technical Rep. STR vol. 98-14, Géophysique et Géodynamique Interne - Univ. Paris-Sud Orsay, EC contract CI1*CT93-0337.

Blaauw, M. and Christen, J. A. (2011). Flexible paleoclimate age-depth models using an autoregressive gamma process. *Bayesian Analysis*, 6(3):457–474.

Clare, M., Chaytor, J., Dabson, O., Gamboa, D., Georgiopoulou, A., Eady, H., Hunt, J., Jackson, C., Katz, O., Krastel, S., León, R., Micallef, A., Moernaut, J., Moriconi, R., Moscardelli, L., Mueller, C., Normandeau, A., Patacci, M., Steventon, M., Urlaub, M., Völker, D., Wood, L., and Jobe, Z. (2019). A consistent global approach for the morphometric characterization of subaqueous landslides. *Geological Society, London, Special Publications*, 477(1):455–477.

Cojean, A. N. Y., Kremer, K., Bartosiewicz, M., Fabbri, S. C., Lehmann, M. F., and Wirth, S. B. (2021). Morphology, Formation, and Activity of Three Different Pockmark Systems in Peri-Alpine Lake Thun, Switzerland. *Frontiers in Water*, 3:666641.

Daxer, C., Sammartini, M., Molenaar, A., Piechl, T., Strasser, M., and Moernaut, J. (2020). Morphology and spatio-temporal distribution of lacustrine mass-transport deposits in Wörthersee, Eastern Alps, Austria. *Geological Society, London, Special Publications*, 500(1):235–254.

Fabbri, S. C., Haas, I., Kremer, K., Motta, D., Girardclos, S., and Anselmetti, F. S. (2021). Subaqueous geomorphology and delta dynamics of Lake Brienz (Switzerland): implications for the sediment budget in the alpine realm. *Swiss Journal of Geosciences*, 114(1):22.

Franco, A., Schneider-Muntau, B., Roberts, N. J., Clague, J. J., and Gems, B. (2021). Geometry-Based Preliminary Quantification of Landslide-Induced

Impulse Wave Attenuation in Mountain Lakes. *Applied Sciences*, 11(24):11614.

Frederik, M. C. G. (2019). First Results of a Bathymetric Survey of Palu Bay, Central Sulawesi, Indonesia following the Tsunamigenic Earthquake of 28 September 2018. *Pure Appl. Geophys.*, 176:14.

Frey-Martínez, J., Cartwright, J., and James, D. (2006). Frontally confined versus frontally emergent submarine landslides: A 3D seismic characterisation. *Marine and Petroleum Geology*, 23(5):585–604.

Galli, P., Galderisi, A., Peronace, E., Giaccio, B., Hajdas, I., Messina, P., Pileggi, D., and Polpetta, F. (2019). The Awakening of the Dormant Mount Vettore Fault (2016 Central Italy Earthquake, M_w 6.6): Paleoseismic Clues on Its Millennial Silences. *Tectonics*, 38(2):687–705.

Galli, P., Messina, P., Peronace, E., Galderisi, A., Ilardo, I., and Polpetta, F. (2023). Paleoseismic evidence of five magnitude 7 earthquakes on the Norcia fault system in the past 8,000 years (Central Italy). *Frontiers in Earth Science*, 11:1188602.

Gamberi, F., Rovere, M., and Marani, M. (2011). Mass-transport complex evolution in a tectonically active margin (Gioia Basin, Southeastern Tyrrhenian Sea). *Marine Geology*, 279(1-4):98–110.

Gastineau, R., de Sigoyer, J., Sabatier, P., Fabbri, S. C., Anselmetti, F. S., Develle, A. L., Şahin, M., Gündüz, S., Niessen, F., and Gebhardt, A. C. (2021). Active Subaquatic Fault Segments in Lake Iznik Along the Middle Strand of the North Anatolian Fault, NW Turkey. *Tectonics*, 40(1):e2020TC006404. _eprint: https://agupubs.onlinelibrary.wiley.com/doi/pdf/10.1029/2020TC006404.

Gastineau, R., Sabatier, P., Fabbri, S. C., Anselmetti, F. S., Roeser, P., Findling, N., Şahin, M., Gündüz, S., Arnaud, F., Franz, S. O., Ünsal, N. D., and De Sigoyer, J. (2023). Lateral variations in the signature of earthquake-generated deposits in Lake Iznik, NW Turkey. *The Depositional Record*, page dep2.232.

Ghazoui, Z., Bertrand, S., Vanneste, K., Yokoyama, Y., Nomade, J., Gajurel, A. P., and Van Der Beek, P. A. (2019). Potentially large post-1505 AD earthquakes in western Nepal revealed by a lake sediment record. *Nature Communications*, 10(1):2258.

Gràcia, E., Vizcaino, A., Escutia, C., Asioli, A., Rodés, Á., Pallàs, R., Garcia-

Orellana, J., Lebreiro, S., and Goldfinger, C. (2010). Holocene earthquake
record offshore Portugal (SW Iberia): testing turbidite paleoseismology in a
slow-convergence margin. *Quaternary Science Reviews*, 29(9-10):1156–1172.

Hall, R. (2009). Southeast Asia's changing palaeogeography. *Southeast Asia*, 54:14.

Hamilton, W. B. (1972). Tectonics of the Indonesian Region. Report 72-1978.
Edition: -.

Hilbe, M. and Anselmetti, F. S. (2014). Signatures of slope failures and river-delta
collapses in a perialpine lake (Lake Lucerne, Switzerland). *Sedimentology*,
61(7):1883–1907.

Hovland, M., Gardner, J. V., and Judd, A. G. (2002). The significance of pockmarks
to understanding fluid flow processes and geohazards. *Geofluids*, 2(2):127–136.

Howarth, J. D., Fitzsimons, S. J., Norris, R. J., and Jacobsen, G. E. (2014). Lake
sediments record high intensity shaking that provides insight into the location
and rupture length of large earthquakes on the Alpine Fault, New Zealand.
Earth and Planetary Science Letters, 403:340–351.

Hutchings, S. J. and Mooney, W. D. (2021). The Seismicity of Indonesia and Tectonic
Implications. *Geochemistry, Geophysics, Geosystems*, 22(9):e2021GC009812.

Inouchi, Y., Kinugasa, Y., Kumon, F., Nakano, S., Yasumatsu, S., and Shiki, T.
(1996). Turbidites as records of intense palaeoearthquakes in Lake Biwa,
Japan. *Sedimentary Geology*, 104(1-4):117–125.

Irsyam, M., Cummins, P. R., Asrurifak, M., Faizal, L., Natawidjaja, D. H.,
Widiyantoro, S., Meilano, I., Triyoso, W., Rudiyanto, A., Hidayati, S.,
Ridwan, M., Hanifa, N. R., and Syahbana, A. J. (2020). Development of
the 2017 national seismic hazard maps of Indonesia. *Earthquake Spectra*,
36(1_suppl):112–136.

Kremer, K., Wirth, S. B., Reusch, A., Fäh, D., Bellwald, B., Anselmetti, F. S.,
Girardclos, S., and Strasser, M. (2017). Lake-sediment based paleoseismology:
Limitations and perspectives from the Swiss Alps. *Quaternary Science
Reviews*, 168:1–18.

Lozano, J. G., Gutierrez, Y. S., Bran, D. M., Lodolo, E., Cerredo, M. E., Tassone, A.,
and Vilas, J. F. (2022). Structure, seismostratigraphy, and tectonic evolution of
Lago Roca (southern Patagonia, Argentina). *Geological Journal*, 57(8):3101–
3113.

Lu, Y., Moernaut, J., Bookman, R., Waldmann, N., Wetzler, N., Agnon, A., Marco, S., Alsop, G. I., Strasser, M., and Hubert-Ferrari, A. (2021a). A New Approach to Constrain the Seismic Origin for Prehistoric Turbidites as Applied to the Dead Sea Basin. *Geophysical Research Letters*, 48(3):e2020GL090947. Publisher: John Wiley & Sons, Ltd.

Lu, Y., Moernaut, J., Waldmann, N., Bookman, R., Alsop, G. I., Hubert-Ferrari, A., Strasser, M., Agnon, A., and Marco, S. (2021b). Orbital- and millennial-scale changes in lake-levels facilitate earthquake-triggered mass failures in the Dead Sea Basin. *Geophysical Research Letters*, e2021GL093391(n/a):24. _eprint: https://agupubs.onlinelibrary.wiley.com/doi/pdf/10.1029/2021GL093391.

Marin, D., Escalona, A., Śliwińska, K. K., Nøhr-Hansen, H., and Mordasova, A. (2017). Sequence stratigraphy and lateral variability of Lower Cretaceous clinoforms in the southwestern Barents Sea. *AAPG Bulletin*, 101(09):1487–1517.

Moernaut, J. and De Batist, M. (2011). Frontal emplacement and mobility of sublacustrine landslides: Results from morphometric and seismostratigraphic analysis. *Marine Geology*, 285(1-4):29–45.

Moernaut, J., De Batist, M., Charlet, F., Heirman, K., Chapron, E., Pino, M., Brümmer, R., and Urrutia, R. (2007). Giant earthquakes in South-Central Chile revealed by Holocene mass-wasting events in Lake Puyehue. *Sedimentary Geology*, 195(3-4):239–256.

Moernaut, J., De Batist, M., Heirman, K., Van Daele, M., Pino, M., Brümmer, R., and Urrutia, R. (2009). Fluidization of buried mass-wasting deposits in lake sediments and its relevance for paleoseismology: Results from a reflection seismic study of lakes Villarrica and Calafquén (South-Central Chile). *Sedimentary Geology*, 213(3-4):121–135.

Moernaut, J., Van Daele, M., Strasser, M., Clare, M. A., Heirman, K., Viel, M., Cardenas, J., Kilian, R., Ladrón de Guevara, B., Pino, M., Urrutia, R., and De Batist, M. (2017). Lacustrine turbidites produced by surficial slope sediment remobilization: A mechanism for continuous and sensitive turbidite paleoseismic records. *Marine Geology*, 384:159–176.

Nigg, V., Bacigaluppi, P., Vetsch, D. F., Vogel, H., Kremer, K., and Anselmetti, F. S. (2021). Shallow-Water Tsunami Deposits: Evidence From Sediment

Cores and Numerical Wave Propagation of the 1601 CE Lake Lucerne Event.
Geochemistry, Geophysics, Geosystems, 22(12):e2021GC009753. _eprint:
https://agupubs.onlinelibrary.wiley.com/doi/pdf/10.1029/2021GC009753.

Nugraha, A. M. S., Adhitama, R., Switzer, A. D., and Hall, R. (2023). Plio-
Pleistocene sedimentation and palaeogeographic reconstruction in the Poso
Depression, Central Sulawesi, Indonesia: from a sea channel to a land bridge.
Journal of Palaeogeography, 12(3):331–357.

Ocakoğlu, F. and Tuncay, E. (2023). Geological and geomechanical evidence from
the Sünnet landslides (NW Anatolia) for an Mw8.0 cascade rupture in the
North Anatolian Fault 8 ky ago. *Tectonophysics*, 846:229682.

Oswald, P., Moernaut, J., Fabbri, S. C., De Batist, M., Hajdas, I., Ortner,
H., Titzler, S., and Strasser, M. (2021). Combined On-Fault and Off-
Fault Paleoseismic Evidence in the Postglacial Infill of the Inner-Alpine Lake
Achensee (Austria, Eastern Alps). *Frontiers in Earth Science*, 9:670952.

Parkinson, C. (1998). An outline of the petrology, structure and age of the
Pompangeo Schist Complex of central Sulawesi, Indonesia. *The Island Arc*,
7(1-2):231–245.

Pasari, S., Simanjuntak, A. V. H., Mehta, A., Neha, and Sharma, Y. (2021). A
synoptic view of the natural time distribution and contemporary earthquake
hazards in Sumatra, Indonesia. *Natural Hazards*, 108(1):309–321.

Patria, A., Natawidjaja, D. H., Daryono, M. R., Hanif, M., Puji, A. R., and
Tsutsumi, H. (2023). Tectonic landform and paleoseismic events of the
easternmost Matano fault in Sulawesi, Indonesia. *Tectonophysics*, 852:229762.

Ratzov, G., Cattaneo, A., Babonneau, N., Déverchère, J., Yelles, K., Bracene, R.,
and Courboulex, F. (2015). Holocene turbidites record earthquake supercycles
at a slow-rate plate boundary. *Geology*, 43(4):331–334.

Ribot, M., Klinger, Y., Jónsson, S., Avsar, U., Pons-Branchu, E., Matrau, R., and
Mallon, F. L. (2021). Active Faults' Geometry in the Gulf of Aqaba, Southern
Dead Sea Fault, Illuminated by Multibeam Bathymetric Data. *Tectonics*,
40(4):e2020TC006443.

Rubin, C. M. and Sieh, K. (1997). Long dormancy, low slip rate, and similar slip-
per-event for the Emerson fault, eastern California shear zone. *Journal of
Geophysical Research: Solid Earth*, 102(B7):15319–15333.

Russell, J. M., Vogel, H., Konecky, B. L., Bijaksana, S., Huang, Y., Melles, M., Wattrus, N., Costa, K., and King, J. W. (2014). Glacial forcing of central Indonesian hydroclimate since 60,000 y B.P. *Proceedings of the National Academy of Sciences*, 111(14):5100–5105.

Sabatier, P., Moernaut, J., Bertrand, S., Van Daele, M., Kremer, K., Chaumillon, E., and Arnaud, F. (2022). A Review of Event Deposits in Lake Sediments. *Quaternary*, 5(3):34.

Salditch, L., Stein, S., Neely, J., Spencer, B. D., Brooks, E. M., Agnon, A., and Liu, M. (2020). Earthquake supercycles and Long-Term Fault Memory. *Tectonophysics*, 774:228289.

Sammartini, M., Moernaut, J., Kopf, A., Stegmann, S., Fabbri, S., Anselmetti, F., and Strasser, M. (2021). Propagation of frontally confined subaqueous landslides: Insights from combining geophysical, sedimentological, and geotechnical analysis. *Sedimentary Geology*, 416:105877.

Schnellmann, M., Anselmetti, F. S., Giardini, D., and Mckenzie, J. A. (2006). 15,000 Years of mass-movement history in Lake Lucerne: Implications for seismic and tsunami hazards. *Eclogae Geologicae Helvetiae*, 99(3):409–428.

Schnellmann, M., Anselmetti, F. S., Giardini, D., McKenzie, J. A., and Ward, S. N. (2002). Prehistoric earthquake history revealed by lacustrine slump deposits. *Geology*, 30(12):1131.

Schulz, W. H. and Wang, G. (2014). Residual shear strength variability as a primary control on movement of landslides reactivated by earthquake-induced ground motion: Implications for coastal Oregon, U.S.: Strength effects on coseismic landslides. *Journal of Geophysical Research: Earth Surface*, 119(7):1617–1635.

Silver, E. A., McCaffrey, R., Joyodiwiryo, Y., and Stevens, S. (1983). Ophiolite emplacement by collision between the Sula Platform and the Sulawesi Island Arc, Indonesia. *Journal of Geophysical Research: Solid Earth*, 88(B11):9419–9435. Publisher: John Wiley & Sons, Ltd.

Simonneau, A., Chapron, E., Vannière, B., Wirth, S. B., Gilli, A., Di Giovanni, C., Anselmetti, F. S., Desmet, M., and Magny, M. (2012). Multidisciplinary distinction of mass-movement and flood-induced deposits in lacustrine environments: implications for Holocene palaeohydrology and natural hazards (Lake Ledro, Southern Alps, Italy). *Climate of the Past Discussions*,

8(4):3205–3249.

Stevens, C., McCaffrey, R., Bock, Y., Genrich, J., Endang, Subarya, C., Puntodewo,
S. S. O., Fauzi, and Vigny, C. (1999). Rapid rotations about a vertical axis in a
collisional setting revealed by the Palu Fault, Sulawesi, Indonesia. *Geophysical
Research Letters*, 26(17):2677–2680.

Stirling, M., Rhoades, D., and Berryman, K. R. (2002). Comparison of Earthquake
Scaling Relations Derived from Data of the Instrumental and Preinstrumental
Era. *Bulletin of the Seismological Society of America*, 92(2):812–830.

Strasser, M., Monecke, K., Schnellmann, M., and Anselmetti, F. S. (2013). Lake
sediments as natural seismographs: A compiled record of Late Quaternary
earthquakes in Central Switzerland and its implication for Alpine deformation.
Sedimentology, 60(1):319–341.

Supendi, P., Widiyantoro, S., Rawlinson, N., Yatimantoro, T., Muhari, A., Hanifa,
N. R., Gunawan, E., Shiddiqi, H. A., Imran, I., Anugrah, S. D., Daryono,
D., Prayitno, B. S., Adi, S. P., Karnawati, D., Faizal, L., and Damanik,
R. (2023). On the potential for megathrust earthquakes and tsunamis off
the southern coast of West Java and southeast Sumatra, Indonesia. *Natural
Hazards*, 116(1):1315–1328.

Titu-Eki, A. and Hall, R. (2020). The Significance of the Banda Sea: Tectonic
Deformation Review in Eastern Sulawesi. *Indonesian Journal on Geoscience*,
7(3):291–303.

Tiwari, P., Maurya, D., Shaikh, M., Patidar, A., Vanik, N., Padmalal, A., Vasaikar,
S., and Chamyal, L. (2021). Surface trace of the active Katrol Hill Fault and
estimation of paleo-earthquake magnitude for seismic hazard, Western India.
Engineering Geology, 295:106416.

Tournier, N., Fabbri, S. C., Anselmetti, F. S., Cahyarini, S. Y., Bijaksana, S.,
Wattrus, N., Russell, J. M., and Vogel, H. (2023). Climate-controlled
sensitivity of lake sediments to record earthquake-related mass wasting in
tropical Lake Towuti during the past 40 kyr. *Quaternary Science Reviews*,
305:108015.

Van Daele, M., Moernaut, J., Doom, L., Boes, E., Fontijn, K., Heirman, K.,
Vandoorne, W., Hebbeln, D., Pino, M., Urrutia, R., Brümmer, R., and
De Batist, M. (2015). A comparison of the sedimentary records of the 1960

and 2010 great Chilean earthquakes in 17 lakes: Implications for quantitative lacustrine palaeoseismology. *Sedimentology*, 62(5):1466–1496.

Vandekerkhove, E., Van Daele, M., Praet, N., Cnudde, V., Haeussler, P. J., and De Batist, M. (2020). Flood-triggered versus earthquake-triggered turbidites: A sedimentological study in clastic lake sediments (Eklutna Lake, Alaska). *Sedimentology*, 67(1):364–389.

Villeneuve, M., Gunawan, W., Cornee, J.-J., and Vidal, O. (2002). Geology of the central Sulawesi belt (eastern Indonesia): constraints for geodynamic models. *International Journal of Earth Sciences*, 91(3):524–537.

Vogel, H., Russell, J. M., Cahyarini, S. Y., Bijaksana, S., Wattrus, N., Rethemeyer, J., and Melles, M. (2015). Depositional modes and lake-level variability at Lake Towuti, Indonesia, during the past ~29 kyr BP. *Journal of Paleolimnology*, 54(4):359–377.

Waldmann, N., Anselmetti, F. S., Ariztegui, D., Austin Jr, J. A., Pirouz, M., Moy, C. M., and Dunbar, R. (2011). Holocene mass-wasting events in Lago Fagnano, Tierra del Fuego (54°S): implications for paleoseismicity of the Magallanes-Fagnano transform fault: Holocene mass-wasting events in Lago Fagnano, Tierra del Fuego (54°S). *Basin Research*, 23(2):171–190.

Watkinson, I. M. and Hall, R. (2017). Fault systems of the eastern Indonesian triple junction: evaluation of Quaternary activity and implications for seismic hazards. *Geological Society, London, Special Publications*, 441(1):71–120.

Wilhelm, Nomade, J., Crouzet, C., Litty, C., Sabatier, P., Belle, S., Rolland, Y., Revel, M., Courboulex, F., Arnaud, F., and Anselmetti, F. S. (2016). Quantified sensitivity of small lake sediments to record historic earthquakes: Implications for paleoseismology: Lake sensitivity to record earthquakes. *Journal of Geophysical Research: Earth Surface*, 121(1):2–16.

Wilhelm, B., Amann, B., Corella, J. P., Rapuc, W., Giguet-Covex, C., Merz, B., and Støren, E. (2022). Reconstructing Paleoflood Occurrence and Magnitude from Lake Sediments. *Quaternary*, 5(1):9.

Wils, K., Deprez, M., Kissel, C., Vervoort, M., Van Daele, M., Daryono, M. R., Cnudde, V., Natawidjaja, D. H., and De Batist, M. (2021). Earthquake doublet revealed by multiple pulses in lacustrine seismo-turbidites. *Geology*, 49(11):1301–1306.
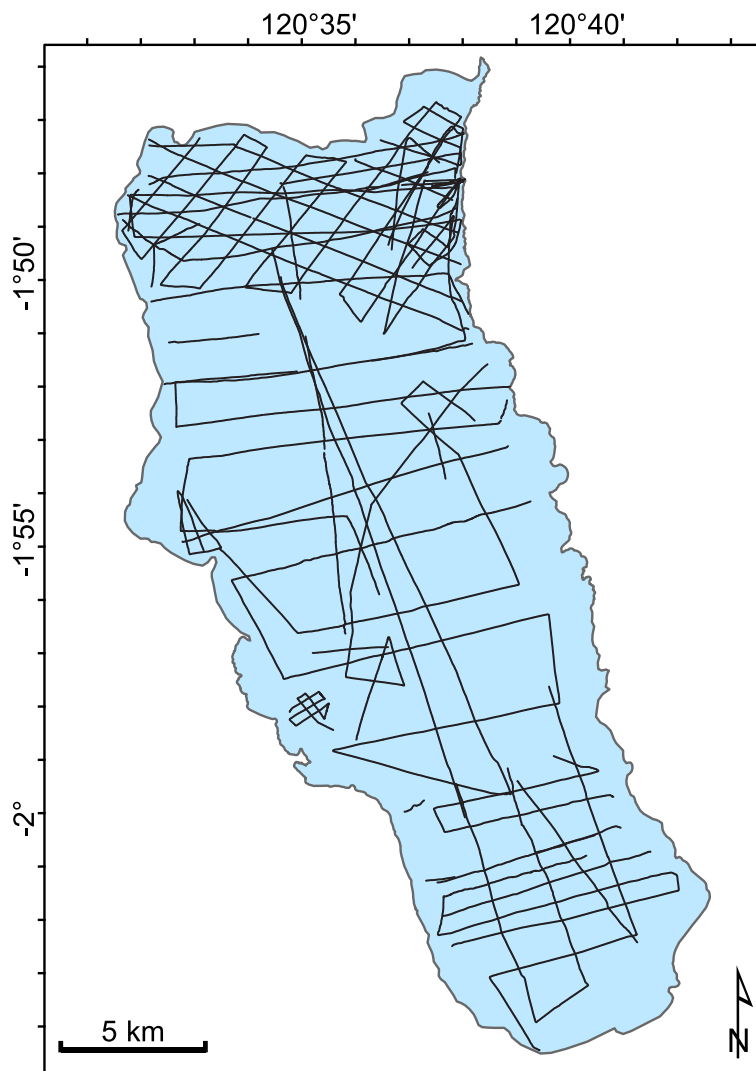
8 Supplementary material

Figure S1: 3.5 kHz seismic grid of the 2022 survey on Lake Poso.

Table S1: Radiocarbon ages measured on the cores used in this article.

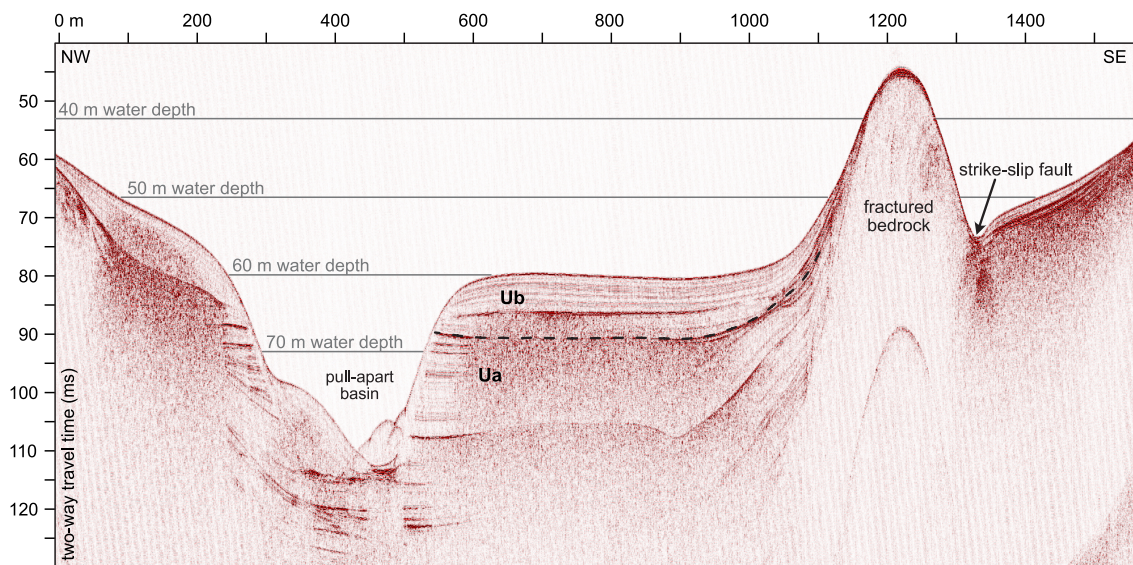| Core Id	Depth (top tube)	Material	Uncalibrated age (y BP)	±1s (y)
POS-22-01	97	macrofossil	**2168**	86
POS-22-18	52	macrofossil	**881**	72
POS-22-23	29	macrofossil	**348**	69
POS-22-23	47	macrofossil	**437**	65

Figure S2: Seismic line crossing the strike-slip fault near Tentena, showing the bedrock outcropping the sediment and the formation of a pull-apart basin.
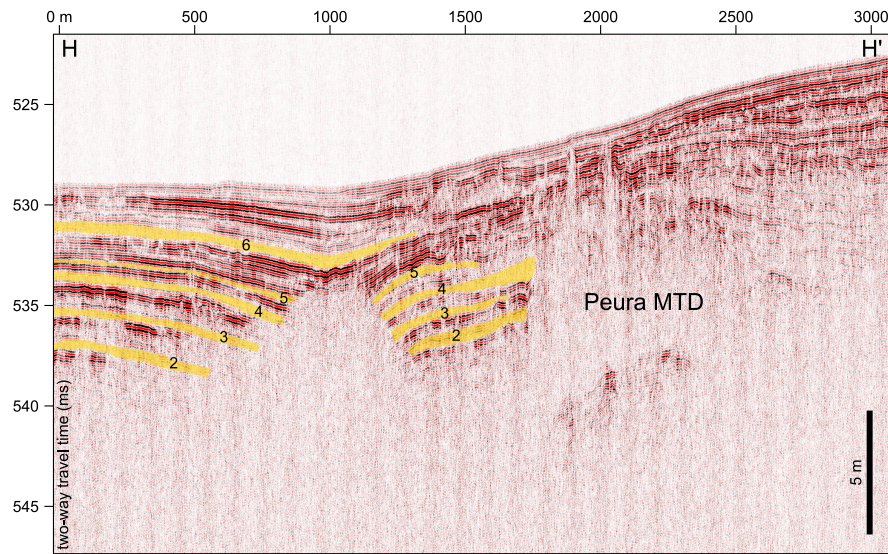
Figure S3: Seismic line in the depocentre, showing 6 event deposits (undefined MTDs or turbidites) underlying the Peura MTD. By correlation, we assume that the Peura MTD is likely related to the turbidite 1, dated at 11.4 kyrs.
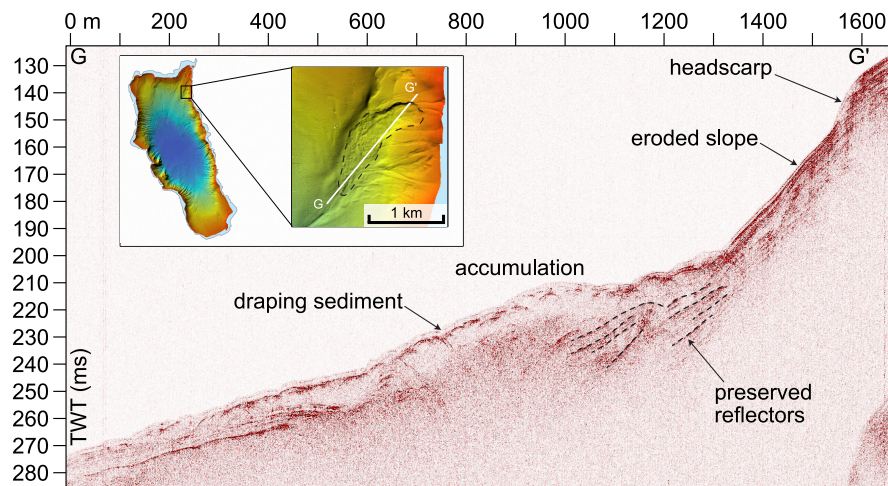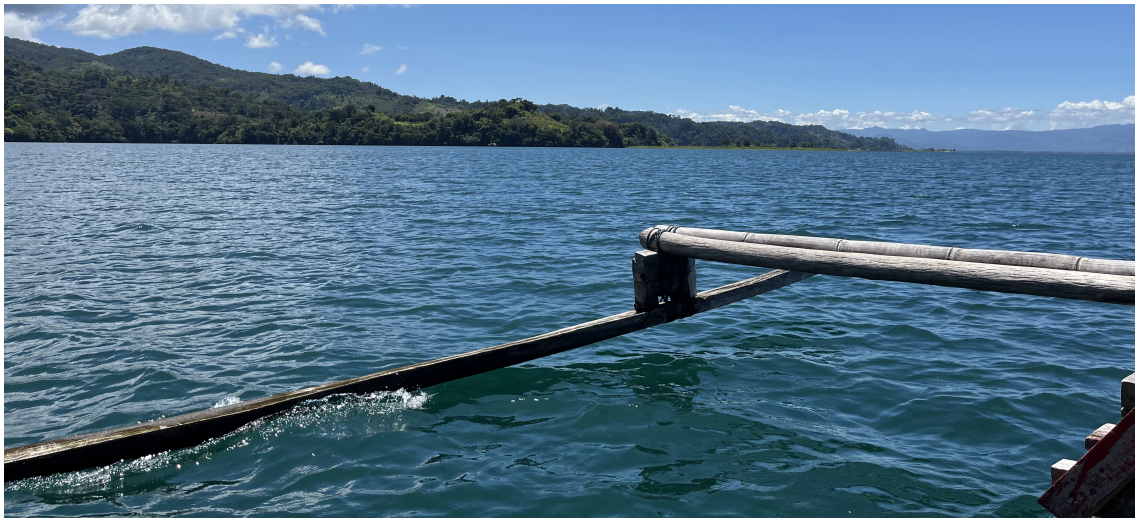

Figure S4: Seismic line in the Tentena Area showing a recent MTD from the eastern shoreline. The location into the fault canyon makes it difficult to date this event.

Chapter 5

Conclusion and outlook

Picture of Lake Poso from the coring boat (personal collection).

1 Conclusion

The Island of Sulawesi is located along a tectonically highly active zone. Apart from the northern section of the PKF, which has been extensively investigated since the Mw 7.5 Palu earthquake in 2018, the Sulawesi strike-slip fault system is poorly studied. Even though Indonesia is the 4th most populous country in the world, seismic risk maps are imprecise in remote areas. To better assess seismic risk, we first need to understand the hazard. However, data on earthquakes only cover modern time from the early 1900s. The time covered by these instruments is not sufficient to identify high-magnitude earthquakes (>7), which can have return periods of several hundred or thousands of years.

Lake Towuti and Lake Poso are two ancient lakes. Their sediments, accumulated over millions of years, are natural seismographs of central Sulawesi. Seismic acquisition missions and sediment core and borehole sampling enable the analysis of the paleoclimate, but also the detection of events that can be interpreted as major seismic episodes since the late Quaternary.

In Lake Towuti, the impact of climate on the sensitivity of the lake to record seismic deposits from the LGM was first demonstrated using piston cores and CHIRP high-resolution seismic reflection. Fluctuating lake levels lead to changes in the stability of the slopes, which can then collapse during seismic events of varying magnitudes.

On the other hand, the study of the TDP boreholes with single- and multi-channel seismic data allowed an extension of the palaeoseismological analysis back to the formation of Lake Towuti 1 Ma ago. First, it was shown that the climatic impact was not significant on this time scale. This is because seismic cycles control the recurrence of earthquakes. The periodicity of turbidites, associated with slope destabilisation, revealed three distinct phases in the sediments with a phase of active tectonics, followed by a quiescent phase, and finally, a rather concentrated turbidite phase controlled by the change in the hydrology of the lake's watershed and the formation of the delta from the Mahalona River. This new input of sediment therefore changes the sensitivity to recording turbidites during seismic events in the northern part of the lake.

Lake Poso is the second study site in this project. The first palaeoseismological survey of this lake was carried out in November 2022. This preliminary study used high-resolution bathymetry to identify massive MTDs, evidence of high-magnitude earthquakes. The faults are also indicators of the area's seismic activity. An estimation of the maximum

magnitude of a fault under the lake indicates that earthquakes of magnitude 6.6 may occur.

2   Outlook

All these studies, with a spatial and temporal distribution (from several thousand years to 1 Ma), show the seismic potential of central Sulawesi. Lake Towuti and Lake Poso demonstrate a particularly virulent tectonic past. However, modern records of earthquakes on the island do not highlight this significant seismicity. Lake paleoseismology provides a better insight into the seismic and tectonic evolution of the Palu-Koro and Matano faults.

However, these data are not yet complete enough to interpret paleoseismology accurately. The TDP aimed to study the palaeoclimate and palaeoenvironments. Therefore, the boreholes and seismic lines are located at sites with little tectonic impact. For an in-depth palaeoseismological study, it would be interesting to carry out boreholes in the southern part of the lake, where tectonic faults appear to have been active recently. In addition, a new seismic survey closer to the shoreline or a bathymetric campaign would enable the identification of potential MTDs.

The survey at Lake Poso revealed the potential of this site for a palaeoseismological study. This pioneering mission to this lake revealed a sensitive area for large magnitude earthquakes, with MTDs and recent faults. It would be judicious to take piston core samples to continue the investigation on this lake. It would also be very useful to carry out a second bathymetric survey in the next few years. In recent years, a new approach has made it possible to calculate erosion and accumulation areas by comparing two bathymetric surveys of a single lake. Lake Poso is one of the few lakes in the world where observing a likely active fault is possible. Using the same bathymetric data comparison approach would be interesting for observing and calculating fault movements.

These new seismic, bathymetric and sediment data will better assess the seismic risk in central Sulawesi and supplement modern records. Few earthquakes of magnitude 7 or more have been identified since the beginning of the 20th century. However, palaeoseismological studies show the potential of Sulawesi's strike-slip faults to generate this type of earthquake. It is, therefore, coherent to say that an event of this magnitude could happen in the near future. However, it has been stated that even where paleoseismologists have pointed out potentially dangerous faults worldwide, local governments have often not used that information to increase public awareness of seismic

hazards or mitigate the effects of future earthquakes.

Declaration of consent

on the basis of Article 18 of the PromR Phil.-nat. 19

Name/First Name: Tournier Nicolas

Registration Number: 19-137-256

Study program: Geological sciences

Bachelor ☐   Master ☐   Dissertation ☑

Title of the thesis: Lake-based paleoseismology in Sulawesi, Indonesia

Supervisor: Prof. Dr. Hendrik Vogel
                     Prof. Dr. Flavio S. Anselmetti

I declare herewith that this thesis is my own work and that I have not used any sources other than those stated. I have indicated the adoption of quotations as well as thoughts taken from other authors as such in the thesis. I am aware that the Senate pursuant to Article 36 paragraph 1 litera r of the University Act of September 5th, 1996 and Article 69 of the University Statute of June 7th, 2011 is authorized to revoke the doctoral degree awarded on the basis of this thesis.

For the purposes of evaluation and verification of compliance with the declaration of originality and the regulations governing plagiarism, I hereby grant the University of Bern the right to process my personal data and to perform the acts of use this requires, in particular, to reproduce the written thesis and to store it permanently in a database, and to use said database, or to make said database available, to enable comparison with theses submitted by others.

Bern, August 5th, 2024

Signature